Fall 12-1-2015

Development of Dual-Cure Hybrid Polybenzoxazine Thermosets

Jananee Narayanan Sivakami
University of Southern Mississippi

The University of Southern Mississippi

DEVELOPMENT OF DUAL-CURE HYBRID POLYBENZOXAZINE THERMOSETS

by

Jananee Narayanan Sivakami

Abstract of a Dissertation
Submitted to the Graduate School
and the School of Polymers and High Performance Materials
at The University of Southern Mississippi
in Partial Fulfillment of the Requirements
for the Degree of Doctor of Philosophy

December 2015

ABSTRACT

DEVELOPMENT OF DUAL-CURE HYBRID

POLYBENZOXAZINE THERMOSETS

by Jananee Narayanan Sivakami

December 2015

Polybenzoxazines are potential high performance thermoset replacements for traditional phenolic resins that can undergo an autocatalytic, thermally initiated ring - opening polymerization, and possess superior processing advantages including excellent shelf-life stability, zero volatile loss and limited volumetric shrinkage. The simplistic monomer synthesis and availability of a wide variety of inexpensive starting materials allows enormous molecular design flexibility for accessing a wide range of tailorable material properties for targeted applications. Despite the fact, once fully cured, benzoxazines are difficult to handle due to their inherent brittleness, leaving a very little scope for any modifications. The motivation of this dissertation is directed towards addressing the common limitations of polybenzoxazines and to enable tailor made material properties for expanding the scope of future applications.

In this work, a unique approach has been demonstrated incorporating a dually polymerizable bifunctional benzoxazine based monomer; designed to form a sequentially addressable intermediate B-staged network, followed by the formation of a final hybrid network *via* thermal curing of benzoxazines. This strategy offers a systematic route to study the formation of glassy polymeric materials in discrete, orthogonal steps, and a handle to access a broad range of material properties within the same system. The dissertation study is focused on manipulating the monomer design, to study different cure

chemistries, in conjunction with benzoxazines. These cure chemistries included - rapid UV curable thiol-ene click chemistry, thermally curable ring-opening metathesis polymerization of norbornene, and free radical photo-polymerization of meth(acrylate) functionalities. A strong fundamental understanding of structure-property relationships with respect to network structure, kinetics, processing control and material properties of the hybrid networks was established.

DEVELOPMENT OF DUAL-CURE HYBRID

POLYBENZOXAZINE THERMOSETS

by

Jananee Narayanan Sivakami

A Dissertation
Submitted to the Graduate School
and the School of Polymers and High Performance Materials
at The University of Southern Mississippi
in Partial Fulfillment of the Requirements
for the Degree of Doctor of Philosophy

Approved:

_____
Dr. Derek L. Patton, Committee Chair
Associate Professor, School of Polymers and High Performance Materials

_____
Dr. Jeffrey S. Wiggins, Committee Member
Associate Professor, School of Polymers and High Performance Materials

_____
Dr. James W. Rawlins, Committee Member
Associate Professor, School of Polymers and High Performance Materials

_____
Dr. Robson F. Storey, Committee Member
Bennett Distinguished Professor, School of Polymers and High Performance Materials

_____
Dr. Joseph R. Lott, Committee Member
Assistant Professor, School of Polymers and High Performance Materials

_____
Dr. Karen S. Coats
Dean of the Graduate School

December 2015

DEDICATION

To my family, K.N. and P.N. Hemalatha Narayanan and brother, Jagdeesh for their endless love, support and encouragement. Thank you for the unconditional love and expressing faith in me. To my cousin brother, Dr. Narayan Raman for his valuable support and guidance. To my best friend, Lalit Kumar Naidu for his care, support and motivation. To all my teachers, for the inspiration and instilling a strong foundation towards my personal and career growth.

ACKNOWLEDGMENTS

I would like to acknowledge my advisor Dr. Derek L. Patton who has been my role model, teacher, philosopher and friend. Thank you for the support and guidance, and much freedom to express and execute my ideas that has been crucial towards my professional and personal growth. I would like to acknowledge my other committee members, Dr. James W. Rawlins, Dr. Jeffrey S. Wiggins, Dr. Robson F. Storey and Dr. Joseph R. Lott for their constructive feedbacks and support that they gave me during my time spent in the graduate school. I would also like to thank all the professors at USM for the guidance and value addition towards the progress of my graduation.

I'd like to thank the administrative staff, specifically Ms. Jody Wiggins and Ms. Beverly McNeese for their valuable support and services.

I would like to thank members of Patton Research Group for inspiring and challenging me every day to evolve as a better researcher and person.

Special thanks to Dr. Joshua U. Otaigbe, Shahab K. Rahimi and Steve Wand for providing me with the opportunity to collaborate with them and adding a new dimension to my research.

I would also like to thank my former laboratory colleagues – Dr. Ryan Hensarling, Dr. Bradley Sparks, Dr. Austin Baranek and Matthew Jungman for their guidance and constructive feedbacks.

Lastly, I would like to thank Dr. Adekunle Olubummo and Jared Cobb for their support and guidance.

TABLE OF CONTENTS

LIST OF TABLES

Tables

LIST OF ILLUSTRATIONS

Figures

LIST OF SCHEMES

Schemes

LIST OF ABBREVIATIONS

Bz	benzoxazine
BPA	bisphenol-A
BA	butyl acrylate
BHT	butylated hydroxytoulene
°C	centigrade
$CDCl_3$	deuterated chloroform
CH_2Cl_2	dichloromethane
DSC	differential scanning calorimetry
DMA	dynamic mechanical analysis
DMPA	2,2-dimethoxy-2-phenyl acetophenone
DCPD	dicyclopentadiene
DCP	dicyclopentadiene
ENB	ethylidene norbornene
E''	loss modulus
E'	storage modulus
FTIR	fourier transform infrared
GDMP	glycol di-(3-mercaptopropionate)
GPa	gigapascal
G'	shear storage modulus
G"	loss shear modulus
g	gram
h	hour

Hz	hertz
H_2O	water
h	hour
ΔH	heat of enthalpy
IPNs	interpenetrating networks
J	joule
KBr	potassium bromide
KOH	potassium hydroxide
L	liter
$MgSO_4$	magnesium sulfate
MHz	megahertz
MPa	megapascal
m	meter
mL	milliliter
mW	milliwat
min	minute
mm	millimeter
mmol	millimole
M_c	molecular weight between cross-links
NMR	nuclear magnetic resonance
nm	nanometer
Nor	norbornene
NaOH	sodium hydroxide

NaCl	sodium chloride
NaOH	sodium hydroxide
N	newton
ppm	parts per million
pBZ	polybenzoxazine
PETMP	pentaerythritol tetra (3-mercaptopropionate)
Pt	platinum
POSS	polyhedral oligomeric silsesquioxane
ρ	density
Pa	pascal
R	gas constant
ROMP	ring-opening metathesis polymerization
ROP	ring opening polymerization
RTIR	real-time fourier transform infrared
rt	room temperature
rpm	revolutions per minute
rad	radian
s	second
S/N	signal-to-noise ratio
T_g	glass transition temperature
T	temperature
TGA	thermo-gravimetric analysis
THF	tertahydrofuran

TMA	thermo-mechanical analysis
Tan δ	tangent delta
t_{gel}	gel point
UV	ultraviolet
v_e	cross-link density
λ	wavelength
w/w	weight ratio
wt	weight

CHAPTER I

INTRODUCTION

Phenolic Resins

Among the most widespread commercial class of high-performance polymers are the phenolic resins, which have found numerous applications from commodity construction materials to high technology applications in electronics and aerospace industry. The widespread use of phenolic resins can be attributed to their outstanding performance characteristics such as excellent heat and chemical resistance, dimensional stability, flame retardancy, and good electrical properties. Nevertheless, they suffer from severe processing limitations including poor shelf life of the precursors, brittle nature of the materials, release of volatiles during polymerization leading to shrinkage, and void formation, and the use of harsh catalyst causing corrosion of the processing equipment.[1-4]

Polybenzoxazines

Polybenzoxazines are an emerging class of non-halogen based high performance thermosetting resins that offer properties comparable and even superior to conventional phenolic, epoxy, bismaleimide and polyimide resins.[5-7] Strikingly, the molecular structure of benzoxazine resins obtained via simple synthetic methodologies offer enormous design flexibility enabling a broad range of tailorable material properties for desired applications.

Monomer- Synthesis and Mechanism

Benzoxazines, a subclass of phenolic resins, are formed by the Mannich condensation of primary amines with phenols and formaldehyde. The synthesis of benzoxazines was first established by Holly and Cope[8] in 1944. Burke et al.[9-15]

significantly contributed to the fundamental understanding of the small molecular weight benzoxazine chemistry in 1949. The studies conducted by Burke showed that formation of the oxazine ring occurred via substitution at the free ortho position of a phenolic compound resulting in the formation of the Mannich bridge structure.[9] Later, Reiss et al.[16], and Schreiber[17] studied the possibility of oligomer formation and polymer development. In 1985, Higginbottom[18-20] initially developed a cross-linked polybenzoxazine based on multifunctional benzoxazine monomers. However, it was not until 1994 that Ning and Ishida[21] shed light on the material properties of cross-linked polybenzoxazines, and they have since significantly contributed to the gain in fundamental understanding of structure-property relationships for numerous polybenzoxazines materials. Several companies, including Huntsman Advanced Materials, have commercialized benzoxazine resins. Also, a variety of benzoxazine-based prepregs, polymeric products, composites and filled resins have been developed and commercialized by Henkel Company.

A typical benzoxazine synthesis involves the use of simple starting materials: a phenolic derivative, formaldehyde and an amine (aliphatic or aromatic) as represented in Scheme 1. A variety of benzoxazine monomers can be designed using substituted phenols and amines to influence the cure kinetics and the network structure, so as to attain a broad range of tailorable material properties. Cross-linked benzoxazine materials for advanced materials applications have been synthesized by employing multifunctional/bifunctional amine or phenol precursors in combination with their respective monofunctional analogues.

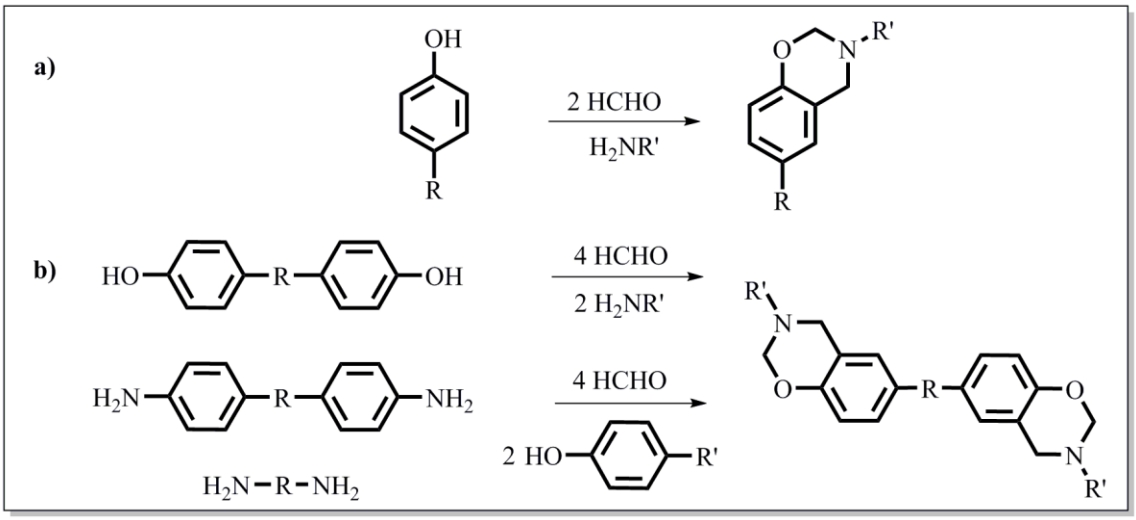

Scheme 1. Typical monomer synthesis of a) Monofunctional benzoxazine b) Bis functional benzoxazine.

Several chemical methodologies have been adopted for benzoxazine monomer synthesis using low cost and commercially available raw materials, which allows significant synthetic flexibility.[22-25] The preferred route of benzoxazine synthesis is the Mannich condensation reaction of phenol, formaldehyde and amine, mixed together in a molar ratio of 1:2:1.[9, 26] However, several variations of the Mannich condensation route to benzoxazines have been reported in literature. The condensation reaction in solution was carried out by first reacting amine with formaldehyde at lower temperature to form N, N-dihydroxymethylamine derivative –N ($-CH_2-OH)_2$, which then undergoes an electrophilic aromatic substitution with phenol, preferably at the ortho position, followed by ring closure with the phenolic hydroxyl group.[14] Alternatively, a mixture of p-substituted phenol, amine and formaldehyde was reacted in a molar ratio of 1:1:1 to yield phenolic Mannich base, which was followed by reaction with formaldehyde in the presence of base.[14]

The course of the condensation is dictated by various factors including the stoichiometry, temperature, nature, position and size of the substituents attached to phenols, and basicity of amines. Consequently, depending on these conditions, the formation of other by-products - N,N-bis(hydroxybenzyl) amine bridge structure and Mannich bases (free base) may be favored more or less relative to the benzoxazine monomer.[9] Bulky substituents at the free ortho position of phenol have been shown to hinder the formation of benzoxazine ring by restricting the free motion of hydroxyl group by steric hindrance and consequently, the N,N-bis(hydroxybenzyl) amine bridge structure is favored over the benzoxazine.[15] On the other hand, the basicity of amine has a significant effect on the course of the condensation. Example, for benzoxazines derived from 2,4-dichlorophenol, strong amines, such as methyl amine favored the formation of N,N-bis(hydroxybenzyl) bridge structure and Mannich base; whereas the use of weak amines, such as benzyl amine led to the isolation of Mannich base in high yield along with some benzoxazines.[27] Generally, a weak electrophile – derived from amines bearing electron-withdrawing groups and formaldehyde – needs high electron density on the aromatic ring of the phenol to easily undergo electrophilic aromatic substitution. Benzoxazines synthesized from weak amines and phenolic precursors bearing weak, but electron donating groups, such as bisphenol-A or 4,4’-thiodiphenol, were easily formed in contrast to 4,4’-dihydroxybenzophenone or 4,4’-dihydoxydiphenylsulfone.[28]

The synthesis of benzoxazine monomer can be conducted using either a solvent or solventless procedure. The course of condensation is strongly influenced by the nature of solvent employed for synthesis of benzoxazine resin. Ning and Ishida[21] found

a strong dependence of the yield of the benzoxazine on the polarity of the solvent. The use of nonpolar solvents, such as 1,4-dioxane and chloroform largely favored the formation of the closed ring over ring-opened structures as compared to the polar solvents, such as water and alcohol. Liu et al.[28] reported that solvents with low dielectric constant favored ring closure; example, the yield of a fluorinated benzoxazine monomer was 80% in 1,4-dioxane (**ε** = 2.2), 70% in ethyl ether (**ε** = 4.2) and 20% in methanol (**ε** = 32.7). Studies conducted by Ishida and Low[29] demonstrated a minimal effect of dielectric constant for nonpolar solvents in contrast to the polar solvents, where the effect was significant. Moreover, the use of high boiling point, nonpolar solvents such as xylene, drives the equilibrium towards ring closure by removing the water - a primary condensation by-product, which promotes ring opening of benzoxazine.[30] The solvent-based benzoxazine synthesis is associated with numerous disadvantages, such as slow reaction rate, cost ineffectiveness, environmental problems, poor solubility of the precursors, and solvent residue, which causes processability issues in benzoxazine resins. Ishida et al.[31] developed an alternative route by developing solventless synthesis under melt conditions. The solventless synthesis was carried out in one pot, simply by physically mixing and melting the monomer precursors – phenol, paraformaldehyde and amine – to complete the ring formation. Short reaction times and fewer side reactions were the major highlights of the melt-based solventless procedure.

Stability and reactivity of benzoxazine

The stability of benzoxazines is highly influenced by the nature of the surrounding medium and the substituents present on them. Benzoxazines have been observed to be quite stable in hot aqueous alkali, but unstable in acid.[9, 26] Some

benzoxazines have been shown to undergo a ring opening reaction in the presence of active hydrogen containing compounds (HY), such as imide, phenol (one of the starting materials), carbazole and aliphatic nitro compounds, to yield a Mannich bridge structure, as shown in Scheme 2.

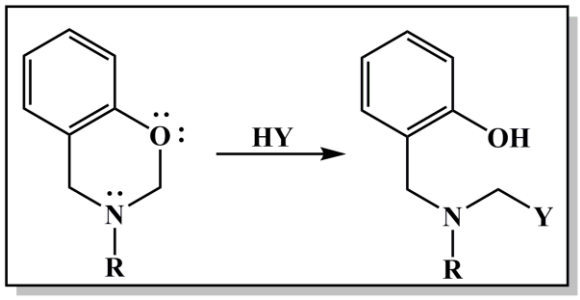

Scheme 2. Ring opening of benzoxazine in the presence of active hydrogen containing compound (HY).

The nature and position of substituents have a key effect on the stability of benzoxazines. Benzoxazine structures bearing a carbonyl group are generally liable to undergo base hydrolysis. The presence of more than one ortho reactive site on benzoxazine may cause another aminoalkylation reaction, eventually resulting in polymerization under appropriate conditions.[32] Likewise, benzoxazines possessing ortho substituents (C-8 position) ring-open more readily to yield a significant amount of ortho aminoalkylated products. The basicity of amine used in the synthesis of benzoxazine has been found to exhibit a correlation with their amino alkylation ability i.e., the ability to undergo ring-opening. The reactivity of benzoxazine based on the basic strength of amines has been found to decrease in the following order: methylamine>cyclohexyl amine>benzyl amine.[28]

Ring opening polymerization of benzoxazines

Benzoxazines undergo thermally accelerated ring opening polymerization with or without an added initiator to yield Mannich Bridge (-CH_2-NR-CH_2-) and phenolic

repeating units as an integral part of the backbone. Ring-opening polymerization of benzoxazines has been demonstrated using various cationic initiators including acids[33-36], photo-cationic initiator[37], thiols[38] and phenols[16]. To date, several mechanisms for benzoxazine polymerization have been proposed; however, a broadly accepted mechanism has not been established. In view of the high basicity of the oxygen and nitrogen center of the oxazine ring, the ring opening polymerization of benzoxazine has been proposed to take place via cationic mechanism.[33-34] In 1968, McDonagh and Smith[39] suggested that benzoxazine polymerization occurred by the formation of iminium ion via the oxygen-nitrogen proton transfer and subsequent ring-chain tautomerism. Reiss et al.[16] proposed that the benzoxazine polymerization proceeds by the condensation of amines with the iminium ions. Later in 1999, Ishida and Dunkers[36] proposed a two-step pathway for the benzoxazine polymerization. The first step involves the formation of iminium ion via the protonation of oxygen existing in equilibrium with the carbocation, which is followed by electrophilic aromatic substitution, taking place preferentially at the free ortho and para position of the phenolic group.

Catalyst-free thermally activated ring opening polymerization of benzoxazine is the most preferred and effective route, as it involves no volatiles or use of corrosive catalyst. The proposed mechanism for the thermal route can be envisaged as a) breakage of –O-CH_2- bond b) tautomerism and finally, electrophilic aromatic substitution,[40] which is represented in Scheme 3.

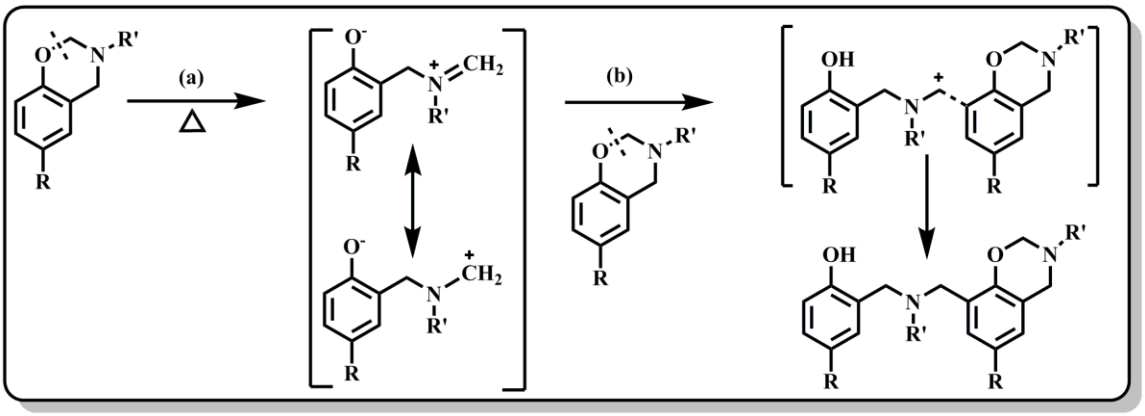

Scheme 3. Mechanism for thermally activated ring - opening polymerization of benzoxazine a) Initiation via oxazine ring-opening b) Electrophilic aromatic substitution reaction.[40]

The presence of trace amounts of phenolic starting materials and/or benzoxazine oligomers acts as cationic initiator and catalyst. Thus, the rate of polymerization is affected by the purity of the monomers and other starting materials. During the course of polymerization, a large amount of acidic phenolic components are produced, which acts as an additional initiator and catalyst, thus enabling an autocatalytic curing process.[41]

Features and applications

With a rich flexibility in molecular design, polybenzoxazines stand out among other traditional thermosetting polymers, featuring a number of unusual and useful properties for a wide variety of industrial applications. The high char yield, lack of smoke generation, and low total heat release during combustion are key characteristics of benzoxazines as excellent flame retardant materials. Their excellent three-dimensional stability, high glass transition temperature, and superior processing advantages make polybenzoxazines suitable for structural matrix composite applications in the aerospace industry.

The ambient storage stability, ease of processability, low water retention, excellent chemical resistance and near-zero volumetric shrinkage offer wide applicability as coatings, adhesives and laminating systems.[6]

Limitations

Despite multiple advantages, polybenzoxazines possess some shortcomings on their use in practical applications. Highly cross-linked polybenzoxazine thermosets typically suffer from severe brittleness due to the presence of low molecular weights between the crosslinks. For many applications, polybenzoxazines require impractically high cure temperatures in the range of 160 °C – 220 °C. Furthermore, most benzoxazine monomers are "brick dust" solids, which presents a major processing challenge for thin film coating applications. Several strategies have been investigated in an attempt to overcome the limitations of polybenzoxazines and for performance enhancement including i) designing novel benzoxazine precursors with additional functionalities (allyl[42], propargyl[43], acetylene[44], nitrile[45-46]) ii) incorporation of benzoxazine into polymer chain as main-chain precursors[47], side-chain precursors[48-49] and cross-linkable telechelics[50] and iii) physical modification via rubber toughening[51], and fabrication of composites with nanofillers (POSS[52,53], silica[54], titania[55]), carbon fibers[56] or clay[57,58]. One of the salient features of benzoxazine is their capability to synergistically blend with non-benzoxazine monomers (epoxies[59,60], polyurethane[61,62]) via reactive phenolic groups, which act as both reactants and catalyst. Moreover, the presence of hydrogen bonding centers – phenolic hydroxyl groups and nitrogen of the Mannich base – in benzoxazines facilitates synergism between other hydrogen bonding polymers including poly (ε-caprolactone)[63-64], polycarbonate[65] and polyurethane[61].

In an attempt to improve the properties of polybenzoxazines, the challenge lies in maintaining the integrity of the network without sacrificing significant properties of polybenzoxazine. Therefore, the most promising strategy is to intrinsically alter the structure of monomer through careful choice of starting materials. Ishida and Allen[66-68] successfully utilized molecular design to achieve inherent flexibility in polybenzoxazine thermosets by synthesizing a series of aliphatic diamine-based bisbenzoxazines that showed improved flexural properties and excellent processing control. In this direction, Baranek et al.[69] designed a series of flexible aliphatic-bridged bisphenol based benzoxazines – a strategy that enabled a broad design space to incorporate a variety of easily assessable amine derivatives.

Molecular Design Flexibility

The simplistic synthetic methodology, and the wide availability of phenols and amines in benzoxazines offer enormous molecular design flexibility, enabling access to a broad range of tailorable material properties. Scheme 4 illustrates the vast synthetic versatility of bifunctional benzoxazine monomers; where each of the design constituents – FG, R, and R′- can be varied to influence polymerization kinetics, network structure, processing control and thermo-mechanical properties.

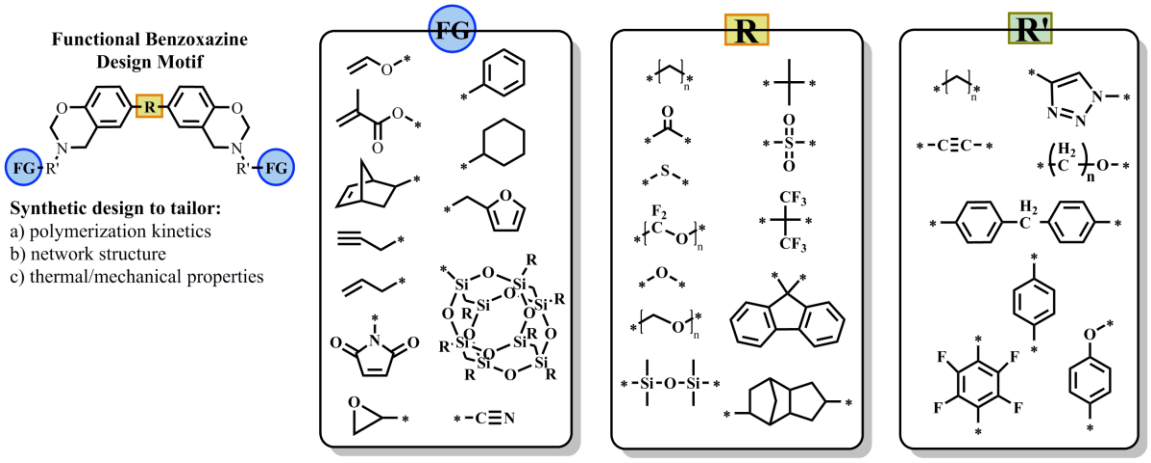

Scheme 4. Demonstration of rich molecular design flexibility in polybenzoxazines.

Benzoxazine chemistry with other orthogonal chemistries

The ring-opening addition polymerization chemistry of benzoxazine allows it to be combined with a vast number of other groups that can polymerize via different mechanisms. The order of formation of the oxazine and functional polymer network (sequential or simultaneous) can be controlled by the choice of functionalities and polymerization conditions such as UV, thermal, or moisture.

To date, numerous reactive crosslinking functional groups have been introduced into benzoxazines, which fall into following categories- thermally curable groups (allyl[42], propargyl[43], acetylene[44], maleimide[70-71], methylol[72]), free-radical UV polymerizable groups (methacrylate[73], maleimide[74]), ionically polymerizable groups (epoxy[75], oxazoline[76], nitrile[77]) and photo-curable groups (coumarin[78]). The incorporation of additional polymerizable groups has a profound effect on final network properties. Thermal stability studies by Low and Ishida[79-83] have revealed that the Mannich bridge (-CH_2-NR-CH_2-) is the weakest link in polybenzoxazine matrix, and this linkage decomposes via loss of amine fragments. The end capping of amine with cross-linkable groups consequently enhances thermal stability by stabilizing early amine

degradation. Also, additional polymerizable moieties contribute to crosslinking density, which enhances the glass transition temperature and stiffness of the final polymer network. For example, acetylene-terminated benzoxazines exhibited an exceptionally high char yield (81%) and high glass transition temperature (320-370 °C) compared to typical difunctional benzoxazines due to the presence of highly cross-linked network arising from additional acetylene crosslinking.[44] In another example, Agag and Takeiechi[42] synthesized allyl-functionalized benzoxazines, in which the curing behavior displayed a dual cure pattern consisting of the thermal addition polymerization of allyl group (ca. 145 °C), followed by benzoxazine polymerization (ca. 220 °C). Thereby, the introduction of allyl group in benzoxazines enhanced the stiffness and thermal stability as compared to non-allyl functional benzoxazines.

UV-curing technology in polybenzoxazines

Photo-initiated polymerization represents state-of-the-art curing technology that has found myriad of applications, especially in the areas of UV-curing of inks, coatings, and adhesives, and photolithography[84-85]. One of the striking features of UV curing processes is rapid and efficient curing, which can be executed without the use of solvent and at ambient temperatures. Photo-initiated polymerization processes fall into two categories – free radical and cationic – both of which have widely been employed because of the wide availability of monomers and photo-initiators that can operate in the near-UV or visible range.

In contrast to rapidly occurring photo-initiated polymerization, thermally curable benzoxazines exhibit a slow rate of polymerization, which makes the combination of the two rather appealing. Moreover, the high UV resistance of benzoxazine resins compared

to epoxies further broadens the scope of applications.[86] To date, very few photo-polymerizable groups have been studied with the benzoxazine system, mostly focusing on the synthesis of linear polymers bearing pendant thermo-labile benzoxazine groups, where some of the examples include radical-mediated polymerization of styrene-co-maleimide[74], methacrylate-co-styrene[87], and methacrylate[73]-based benzoxazine polymer systems. Additionally, the photo-initiated cationic polymerization and free-radical -promoted cationic polymerization of benzoxazine monomer[37], and its application as hydrogen donor for conducting free radical mediated photo-polymerization of vinyl-based compounds[88] have been documented.

Dual-cure/hybrid-cure methodology

Dual-cure/hybrid-cure methodologies – processes that combine two independent curing mechanisms – facilitate the formation of a multicomponent polymer network with versatile tailoring of thermo-mechanical properties of final network. Hybrid cure systems are associated with two polymerization/crosslinking reactions occurring simultaneously; whereas in dual-cure systems, the cure mechanisms take place serially. Whether the two curing mechanisms occur serially (dual-cure) or simultaneously (hybrid-cure) are determined by the choice of curing chemistries and curing parameters, such as the source of trigger, type and concentration of initiator, and the environmental factors.

Dual cure/hybrid-cure systems based on UV radiation curing are widely employed because of their many advantages, including ambient temperature cure capability, high selectivity, rapid reaction kinetics, and broad tailorability by virtue of the choice of monomers and photoinitators[89]. Many different dual-cure/hybrid-cure systems have been proposed and/or developed. Some of the proposed systems include the combination of

UV radical polymerization (example of acrylates) with a variety of other processes including cationic UV curing (vinyl ethers, oxetanes and epoxides), radical thermal curing (acrylates), cationic thermal curing (epoxides), thermal curing *via* polyaddition (isocyanates with polyols), air curing (alkyds) and moisture curing (siloxanes, isocyanates).[90] The practical applicability of hybrid-cure/dual-cure processes would depend on the nature of substrate, application technique, and the desired material properties of the finished product. Furthermore, the order of cure sequence and monomer composition/ratio has been shown to have a profound effect on the polymerization kinetics, network formation and final material properties.[91,92,93]

The utilization of hybrid systems offers access to a broad range of tailorable material properties through a careful choice of monomer composition/functionality and curing conditions. Aside from unique network characteristics, the hybrid system could be considered as a potential solution in overcoming the limitations of the pure systems. For example, UV-initiated radical polymerizations of acrylates are widely employed owing to their rapid rates, and wide choice of monomers. However, acrylates are inhibited by oxygen, and exhibit high viscosity, skin toxicity, and unpleasant odor. In contrast, cationic photo-initiated polymerizations – mainly based on epoxides and vinyl ethers – combine high reactivity and absence of oxygen inhibition with low toxicity and irritation properties.[94] Studies based on the hybrid-cure systems of acrylates/vinyl ethers[95,96] or acrylates/epoxides[97], when compared to individual systems, showed improved polymerization kinetics with less sensitivity to oxygen and moisture in the respective radical and cationic processes, yielding materials with superior performance characteristics.

Unlike a hybrid system, a dual-cure system offers an additional advantage of controlled network formation that can be employed to overcome the common limitations of coating systems. For example, high crosslink density often results in a brittle coating unsuitable for substrates that must be subsequently stamped or bent into final form. The dual-cure systems can provide an opportunity to first apply the coating formulation on flat substrates and execute a first stage cure to yield an easily deformable, flexible coating. Subsequently, the B-stage coating can be deformed to the final form, and fully cured to produce a hard coating with desired final properties. Examples of two-step cure processes based on different polymerization mechanisms include UV-initiated radical polymerization (acrylates) followed by UV-mediated cationic polymerization (epoxides[98], oxetane[99,100,101]), wherein two photo-initiators with different spectral absorptivity were employed. Another type of system is based on the combination of UV free-radical polymerization (acrylates) and thermal-initiated polymerization (vinyl ethers[102], epoxides[103,104]). Additionally, the dual-cure systems combining thermal (based on polyaddition of isocyanate and alcohol) and UV cure processes are advantageously employed in the curing of dark areas that are inaccessible by UV light, thus promoting an efficient cure throughout the thickness of the film.[105]

The hybrid networks can be classified into two main categories: interpenetrating networks (IPNs) and covalently cross-linked networks. Interpenetrating networks are composed of two or more networks which are at least partially interlocked on a molecular scale, but are not covalently bonded to each other.[106] The concept of a dual-cure/hybrid-cure approach is not new and indeed, has been studied for various interpenetrating networks developed either via sequential or simultaneous cure mechanisms.[92, 107-109]

Much less studied are hybrid systems that incorporate orthogonal cure mechanisms within the same molecule.

Unlike IPNs and blends, a covalently cross-linked hybrid network potentially improves phase homogeneity and reaction kinetics by the virtue of chemical bonds between the two networks during or after the first curing step. Another possible way to develop a hybrid network is to copolymerize functionally different monomers/polymers utilizing a common curing mechanism. The copolymerization method offers a straightforward and easy route to access a broad range of network properties, tailored through the careful selection of co-monomers and their relative ratios. Another route to develop a one-component system is where both the networks are derived from the same molecule bearing different reactive functional groups. An example by Itoh et al.[110] showcased a new hybrid system derived from a multifunctional vinyl monomer bearing both cationic and free radical polymerizable vinyl groups. Other examples of one-component hybrid networks based on a multifunctional monomer systems include acrylate-oxetane[100], acrylate-polyester[99], acrylate-vinyl ether[110,111] and acrylate-epoxy[104].

Dual cure hybrid methodology in polybenzoxazines

In view of the aforementioned advantages, the dual-cure hybrid methodology could be used to render processing advantages in polybenzoxazines, which are brittle and difficult to handle. The dual cure process could be used to prepare easy-to-handle, B-staged films prior to the full final cure. Moreover, the final properties of the network could be manipulated by various parameters including choice of monomers with varying cross-linkable functionalities associated with the primary network, curing conditions, cure time and temperature, source of trigger, and type and concentration of the initiator.

Overall, this approach could yield fundamentally different network structures, polymerization kinetics, thermo-mechanical properties, and processing control from benzoxazines.

To date, few studies of the application of dual-cure hybrid methodology to polybenzoxazines have been reported. Lu et al.[112] developed polyacrylate-polybenzoxazine interpenetrating networks via sequential UV-induced polymerization of trimethyoylpropane triacrylate and thermal ring-opening polymerization of benzoxazines. Rapid UV-induced polymerization resulted in improved miscibility within fully interpenetrating polyacrylate and polybenzoxazine networks; however the system exhibited substantial phase inhomogeneity at high benzoxazine content because of presence of strong intra-molecular hydrogen bonding interactions within the PBZ network. Although no studies on mechanical properties were reported, the authors showed the ability to tailor both thermal and surface energy properties of interpenetrating network structures. Recently, Beyazkilic et al.[113] synthesized benzoxazine polymer precursors via simultaneous thiol-ene photo-polymerization (radical-mediated) and thiol-mediated ring opening of benzoxazine. Beyazkilic et al.[113] initially targeted the synthesis of main-chain benzoxazine precursors by employing allyl functional bis-benzoxazine and difunctional thiol. They found, however, that the primary reaction products were cross-linked rather than linear, and that additional crosslinking subsequently occurred owing to the presence of residual benzoxazine functionalities. Sponton et al.[114] developed polybenzoxazine/polysiloxane hybrid material based on trimethoxysilane-functionalized benzoxazine, wherein a partially condensed polysiloxane hybrid precursor was formed by sol-gel process (hydrolysis followed by condensation) followed by polycondensation of

the residual siloxane groups and thermal ring opening polymerization of benzoxazine. Although, the two curing processes could not be completely separated due to incomplete sol-gel process, the authors demonstrated the utility of incorporating dual-cure orthogonal mechanisms to produce homogeneous hybrid materials with enhanced thermal stability, thermo-mechanical properties, and excellent flame-retardancy compared to that of typical polybenzoxazine.

Summary

Simple synthesis and rich molecular design flexibility provide the impetus for development of improved and novel polybenzoxazine materials for a variety of applications. Considering this body of literature, there are bountiful possibilities to utilize a variety of versatile chemistries with the catalyst-free thermal polymerization of benzoxazines. The application of dual-cure hybrid methodology in polybenzoxazines is a potentially promising solution to the limitations of polybenzoxazines, and as well, offers access to a broad array of improved and tailorable material properties. Moreover, a fundamental understanding of structure-property relationships in dual-cure hybrid networks, especially as affected by reaction kinetics and conversion would be highly beneficial. This information would provide a platform to develop tailor made solutions for specific end-use applications in the areas of coatings, adhesives, sealants and high performance composites.

References

1. Nair, C. P. R., Advances in addition-cure phenolic resins. *Progress in Polymer Science* **2004,** *29* (5), 401-498.
2. Knop, A.; Pilato, L. A., *Phenolic resins: Chemistry, application and performance—future directions*. Springer-Verlag, Berlin: 1987.
3. Dodiuk, H.; Goodman, S. H., *Handbook of thermoset plastics*. William Andrew: 2013.
4. Matsumoto, A., In *Polymeric Materials Encyclopedia*, Salomone, J. C., Ed. CRC Press: Baton Raton, FL, 1996; p 5039.
5. Takeichi, T.; Kawauchi, T.; Agag, T., High Performance Polybenzoxazines as a Novel Type of Phenolic Resin. *Polym. J* **2008,** *40* (12), 1121-1131.
6. Ishida, H.; Agag, T., *Handbook of benzoxazine resins*. Elsevier: 2011.
7. Ghosh, N. N.; Kiskan, B.; Yagci, Y., Polybenzoxazines—New high performance thermosetting resins: Synthesis and properties. *Progress in Polymer Science* **2007,** *32* (11), 1344-1391.
8. Holly, F. W.; Cope, A. C., Condensation Products of Aldehydes and Ketones with o-Aminobenzyl Alcohol and o-Hydroxybenzylamine. *Journal of the American Chemical Society* **1944,** *66* (11), 1875-1879.
9. Burke, W. J., 3,4-Dihydro-1,3,2H-Benzoxazines. Reaction of p-Substituted Phenols with N,N-Dimethylolamines. *Journal of the American Chemical Society* **1949,** *71* (2), 609-612.
10. Burke, W. J.; Weatherbee, C., 3,4-Dihydro-1,3,2H-Benzoxazines. Reaction of Polyhydroxybenzenes with N-Methylolamines1. *Journal of the American*

Chemical Society **1950,** *72* (10), 4691-4694.

11. Burke, W. J.; Stephens, C. W., Monomeric Products from the Condensation of Phenol with Formaldehyde and Primary Amines. *Journal of the American Chemical Society* **1952,** *74* (6), 1518-1520.
12. Burke, W. J.; Kolbezen, M. J.; Stephens, C. W., Condensation of Naphthols with Formaldehyde and Primary Amines1. *Journal of the American Chemical Society* **1952,** *74* (14), 3601-3605.
13. Burke, W. J.; Glennie, E. L. M.; Weatherbee, C., Condensation of Halophenols with Formaldehyde and Primary Amines1. *The Journal of Organic Chemistry* **1964,** *29* (4), 909-912.
14. Burke, W. J.; Bishop, J. L.; Glennie, E. L. M.; Bauer, W. N., A New Aminoalkylation Reaction. Condensation of Phenols with Dihydro-1,3-aroxazines1. *The Journal of Organic Chemistry* **1965,** *30* (10), 3423-3427.
15. Burke, W.; Smith, R. P.; Weatherbee, C., N, N-Bis-(hydroxybenzyl)-amines: Synthesis from Phenols, Formaldehyde and Primary Amines1. *Journal of the American Chemical Society* **1952,** *74* (3), 602-605.
16. Reiss, G.; Schwob, J. M.; Guth, G.; Roche, M.; Lande, B., In *Advances in Polymer Synthesis*, Culberston, B. M.; McGrath, J. E., Eds. Plenum: New York, 1985; pp 27-49.
17. Schreiber, H. German. Offen. 2,255,504, 1973.
18. Higginbottom, H. P. Polymerizable compositions comprising polyamines and poly(dihydrobenzoxazines), U.S. Pat. 4,501,864, 1985.
19. Higginbottom, H. P. Aqueous dispersions of polyamines and

poly(dihydrobenzoxazines), U.S. Pat. 4,507,428, 1985.

20. Higginbottom, H. P. Process for deposition of resin dispersions on metal substrates, U.S. Pat. 4,557,979, 1985.

21. Ning, X.; Ishida, H., Phenolic materials via ring-opening polymerization: Synthesis and characterization of bisphenol-A based benzoxazines and their polymers. *Journal of Polymer Science Part A: Polymer Chemistry* **1994,** *32* (6), 1121-1129.

22. Aversa, M. C.; Giannetto, P.; Caristi, C.; Ferlazzo, A., Behaviour of an N-(o-hydroxybenzyl)-[small beta]-amino-acid in the presence of dehydrating agents. Synthesis of a 3,4-dihydro-2H-1,3-benzoxazine. *Journal of the Chemical Society, Chemical Communications* **1982,** (8), 469-470.

23. FW, H.; AC, C., Condensation products of aldehydes and ketones with o-aminobenzyl alcohol and o-hydroxy- benzylamine. *Journal of American Chemical Society* **1944,** *66*, 1875-9.

24. Katritzky, A. R.; Xu, Y.-J.; Jain, R., A Novel Dilithiation Approach to 3,4-Dihydro-2H-1,3-benzothiazines, 3,4-Dihydro-2H-1,3-benzoxazines, and 2,3,4,5-Tetrahydro-1,3-benzothiazepines. *The Journal of Organic Chemistry* **2002,** *67* (23), 8234-8236.

25. Snieckus, V., Directed ortho metalation. Tertiary amide and O-carbamate directors in synthetic strategies for polysubstituted aromatics. *Chemical Reviews* **1990,** *90* (6), 879-933.

26. Elderfield, R. C.; Todd, W. H.; Gerber, S., In *Heterocyclic compounds*, Elderfield, R. C., Ed. John Wiley & Sons: New York, 1957; Vol. 6.

27. Burke, W. J.; Hammer, C. R.; Weatherbee, C., Bis-m-oxazines from Hydroquinone1. *The Journal of Organic Chemistry* **1961,** *26* (11), 4403-4407.

28. Liu, J. Synthesis, characterization, reaction mechanism and kinetics of 3,4-dihydro-2H-1,3-benzoxazine and its polymer, Ph.D. Thesis. Case Western Reserve University, Cleveland, OH, May 1995.

29. Ishida, H.; Low, H. Y., Synthesis of benzoxazine functional silane and adhesion properties of glass-fiber-reinforced polybenzoxazine composites. *Journal of Applied Polymer Science* **1998,** *69* (13), 2559-2567.

30. Agag, T.; Jin, L.; Ishida, H., A new synthetic approach for difficult benzoxazines: Preparation and polymerization of 4,4′-diaminodiphenyl sulfone-based benzoxazine monomer. *Polymer* **2009,** *50* (25), 5940-5944.

31. Ishida, H. U.S. Pat. 5,543,516, assigned to Edison Polymer Innovation Corporation.

32. McDonagh, A. F.; Smith, H. E., Ring-chain tautomerism of derivatives of o-hydroxybenzylamine with aldehydes and ketones. *The Journal of Organic Chemistry* **1968,** *33* (1), 1-8.

33. Wang, Y. X.; Ishida, H., Cationic ring-opening polymerization of benzoxazines. *Polymer* **1999,** *40* (16), 4563-4570.

34. Wang, Y.-X.; Ishida, H., Synthesis and Properties of New Thermoplastic Polymers from Substituted 3,4-Dihydro-2H-1,3-benzoxazines. *Macromolecules* **2000,** *33* (8), 2839-2847.

35. Ishida, H.; Rodriguez, Y., Catalyzing the curing reaction of a new benzoxazine-based phenolic resin. *Journal of Applied Polymer Science* **1995,** *58* (10), 1751-

1760.

36. Dunkers, J.; Ishida, H., Reaction of benzoxazine-based phenolic resins with strong and weak carboxylic acids and phenols as catalysts. *Journal of Polymer Science Part A: Polymer Chemistry* **1999,** *37* (13), 1913-1921.

37. Kasapoglu, F.; Cianga, I.; Yagci, Y.; Takeichi, T., Photoinitiated cationic polymerization of monofunctional benzoxazine. *Journal of Polymer Science Part A: Polymer Chemistry* **2003,** *41* (21), 3320-3328.

38. Gorodisher, I.; DeVoe, R. J.; Webb, R. J., Chapter 11 - Catalytic Opening of Lateral Benzoxazine Rings by Thiols. In *Handbook of benzoxazine resins*, Ishida, H.; Agag, T., Eds. Elsevier: Amsterdam, 2011; pp 211-234.

39. McDonagh, A. F.; Smith, H. E., Ring-chain tautomerism of derivatives of o-hydroxybenzylamine with aromatic aldehydes. *Chemical Communications (London)* **1966,** (12), 374-374.

40. Russell, V. M.; Koenig, J. L.; Low, H. Y.; Ishida, H., Study of the characterization and curing of benzoxazines using 13C solid-state nuclear magnetic resonance. *Journal of Applied Polymer Science* **1998,** *70* (7), 1413-1425.

41. Ishida, H.; Rodriguez, Y., *Journal of Applied Polymer Science* **1995,** *58* (10), 1751-1760.

42. Agag, T.; Takeichi, T., Synthesis and characterization of novel benzoxazine monomers containing allyl groups and their high performance thermosets. *Macromolecules* **2003,** *36* (16), 6010-6017.

43. Agag, T.; Takeichi, T., Novel benzoxazine monomers containing p-phenyl

propargyl ether: polymerization of monomers and properties of polybenzoxazines. *Macromolecules* **2001,** *34* (21), 7257-7263.

44. Kim, H.; Brunovska, Z.; Ishida, H., Synthesis and thermal characterization of polybenzoxazines based on acetylene-functional monomers. *Polymer* **1999,** *40* (23), 6565-6573.

45. Brunovska, Z.; Ishida, H., Thermal study on the copolymers of phthalonitrile and phenylnitrile-functional benzoxazines. *J. Appl. Polym. Sci.* **1999,** *73* (14), 2937-2949.

46. Brunovska, Z.; Lyon, R.; Ishida, H., Thermal properties of phthalonitrile functional polybenzoxazines. *Thermochimica Acta* **2000,** *357–358*, 195-203.

47. Takeichi, T.; Kano, T.; Agag, T., Synthesis and thermal cure of high molecular weight polybenzoxazine precursors and the properties of the thermosets. *Polymer* **2005,** *46* (26), 12172-12180.

48. Kiskan, B.; Yagci, Y.; Sahmetlioglu, E.; Toppare, L., Preparation of conductive polybenzoxazines by oxidative polymerization. *Journal of Polymer Science Part A: Polymer Chemistry* **2007,** *45* (6), 999-1006.

49. Kiskan, B.; Demiray, G.; Yagci, Y., Thermally curable polyvinylchloride via click chemistry. *Journal of Polymer Science Part A: Polymer Chemistry* **2008,** *46* (11), 3512-3518.

50. Kiskan, B.; Colak, D.; Muftuoglu, A. E.; Cianga, I.; Yagci, Y., *Macromolecular Rapid Communications* **2005,** *26* (10), 819-824.

51. Jang, J.; Seo, D., Performance improvement of rubber-modified polybenzoxazine. *Journal of Applied Polymer Science* **1998,** *67* (1), 1-10.

52. Lee, Y.-J.; Kuo, S.-W.; Su, Y.-C.; Chen, J.-K.; Tu, C.-W.; Chang, F.-C., Syntheses, thermal properties, and phase morphologies of novel benzoxazines functionalized with polyhedral oligomeric silsesquioxane (POSS) nanocomposites. *Polymer* **2004,** *45* (18), 6321-6331.

53. Lee, Y.-J.; Huang, J.-M.; Kuo, S.-W.; Chen, J.-K.; Chang, F.-C., Synthesis and characterizations of a vinyl-terminated benzoxazine monomer and its blending with polyhedral oligomeric silsesquioxane (POSS). *Polymer* **2005,** *46* (7), 2320-2330.

54. Agag, T.; Takeichi, T. In *Synthesis and properties of silica-modified polybenzoxazine*, Materials Science Forum, Trans Tech Publ: 2004; pp 1157-1160.

55. Agag, T.; Tsuchiya, H.; Takeichi, T., Novel organic–inorganic hybrids prepared from polybenzoxazine and titania using sol–gel process. *Polymer* **2004,** *45* (23), 7903-7910.

56. Shen, S. B.; Ishida, H., Development and characterization of high-performance polybenzoxazine composites. *Polymer Composites* **1996,** *17* (5), 710-719.

57. Agag, T.; Takeichi, T., Polybenzoxazine–montmorillonite hybrid nanocomposites: synthesis and characterization. *Polymer* **2000,** *41* (19), 7083-7090.

58. Takeichi, T.; Zeidam, R.; Agag, T., Polybenzoxazine/clay hybrid nanocomposites: influence of preparation method on the curing behavior and properties of polybenzoxazines. *Polymer* **2002,** *43* (1), 45-53.

59. Ishida, H.; Allen, D. J., Mechanical characterization of copolymers based on

benzoxazine and epoxy. *Polymer* **1996,** *37* (20), 4487-4495.

60. Grishchuk, S.; Mbhele, Z.; Schmitt, S.; Karger-Kocsis, J., Structure, thermal and fracture mechanical properties of benzoxazine-modified amine-cured DGEBA epoxy resins. *Express Polymer Letters* **2011,** *5* (3), 273-282.

61. Takeichi, T.; Guo, Y.; Agag, T., Synthesis and characterization of poly(urethane-benzoxazine) films as novel type of polyurethane/phenolic resin composites. *Journal of Polymer Science Part A: Polymer Chemistry* **2000,** *38* (22), 4165-4176.

62. Takeichi, T.; Guo, Y., Preparation and Properties of Poly(urethane-benzoxazine)s Based on Monofunctional Benzoxazine Monomer. *Polym J* **2001,** *33* (5), 437-443.

63. Ishida, H.; Lee, Y. H., Synergism observed in polybenzoxazine and poly(ε-caprolactone) blends by dynamic mechanical and thermogravimetric analysis. *Polymer* **2001,** *42* (16), 6971-6979.

64. Ishida, H.; Lee, Y.-H., Study of hydrogen bonding and thermal properties of polybenzoxazine and poly-(ε-caprolactone) blends. *Journal of Polymer Science Part B: Polymer Physics* **2001,** *39* (7), 736-749.

65. Ishida, H.; Lee, Y.-H., Infrared and thermal analyses of polybenzoxazine and polycarbonate blends. *Journal of Applied Polymer Science* **2001,** *81* (4), 1021-1034.

66. Allen, D. J.; Ishida, H., Physical and mechanical properties of flexible polybenzoxazine resins: Effect of aliphatic diamine chain length. *Journal of Applied Polymer Science* **2006,** *101* (5), 2798-2809.

67. Allen, D. J.; Ishida, H., Polymerization of linear aliphatic diamine-based

benzoxazine resins under inert and oxidative environments. *Polymer* **2007,** *48* (23), 6763-6772.

68. Allen, D. J.; Ishida, H., Effect of phenol substitution on the network structure and properties of linear aliphatic diamine-based benzoxazines. *Polymer* **2009,** *50* (2), 613-626.

69. Baranek, A. D.; Kendrick, L. L.; Narayanan, J.; Tyson, G. E.; Wand, S.; Patton, D. L., Flexible aliphatic-bridged bisphenol-based polybenzoxazines. *Polymer Chemistry* **2012,** *3* (10), 2892-2900.

70. Ishida, H.; Ohba, S., Synthesis and characterization of maleimide and norbornene functionalized benzoxazines. *Polymer* **2005,** *46* (15), 5588-5595.

71. Liu, Y.-L.; Yu, J.-M.; Chou, C.-I., Preparation and properties of novel benzoxazine and polybenzoxazine with maleimide groups. *Journal of Polymer Science Part A: Polymer Chemistry* **2004,** *42* (23), 5954-5963.

72. BAQAR, M. S. Methylol-Functional Benzoxazines: Novel Precursors for Phenolic Thermoset Polymers and Nanocomposite Applications. Case Western Reserve University, 2013.

73. Jin, L.; Agag, T.; Yagci, Y.; Ishida, H., Methacryloyl-functional benzoxazine: photopolymerization and thermally activated polymerization. *Macromolecules* **2011,** *44* (4), 767-772.

74. Gacal, B.; Cianga, L.; Agag, T.; Takeichi, T.; Yagci, Y., Synthesis and characterization of maleimide (Co)polymers with pendant benzoxazine groups by photoinduced radical polymerization and their thermal curing. *Journal of Polymer Science Part A: Polymer Chemistry* **2007,** *45* (13), 2774-2786.

75. Andreu, R.; Espinosa, M. A.; Galià, M.; Cádiz, V.; Ronda, J. C.; Reina, J. A., Synthesis of novel benzoxazines containing glycidyl groups: A study of the crosslinking behavior. *Journal of Polymer Science Part A: Polymer Chemistry* **2006,** *44* (4), 1529-1540.

76. Cao, H.; Xu, R.; Yu, D., Synthesis and characterization of 2-oxazoline-benzoxazine compound and its polymer. *Journal of Applied Polymer Science* **2008,** *110* (3), 1502-1508.

77. Chaisuwan, T.; Ishida, H., High-performance maleimide and nitrile-functionalized benzoxazines with good processibility for advanced composites applications. *Journal of Applied Polymer Science* **2006,** *101* (1), 548-558.

78. Kiskan, B.; Yagci, Y., Thermally curable benzoxazine monomer with a photodimerizable coumarin group. *Journal of Polymer Science Part A: Polymer Chemistry* **2007,** *45* (9), 1670-1676.

79. Low, H. Y.; Ishida, H., Mechanistic study on the thermal decomposition of polybenzoxazines: Effects of aliphatic amines. *Journal of Polymer Science Part B: Polymer Physics* **1998,** *36* (11), 1935-1946.

80. Yee Low, H.; Ishida, H., Structural effects of phenols on the thermal and thermo-oxidative degradation of polybenzoxazines. *Polymer* **1999,** *40* (15), 4365-4376.

81. Hemvichian, K.; Ishida, H., Thermal decomposition processes in aromatic amine-based polybenzoxazines investigated by TGA and GC–MS. *Polymer* **2002,** *43* (16), 4391-4402.

82. Hemvichian, K.; Laobuthee, A.; Chirachanchai, S.; Ishida, H., Thermal decomposition processes in polybenzoxazine model dimers investigated by TGA–

FTIR and GC–MS. *Polymer degradation and stability* **2002,** *76* (1), 1-15.

83. Hemvichian, K.; Kim, H. D.; Ishida, H., Identification of volatile products and determination of thermal degradation mechanisms of polybenzoxazine model oligomers by GC–MS. *Polymer degradation and stability* **2005,** *87* (2), 213-224.

84. Fouassier, J. P., In *Photoinitiation, Photopolymerization, and Photocuring: Fundamentals and Applications,* Hanser/Gardner Publications: Munich, 1995.

85. Yagci, Y.; Jockusch, S.; Turro, N. J., Photoinitiated polymerization: advances, challenges, and opportunities. *Macromolecules* **2010,** *43* (15), 6245-6260.

86. Macko, J. A.; Ishida, H., Behavior of a bisphenol- A- based polybenzoxazine exposed to ultraviolet radiation. *Journal of Polymer Science Part B: Polymer Physics* **2000,** *38* (20), 2687-2701.

87. Koz, B.; Kiskan, B.; Yagci, Y., A novel benzoxazine monomer with methacrylate functionality and its thermally curable (co)polymers. *Polym. Bull.* **2011,** *66* (2), 165-174.

88. Tasdelen, M. A.; Kiskan, B.; Yagci, Y., Photoinitiated free radical polymerization using benzoxazines as hydrogen donors. *Macromolecular rapid communications* **2006,** *27* (18), 1539-1544.

89. Schwalm, R., UV Coatings: Basics Recent Developments and New Applications. Elsevier Science Ltd.: 2007.

90. Peeters, S., In *Overview of dual-cure and hybrid-cure systems in radiation curing, In "Radiation Curing in Polymer Science and Technology, Vol. III, Polymerization Mechanism", J.P. Fouassier and J.F. Rabek, eds.*, Elsevier Applied Science, 1993, Chapter 6.

91. Dean, K.; Cook, W. D., Effect of Curing Sequence on the Photopolymerization and Thermal Curing Kinetics of Dimethacrylate/Epoxy Interpenetrating Polymer Networks. *Macromolecules* **2002,** *35* (21), 7942-7954.

92. Lin, Y.; Stansbury, J. W., Kinetics studies of hybrid structure formation by controlled photopolymerization. *Polymer* **2003,** *44* (17), 4781-4789.

93. Carioscia, J. A.; Stansbury, J. W.; Bowman, C. N., Evaluation and Control of Thiol-ene/Thiol-epoxy Hybrid Networks. *Polymer* **2007,** *48* (6), 1526-1532.

94. Decker, C.; Bianchi, C.; Decker, D.; Morel, F., Photoinitiated polymerization of vinyl ether-based systems. *Progress in Organic Coatings* **2001,** *42* (3–4), 253-266.

95. Cho, J.-D.; Hong, J.-W., UV-initiated free radical and cationic photopolymerizations of acrylate/epoxide and acrylate/vinyl ether hybrid systems with and without photosensitizer. *Journal of Applied Polymer Science* **2004,** *93* (3), 1473-1483.

96. Lin, Y.; Stansbury, J. W., The impact of water on photopolymerization kinetics of methacrylate/vinyl ether hybrid systems. *Polymers for Advanced Technologies* **2005,** *16* (2-3), 195-199.

97. Decker, C.; Nguyen Thi Viet, T.; Decker, D.; Weber-Koehl, E., UV-radiation curing of acrylate/epoxide systems. *Polymer* **2001,** *42* (13), 5531-5541.

98. Rohm and Haas Co. Eur. Patent. EP 0 335 629 A2, 1989.

99. El-ghayoury, A.; Boukaftane, C.; de Ruiter, B.; van der Linde, R., Dual-cure processes: towards deformable crosslinked coatings. *Macromolecular Symposia* **2002,** *187* (1), 553-562.

100. El-ghayoury, A.; Boukaftane, C.; de Ruiter, B.; van der Linde, R., Ultraviolet–ultraviolet dual-cure process based on acrylate oxetane monomers. *Journal of Polymer Science Part A: Polymer Chemistry* **2003,** *41* (4), 469-475.

101. de Ruiter, B.; El-ghayoury, A.; Hofmeier, H.; Schubert, U. S.; Manea, M., Two-step curing processes for coating application. *Progress in Organic Coatings* **2006,** *55* (2), 154-159.

102. Vansteenkiste, S.; Matthijs, G.; Schacht, E.; De Schrijver, F. C.; Van Damme, M.; Vermeersch, J., Preparation of Tailor-Made Multifunctional Propenyl Ethers by Radical Copolymerization of 2-(1-Propenyl)oxyethyl Methacrylate. *Macromolecules* **1999,** *32* (1), 55-59.

103. Yu, X.; Chen, J.; Yang, J.; Zeng, Z.; Chen, Y., Synthesis of a novel quaternary ammonium tetraphenylborate salt and its use for photo-induced thermal curing of epoxides and radical polymerization of acrylates. *Polymer International* **2005,** *54* (8), 1212-1219.

104. Park, Y.-J.; Lim, D.-H.; Kim, H.-J.; Park, D.-S.; Sung, I.-K., UV- and thermal-curing behaviors of dual-curable adhesives based on epoxy acrylate oligomers. *International Journal of Adhesion and Adhesives* **2009,** *29* (7), 710-717.

105. Studer, K.; Decker, C.; Beck, E.; Schwalm, R., Thermal and photochemical curing of isocyanate and acrylate functionalized oligomers. *European Polymer Journal* **2005,** *41* (1), 157-167.

106. Sperling, L. H., Interpenetrating Polymer Networks. In *Encyclopedia of Polymer Science and Technology*, John Wiley & Sons, Inc.: 2002.

107. Sperling, L. H., An Overview of Interpenetrating Networks. In Polymeric

Materials Encyclopedia. Salamone, J. C., Ed. CRC Press: Boca Raton, FL, 1996; Vol. 5.

108. Wei, H.; Li, Q.; Ojelade, M.; Madbouly, S.; Otaigbe, J. U.; Hoyle, C. E., Thiol−Ene Free-Radical and Vinyl Ether Cationic Hybrid Photopolymerization. *Macromolecules* **2007,** *40* (24), 8788-8793.

109. Xu, L. Q.; Yao, F.; Fu, G. D.; Kang, E. T., Interpenetrating Network Hydrogels via Simultaneous "Click Chemistry" and Atom Transfer Radical Polymerization. *Biomacromolecules* **2010,** *11* (7), 1810-1817.

110. Itoh, H.; Kameyama, A.; Nishikubo, T., Synthesis of new hybrid monomers and oligomers containing cationic and radical polymerizable vinyl groups and their photoinitiated polymerization. *Journal of Polymer Science Part A: Polymer Chemistry* **1996,** *34* (2), 217-225.

111. Li, S.; He, Y.; Nie, J., Photopolymerization of hybrid monomer 3-(1-propenyl)oxypropyl acrylate. *Journal of Photochemistry and Photobiology A: Chemistry* **2007,** *191* (1), 25-31.

112. Lu, C.; Su, Y.; Wang, C.; Huang, C.; Sheen, Y.; Chang, F., Thermal properties and surface energy characteristics of interpenetrating polyacrylate and polybenzoxazine networks. *Polymer* **2008,** *49* (22), 4852-4860.

113. Beyazkilic, Z.; Kahveci, M. U.; Aydogan, B.; Kiskan, B.; Yagci, Y., Synthesis of polybenzoxazine precursors using thiols: Simultaneous thiol–ene and ring-opening reactions. *Journal of Polymer Science Part A: Polymer Chemistry* **2012,** *50* (19), 4029-4036.

114. Spontón, M.; Estenoz, D.; Lligadas, G.; Ronda, J. C.; Galià, M.; Cádiz, V.,

Synthesis and characterization of a hybrid material based on a trimethoxysilane functionalized benzoxazine. *Journal of Applied Polymer Science* **2012,** *126* (4), 1369-1376.

CHAPTER II

RESEARCH OBJECTIVES

The goal of this dissertation is to incorporate different orthogonal cure mechanisms in conjunction with benzoxazine for the design of a unique class of dual cure hybrid polybenzoxazine thermosets with an aim to improve processability and achieve a broad range of tailorable material properties in polybenzoxazines. The unique high performance characteristics and unprecedented molecular design flexibility of benzoxazines are essentially unparalleled by conventional thermosetting materials. Motivation of this dissertation emerges from addressing the common limitations of glassy thermosets such as polybenzoxazines, which suffer from high brittleness and difficulty to process into mechanically robust thin films.

The dual cure hybrid approach used in this study relies on the design of a bis-functional benzoxazine monomer bearing a suitable cross-linkable functionality- the one which can primarily be addressed by an independent curing mechanism to form an intermediate B-staged network (stable and easy to handle), followed by thermally initiated polymerization of benzoxazines at a high temperature, as illustrated in Scheme 5. The sequential intermediate network formation aids in ease of handling/application-with a handle to manipulate the properties using a variety of parameters including cure chemistry and choice of trigger, structurally different co-monomers and co-monomer compositions, and cure time and temperature. Aside from unique network characteristics, the sequential formation of network synthesis offers opportunities to provide transformative fundamental knowledge of network formation and structure in glassy polymeric materials.

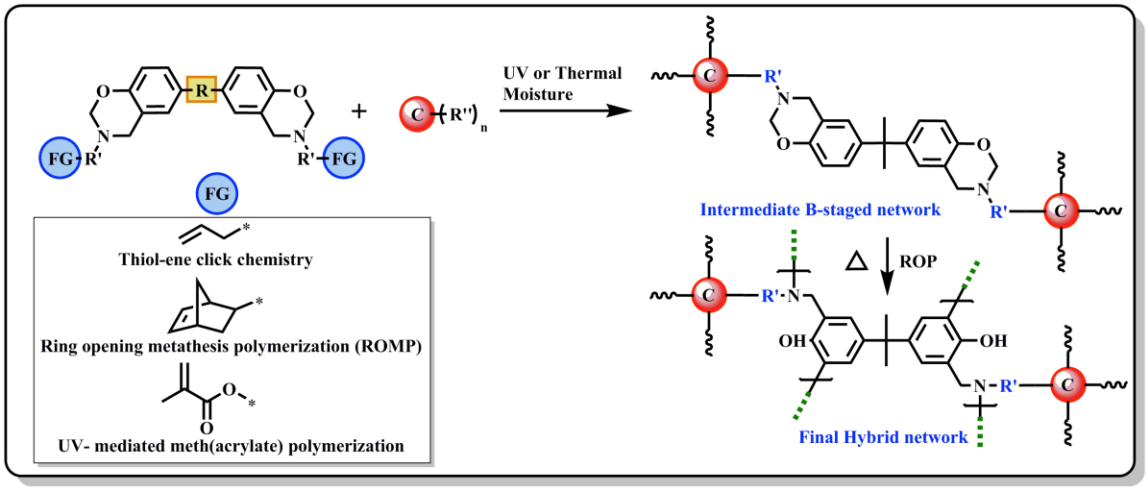

Scheme 5. Research methodology design for development of dual-cure hybrid polybenzoxazine thermosets.

The dual-cure hybrid polybenzoxazine thermosets serve as potential candidates for use in a variety of applications including coatings, inks, adhesives, electronics, and high performance composite materials. The objectives of this dissertation include:

1. Development of dual cure hybrid polymer networks via sequential thiol-ene photo-polymerization and thermal polymerization of benzoxazines.
2. Synthesis and characterization of covalently linked dual-cure hybrid cross-linked materials bearing polynorbornene and polybenzoxazine network.
3. Structure-property relationship studies of development of dual-cure hybrid polybenzoxazine network based on UV curable meth(acrylate) and thermally curable benzoxazine moieties.

The main chapters in this dissertation are either published in a peer-reviewed journal or in the process of submission to a scholarly journal.

Objective 1 (Chapter III) of this dissertation focuses on combining orthogonal UV mediated thiol-click and thermally activated benzoxazine chemistries for the design of a unique class of hybrid cure network. The two-staged network comprising of covalently linked low and high modulus components, yielded high glass transition thiol-ene materials, while offering improved processability and the flexibility to tailor the properties of the final hybrid polybenzoxazines.

Objective 2 (Chapter IV) involves the utilization of versatile ROMP (ring-opening polymerization) curing chemistry and thermally curable benzoxazines. The norbornene functional bis-benzoxazine monomer was synthesized and co-polymerized with varying concentrations of two different reactive co-monomers: DCPD and ENB, using Grubbs 3rd catalyst. The combined network characteristics of polynorbornene and polybenzoxazine networks yielded homogeneous networks with excellent thermal stability and high glass transition temperature.

Objective 3 (Chapter V) involves the development of hybrid networks based on UV curable meth(acrylate) in combination with benzoxazine chemistries. Monofunctional n-butyl acrylate was used as a reactive diluent and incorporated in varying concentrations to tailor and establish structure property relationship of structural composition, viscosity, reaction kinetics and final material properties. The incorporation of varying concentrations of highly flexible and reactive co-monomer enabled excellent processability and flexibility with an attainment of a broad range of thermo-mechanical properties in both of the sequential cured stages of network formation.

CHAPTER III

HYBRID DUAL-CURE POLYMER NETWORKS VIA SEQUENTIAL THIOL-ENE PHOTOPOLYMERIZATION AND THERMAL RING-OPENING POLYMERIZATION OF BENZOXAZINES

Introduction

Cross-linked polymer networks, or thermosets, are used extensively as structural materials in a vast array of applications. As a class of thermosets, thiol-ene networks have garnered significant interest as candidates for a broad range of applications including coatings, adhesives, optics, dental materials, and imprint lithography.[1-3] Thiol-ene networks are readily synthesized via photopolymerization of multifunctional thiols and alkenes. One of the prominent features of thiol-ene photopolymerizations is that practically any type of ene can participate in the reaction. This feature enables, through judicious choice of the chemical structure of the thiol and ene, precise tailorability of physical, mechanical, thermal, and optical properties of the network. The appealing aspects of thiol-ene materials arise from their unique combination of attributes including high gel-point monomer conversions, low shrinkage, photoinitiator-free formulations,[4] high tolerance to oxygen inhibition and homogeneity in mechanical properties – all of which result from a radical-mediated step-growth polymerization mechanism.

The inherent flexibility of the thioether linkages comprising the structure of most thiol-ene networks results in low glass transitions, which are generally observed at or below room temperature. Consequently, applications requiring high T_g materials such as naval/aerospace composites are inaccessible by thiol-ene polymerizations – as there are relatively few viable options within traditional thiol and ene combinations capable of

achieving high T_g. In this direction, several approaches have been reported with the aim of improving thermomechanical properties including thiol-norbornene networks (T_g > 80 °C),[5] thiourethane-based networks (T_g ~ 100 °C),[6] thiol-alkyne networks (T_g ~ 60 °C),[7] and hybrid, dual-cure thiol-ene/thiol-epoxy networks.[8] Other approaches to improve the range of thermal applicability include hybrid inorganic-organic thiol-ene networks.[9-11] Nonetheless, thiol-ene materials that exhibit T_g above 100 °C are all but non-existent in the literature. The development of such high glass transition networks would certainly expand the scope of thiol-ene photopolymerization and open the door to new application opportunities. In this direction, we are interested in the application of dual chemistries for synthesizing multicomponent networks that exhibit properties unachievable with traditional thiol-ene systems.

Polybenzoxazines are a relatively new class of thermoset resins, which provide attractive alternatives to traditional phenolic and epoxy resins for a variety of high performance and high temperature applications.[12-15] Benzoxazine monomers are synthesized via the Mannich condensation of phenolic and primary amine derivatives and formaldehyde.[16] The simplistic nature of benzoxazine synthesis and the broad availability of starting materials offer unprecedented flexibility in the molecular design of monomers. Benzoxazines undergo thermally activated ring-opening polymerization in the absence of the catalyst yielding a polymer backbone consisting of a phenol and a tertiary amine bridge as the repeating motif. Consequently, polybenzoxazines exhibit advantageous properties such as high glass transition temperatures, near-zero shrinkage (zero volatile byproducts), high thermal stability, excellent flame resistance (high char yields), low surface energy and low water absorption. Despite these advantageous properties,

polybenzoxazines suffer from several disadvantages including poor mechanical properties and poor processing particularly into thin films and coatings. To address these shortcomings, benzoxazines have been incorporated into polymeric precursors as pendent moieties – via thermal and photochemical polymerization of benzoxazine pendant monomers (allyl,[17-19] acetylene,[20] propargyl ether,[21] nitrile,[22] maleimide[23-26] and methacrylate[27-28]) or through postpolymerization modification – and as linear main-chain derivatives – via condensation reactions, Pt-catalyzed hydrosilylation,[18, 29] and copper-catalyzed azide-alkyne click reactions.[30-31] Thus far, the incorporation of benzoxazines into sequentially addressable (i.e. dual-cure), *multicomponent networks* has been scarcely reported. Lu and coworkers[32] recently reported interpenetrating polyacrylate/polybenzoxazine networks that could be sequentially cured by photochemical polymerization of a multifunctional acrylate and thermal polymerization of a bisfunctional benzoxazine. Although no mechanical properties were reported, the authors showed the ability the tailor both thermal and surface properties of the interpenetrating network materials. While the current manuscript was under review, Beyazkilic and coworkers[33] reported the synthesis of benzoxazine precursor polymers using simultaneous radical-mediated thiol-ene photopolymerization and thiol-mediated benzoxazine ring-opening reactions. In an effort to prepare linear main-chain benzoxazine precursors from a difunctional allyl-benzoxazine and a difunctional thiol, Beyazkilic found the reaction products were cross-linked, rather than linear, due to the occurrence of competing thiol-ene and thiol-benzoxazine reactions, and that these materials could undergo additional thermal polymerization via residual, unopened benzoxazines. The results reported by Beyazkilic et al.[33] are consistent and

complementary to our approach reported herein using tetrafunctional thiols to deliberately establish a dual network structure. The reaction of benzoxazines with thiols was recently elucidated as the COLBERT (catalytic opening of lateral benzoxazine rings by thiols) reaction (*vide infra*) by Gorodisher and coworkers[34] towards materials with potential adhesive applications.

In this work, we describe the combination of thiol-ene and polybenzoxazines for the development of hybrid, dual-cure polymer networks. Our approach, as illustrated in Figure 1, relies on the use of a multifunctional, dually-polymerizable monomer possessing both bis-"ene" and bis-benzoxazine moieties within the same molecule. This represents a unique approach to polymer network chemistry since both networks are derived in a semi-sequential manner through a common monomer constituent, i.e. a primary thiol-ene network sequentially templates a secondary polybenzoxazine network. Although complicated by the COLBERT reaction, the functional moieties are sequentially addressable via distinct polymerization mechanisms – photoinitiated thiol-ene polymerization followed by thermal ring-opening polymerization of benzoxazines – resulting in hybrid polymer networks (the term "hybrid" is used since the resulting networks cannot be classified as traditional interpenetrating networks). Hybridized, these materials combine advantages of thiol-ene reactions (photoinitiated, rapid reaction rates, low shrinkage/stress) with advantages of polybenzoxazines (high glass transition temperature, near-zero shrinkage, excellent flame resistance, low surface energy and low water absorption) yielding a sequentially processable, high T_g thermoset (150 °C) of interest for coatings, adhesives and composite applications.

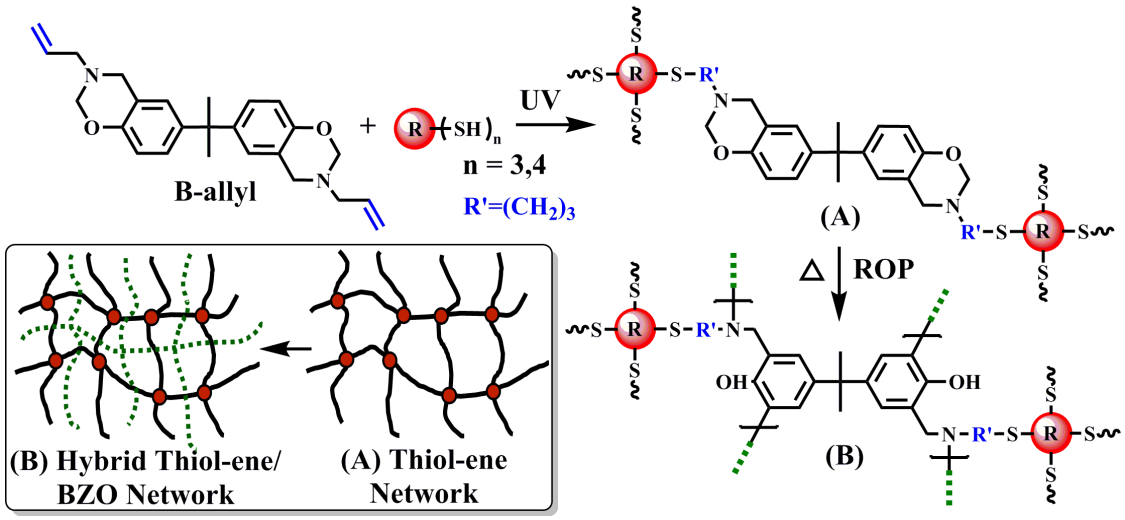

Figure 1. Ideal representation of the approach for dual cure thiol-ene/polybenzoxazine networks. For simplicity, the thiol-benzoxazine ring-opening reaction is not represented in the network structure.

Experimental

Materials

All the solvents and reagents were obtained at the highest purity available from Aldrich Chemical Company or Fisher Scientific and were used as received unless otherwise specified. Pentaerythritol tetra(3-mercaptopropionate) (PETMP) and glycol di-(3-mercaptopropionate) (GDMP) were obtained from Bruno Bock. The allyl functionalized bis-benzoxazine monomer (B-allyl)[35-36] and bisallyl ether of bisphenol A (bisallyl-BPA)[37] were synthesized according to the published procedures. Araldite© MT-35600 was obtained as a complimentary sample from Hunstman Advanced Materials. The abbreviations pB-allyl, B-allyl-PETMP, pB-allyl-PETMP are used to represent the thermally cured allyl functionalized bis-benzoxazine network in the absence of thiol, the UV cured allyl functionalized bis-benzoxazine/PETMP network, and the dual UV/thermally cured allyl functionalized bis-benzoxazine/PETMP network, respectively.

Characterization and Measurements

^{1}H- NMR and ^{13}C-NMR measurements were performed in deuterated chloroform ($CDCl_3$) using a Varian Mercury Plus 300 MHz NMR spectrometer operating at a frequency of 300 MHz with tetramethylsilane as an internal standard. The number of transients for ^{1}H and ^{13}C are 32 and 256, respectively. A relaxation time of 5 s was used for the integrated intensity determination of ^{1}H NMR spectra. Kinetic analysis was conducted using real-time FTIR spectroscopy to determine the conversions of thiol and ene functional groups. FTIR studies were conducted using a Nicolet 8700 FTIR spectrometer with a KBr beam splitter and an MCT/A detector with a 320-500 nm filtered (λ_{max} = 365 nm) ultraviolet light source (Omnicure S1000). A thiol/B-allyl solution mixture consisting of 0.5 wt% 2,2-dimethoxy-2-phenyl acetophenone (DMPA) photoinitiator was spin coated on a NaCl plate at 1800 rpm for 60 s and exposed to UV light with an intensity of 36.0 mW cm^2 using a liquid light guide. Series scans were recorded, where spectra were recorded approximately 4 scans/s, each with a resolution of 4 cm^{-1}. All FTIR experiments were carried out under a nitrogen atmosphere. Plots shown are representative data of a repeatable process. Differential scanning calorimetry (DSC) was performed on a TA instruments DSC Q200 differential scanning calorimeter at a heating rate of 15 °C/min and a nitrogen flow rate of 50 mL/min. Samples were crimped in hermetic aluminum pans with lids. Thermogravimetric analysis (TGA) was performed using a TA Instruments Q50 thermogravimetric analyzer with a platinum pan. Samples were heated at 20 °C/min from 40 °C to 800 °C under a nitrogen atmosphere. Thermomechanical analysis (TMA) was performed using a TA Instruments Q400 thermomechanical analyzer equipped with a penetration probe at a heating rate of 5 °C/min from 25 °C to 350 °C, where the sample was subjected to a force of 0.08 N.

Dynamic mechanical analysis (DMA) was performed on a TA Instruments Q800 DMA in tension film mode with a heating rate of 2 °C/min from 25 °C to 250 °C at 1 Hz. Samples were prepared using a silicone rubber mold and the dimensions of a rectangular specimen were 6.2 x 5.3 x 0.8 mm (Length x Width x Thickness).

Preparation of dual-cured polymer films

The thiol-ene/benzoxazine dual cure hybrid networks were developed by sequential thiol-ene photopolymerization followed by thermal ring-opening of benzoxazine as represented in Scheme 6. The allyl functionalized bis-benzoxazine (B-allyl) monomer (1.0 g, 2.56 mmol) was dissolved in a minimal amount of THF (1.0 mL), followed by the addition of 0.5 wt % of DMPA photoinitiator and stoichiometric amount of PETMP (0.6 g, 1.28 mmol) (ene : thiol 1:1). The solution was degassed by ultrasonication and casted onto a silicone mold. The films were kept at 45 °C for 30 min under vacuum to remove residual THF, and were then exposed to UV light for 30 min yielding a yellow transparent, tack-free film (film thickness 1 mm). The UV cured film was used for DSC analysis to study the thermal curing behavior. The UV cured films were kept at 65 °C under vacuum overnight to remove traces of residual solvent. UV cured films were subsequently cured step-wise at 100 °C, 120 °C, 140 °C for 1 h each, 160 °C, 180 °C for 2 h each and 200 °C, 220 °C for 1 h each in an air-circulating oven. The samples were then post cured at 240 °C for 1 h in an air circulating oven.

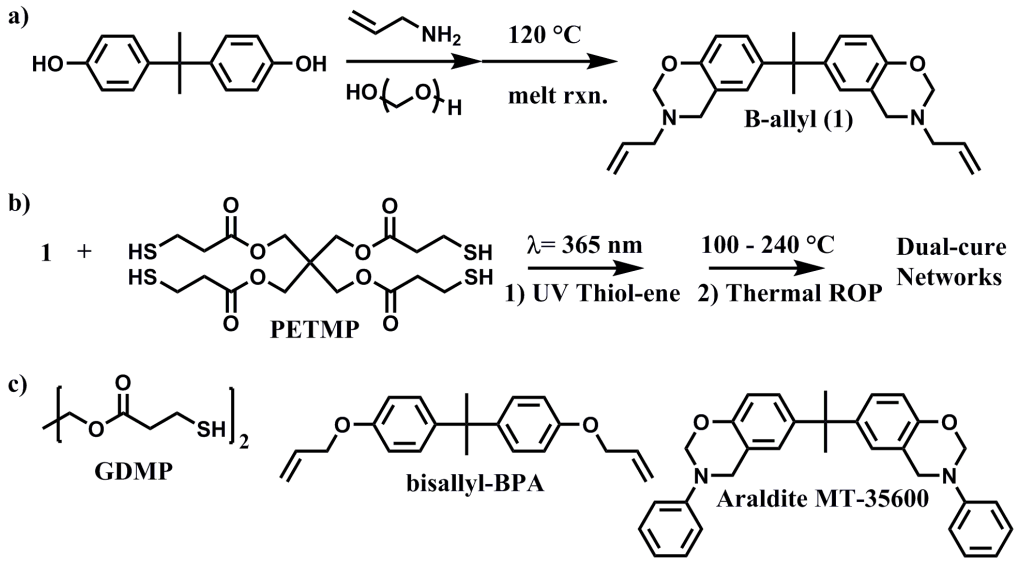

Scheme 6. (a) Preparation of B-allyl monomer and (b) pB-allyl-PETMP dual cure hybrid networks. (c) Structures of glycol di-(3-mercaptopropionate) (GDMP), bisallyl-bisphenol-A (bisallyl-BPA), and Araldite MT-35600.

Results and Discussion

Monomer Synthesis

The allyl based bis-benzoxazine monomer (B-allyl) was initially prepared by the Mannich condensation of bisphenol A, allyl amine and paraformaldehyde using a solventless method reported by Ishida and coworkers.[36] This approach provided B-allyl at 75 – 80% yield; however, purification by column chromatography was necessary to remove partially ring-opened oligomers, which significantly reduced the yield of the final high purity product (18%). Consequently, an alternate synthetic methodology was adopted where the synthesis of allyl functionalized bis-benzoxazine was carried out in xylene in an attempt to minimize the formation of oligomeric side products.[35] The use of a high boiling non-polar solvent allows increased solubility of the reactants at high temperature and facilitates removal of water, which is influential in inducing ring opening of benzoxazine leading to the formation of oligomers. Moreover, the benzoxazine ring formation is found to be more efficient in a reaction medium with a

lower dielectric constant. Also, the use of a high boiling solvent facilitates lowering of dielectric constant with increase in the reaction temperature.[35] The reaction conditions were optimized to achieve the best conversion to benzoxazine ring formation (30% yield). The details of the optimized synthetic procedure for the B-allyl monomer are given in Appendix A (Figure A1 and Figure A2).

Photopolymerization behavior of the B-allyl-PETMP system

Thiol-ene photopolymerization kinetics of the B-allyl-PETMP system were monitored using real-time FTIR (RTIR). For these measurements, the formulated resins were sandwiched between two NaCl windows (5 mm × 25 mm) and irradiated with UV light (filtered 320-500 nm) with an intensity of approximately 36 mW/cm^2.

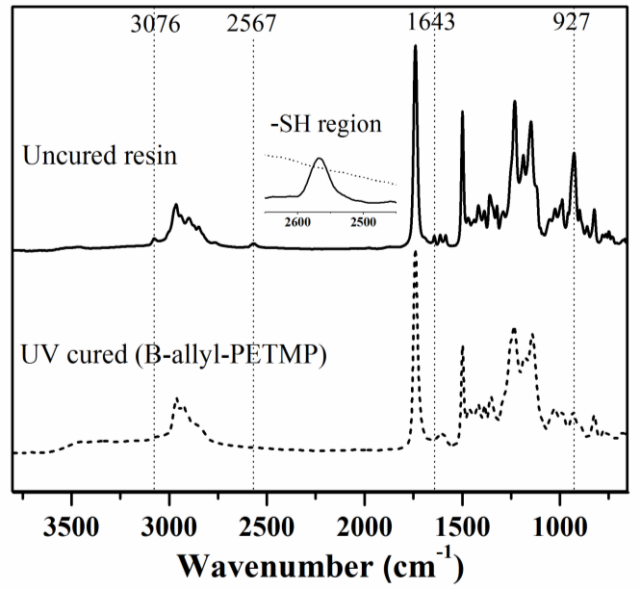

Figure 2. FTIR spectra for the uncured (upper) and UV cured B-allyl-PETMP resins (lower).

Figure 2 shows exemplary FTIR spectra for the uncured and photocured resins. Thiol conversion was monitored using the –SH absorption peak at 2567 cm^{-1}, while the allyl group conversions were monitored using the carbon-carbon double bond absorption peak at 1643 cm^{-1} (similar conversions were also obtained using the alkene peak at 3076

cm^{-1}) The aromatic out-of-phase C-H deformation vibration from DMPA photoinitiator at 824 cm^{-1} was used as an internal standard, since this peak remained unchanged during the course of the experiment. Conversions values were calculated as the change in the area under the peaks related to the thiol and alkene moieties. Conversion vs. irradiation time plots for thiol and alkene functional groups are shown in Figure 3. Under ambient conditions, the high viscosity of the resin and rapid vitrification of the films under UV irradiation yield rather slow reaction kinetics (compared to typical thiol-ene systems) and less than quantitative –SH and C=C conversions.

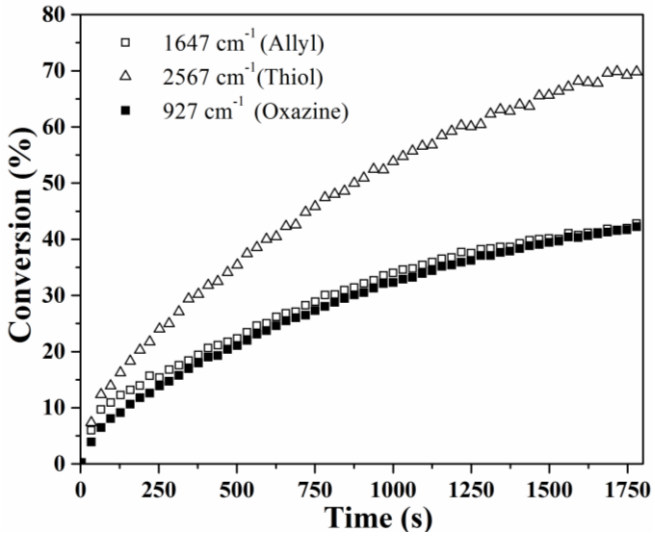

Figure 3. Real-time conversion plots of the thiol-ene photopolymerization with B-allyl and PETMP using 0.5 wt % DMPA photoinitiator exposed to UV irradiation (36.0 mW/cm^2) at room temperature.

Although stoichiometric conditions were utilized, a disparity was observed between thiol and ene conversion values leading to approximately 30% greater thiol conversion than ene conversion at 30 min. The presence of the benzoxazine ring is indicated by the out of plane C-H vibration of the aromatic ring attached to the oxazine ring observed at 927 cm^{-1}. The conversion of the benzoxazine ring of B-allyl at 927 cm^{-1} and inequality in thiol and ene conversions previously mentioned can be predominately attributed to a ring-

opening reaction between the thiol and benzoxazine ring. As shown in Figure 3, the benzoxazine conversion (42% conversion at 30 min) closely approximates the excess thiol conversion observed under UV irradiation. It should also be noted that Jin and coworkers[27] have shown exposure to UV light results in minimal ring-opening of the benzoxazine ring, but this is nonetheless contributor to the observed benzoxazine conversion in Figure 3. Similar results were obtained for thiol and benzoxazine conversions in model studies using a non-functional aniline-based benzoxazine (i.e. one that should not participate in the radical-mediated thiol-ene reaction; see Figure A3 of Appendix A). The recent work of Gorodisher *et al.*[34] describing the catalytic opening of lateral benzoxazine rings by thiols showed that thiols readily react with benzoxazines under ambient conditions. The ring-opening reaction appears to proceed via protonation of the benzoxazine nitrogen to create an ammonium cation **2**, followed by nucleophilic attack by the thiolate anion at the methylene carbon adjacent to the benzoxazine oxygen to give intermediate **3**. Proton transfer from the ammonium cation to the phenoxide yields the adduct **4** (Scheme 7).

Our own model studies involving the reaction of B-allyl with a difunctional thiol structurally similar to PETMP (the difunctional thiol GDMP was employed to avoid cross-linking and facilitate facile solution characterization by ^{1}H NMR) support the observations reported by Gorodisher and confirm the occurrence of the thiol-benzoxazine reaction during the previously described photopolymerization studies. A THF solution containing a stoichiometric amount of allyl based bisbenzoxazine (B-allyl) and GDMP were stirred at room temperature for 6 h. Figure 4 shows the ^{1}H-NMR spectrum of ring-opened adduct of benzoxazine with thiol at initial 0 h and after 6 h. The progress of the

reaction was monitored by observing the disappearance of the characteristic peaks of oxazine ring at 4.83 and 3.94 ppm corresponding to -O-CH_2-N- and Ar-CH_2-N-, respectively, and the thiol peak (-SH) at 1.56 pm (triplet). Whereas after 6 h, two new peaks appeared at 3.99 ppm and 3.81 ppm which can be attributed to Ar-CH_2-N- and -N-CH_2-S- , respectively of the Mannich bridge of the ring opened adduct.

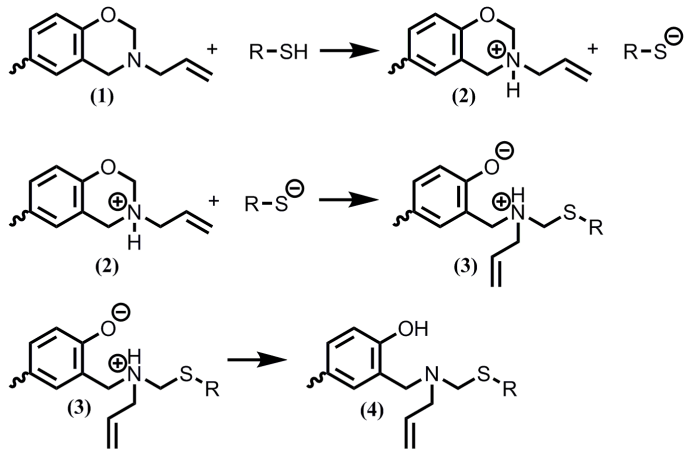

Scheme 7. Mechanism for ring-opening of benzoxazine with thiol (adapted from Gorodisher et al.[34]

The results obtained were found to be in good correlation with the proposed structure (**4**, Scheme 7) confirming the ring-opening of benzoxazine with thiol. As a result of the mechanism, it should be possible to suppress the thiol-benzoxazine ring-opening reaction by addition of a base stronger than the benzoxazine, such as triethylamine, thereby impeding the protonation of the benzoxazine by the thiol. Indeed, Gorodisher *et al.*[34] showed a significant decrease in the rate of the thiol-benzoxazine ring-opening in the presence of pyridine, and essentially no reaction in the presence of triethylamine. Although the addition of triethylamine interferes with the radical mediated thiol-ene polymerization, ongoing work in our lab suggests this strategy is a viable approach to combine base-catalyzed thiol-ene (i.e. thiol-methacrylate) with thermal ring-

opening polymerization of benzoxazines for the sequential synthesis of well-defined hybrid networks.

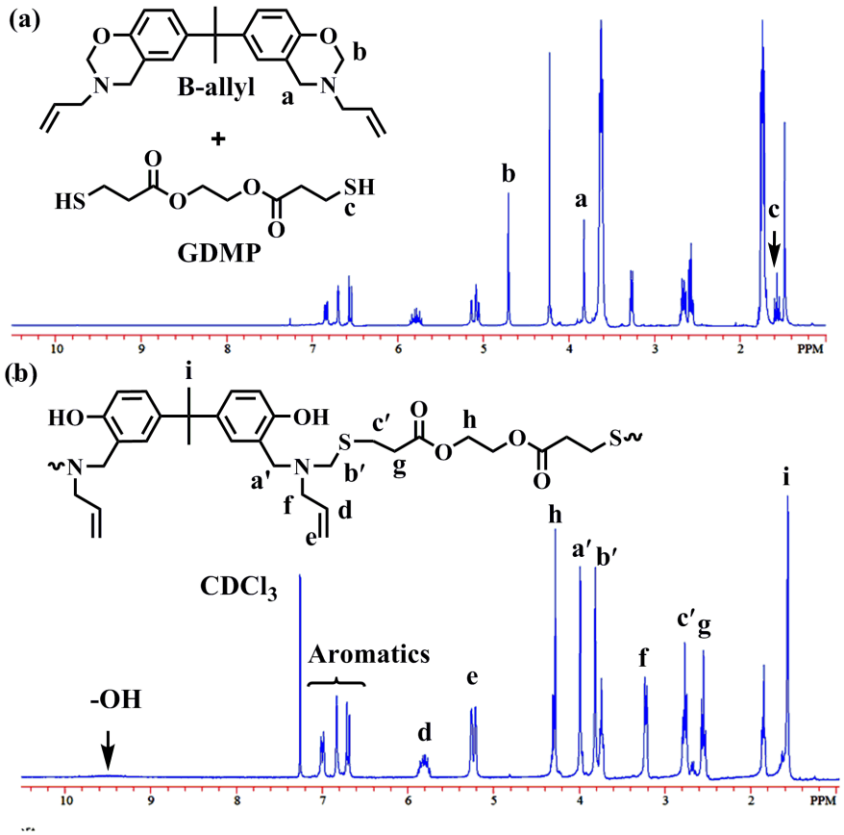

Figure 4. ^{1}H-NMR spectrum of solution of allyl based benzoxazine (B-allyl) with GDMP stirred at room temperature in THF in the absence of UV light a) initial 0 h b) after 6 h.

Thermal ring-opening polymerization of B-allyl-PETMP system

The thermal polymerization behavior of the UV cured resin was investigated by FTIR by stepwise heating at 120, 140, and 160 °C for 1 h each, 180 and 200 °C for 2 h each, and 220 and 240 °C for 1 h each. Figure 5 shows the FTIR spectra for the UV cured B-allyl-PEMTP resin during each of the aforementioned stages of the thermal cure. The intensities of the characteristic benzoxazine peaks – one at 927 cm^{-1} due to out of plane C-H vibrations of benzene ring attached to oxazine ring and another at 1498 cm^{-1}

assigned to the vibration of the tri-substituted benzene ring – decrease gradually until both peaks disappear by the end of the 240 ˚C cycle.

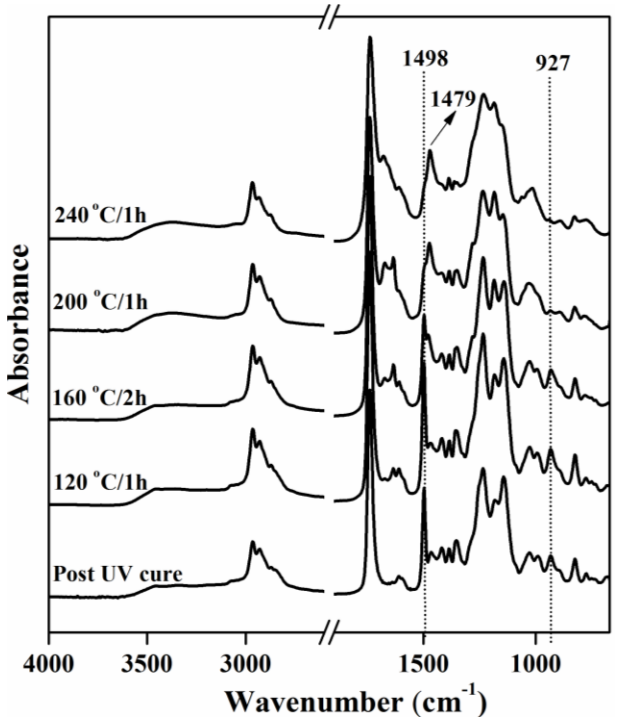

Figure 5. FTIR plots of B-allyl-PETMP resin after each cure stage.

Additionally, a new peak appears at 1479 cm^{-1} corresponding to the tetra-substituted benzene ring that results from thermal ring-opening polymerization of the benzoxazine. The appearance of a broad band around 3400 cm^{-1} with increasing temperature is also consistent with the phenolic OH resulting from the formation of a polybenzoxazine network.

The thermal polymerization behavior of the UV cured B-allyl-PETMP was also investigated using DSC analysis. The DSC thermograms of B-allyl-PETMP after each stage of cure are shown in Figure 6. DSC of UV cured B-allyl-PETMP showed two exothermic peaks. The onset of the first exotherm occurred at 142 °C with an exotherm

peak maximum at 202 °C, while the peak maximum of the second exotherm was observed at 266 °C.

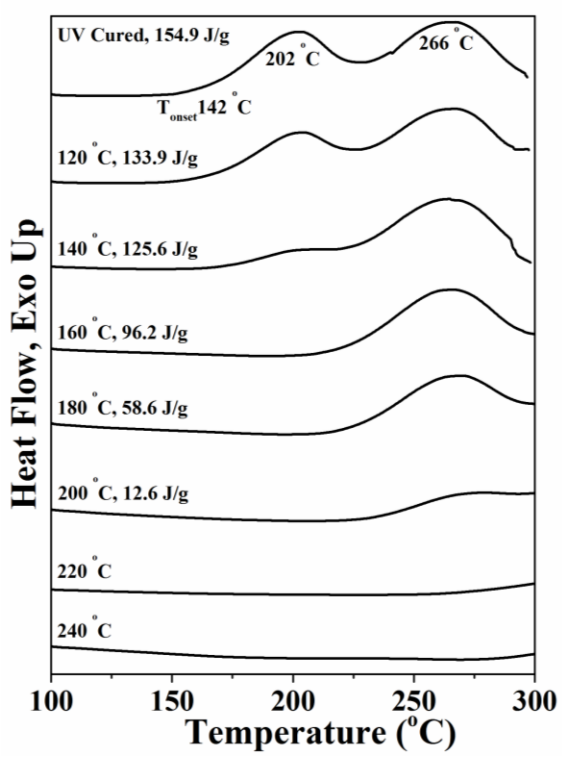

*Figure 6***.** DSC thermograms of B-allyl-PETMP after each stage of cure.

The total heat of polymerization was 154.9 J/g. The first exotherm recorded at lower temperature can be attributed predominately to the thermal polymerization of the residual allyl functional groups within the network. Thermal polymerization of the N-allyl group is known to occur at lower temperature and the results shown are consistent with previously reported thermal polymerization of B-allyl.[17, 38] The second exotherm can be attributed to the polymerization of residual fraction of benzoxazine functional groups within the thiol-ene network. The presence of the thiol-ene network restricts the mobility of the benzoxazine units and shifts the second exotherm maximum to 266 °C – a higher temperature range than typically observed for non-functionalized benzoxazine monomers.

As shown in Figure 8, the first exotherm gradually decreases and disappears after the cure at 160 °C, while the second exotherm is no longer observed after the cure at 220 °C.

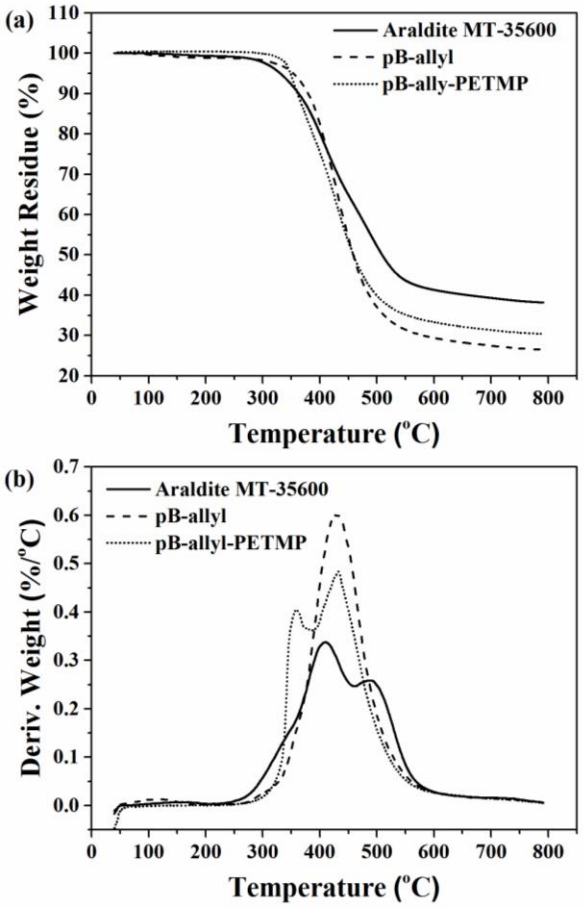

Figure 7. a) TGA degradation profiles and b) derivatives of pB-allyl, pB-allyl-PETMP and Araldite MT- 35600.

Thermal stability of dual cure hybrid networks

Figure 7 shows the results of thermogravimetric analysis for pB-ally-PETMP and pB-allyl, compared with a commercially available polybenzoxazine derived from Huntsman's aniline-based bis-benzoxazine (Araldite® MT-35600). The data are also summarized in Table 1. The 5 % ($T_{5\%}$) and 10 % ($T_{10\%}$) weight loss temperatures of pB-allyl-PETMP were 347 °C and 360 °C, respectively. These values were lower in

comparison to pB-allyl which showed $T_{5\%}$ and $T_{10\%}$ temperatures at 353 °C and 379 °C, respectively.

Table 1.

TGA analysis of dual cure hybrid network pB-allyl-PETMP, thermal cured pB-allyl and thermal cured Araldite MT-35600

Sample	**$T_{5\%}$ (°C)[a]**	**$T_{10\%}$ (°C)[b]**	**Char Yield (800 °C)**
pB-allyl	353	379	26
pB-allyl-PETMP	347	360	31
Araldite MT-35600	330	362	38

[a] Temperature at which 5% weight loss occurs; [b] Temperature at which 10% weight loss occurs

In the thermally cured pB-allyl network, the cross-linking of the allyl group augments the thermal stability by preventing the loss of Mannich bridge during the early stages of decomposition of polybenzoxazine,[39] whereas in the hybrid thiol-ene benzoxazine network, incorporation of the aliphatic PETMP significantly reduces the aromatic content within the network and likely contributes to the lower thermal stability of the hybrid network. Both pB-allyl-PETMP and pB-allyl showed improved onset of degradation in comparison to the Araldite® MT-35600. The char yield at 800 °C for pB-allyl-PETMP (31 %) was slightly more than that of pB-allyl (26 %). This increase can be attributed to the sulfur content in the pB-allyl-PETMP network; sulfur is known to promote char formation upon thermal degradation of sulfur-containing polymers.[40-41] The char yields of pB-allyl-PETMP and pB-allyl were both lower than the aniline-based bis-benzoxazine (Araldite® MT-35600) owing to the presence of aliphatic crosslinks and a reduction in aromatic content of the polymer network. While lower char yields for the hybrid thiol-ene benzoxazine networks may indicate a reduction in flame resistance typically

associated with polybenzoxazines, the hybrid approach improves film processability and enables tailoring of thermomechanical properties as discussed in the TMA section.

Thermomechanical Analysis of pB-allyl-PETMP

Thermomechanical transitions of the dual-cured thiol-ene/polybenzoxazine networks were investigated using dynamic mechanical analysis in tension mode and thermomechanical analysis in penetration mode. DMA was used to obtain storage (E') and loss moduli (E") as a function of temperature. The ratio E"/E' of the loss and storage moduli gives tan δ, a damping term, which relates the energy dissipation relative to the energy stored in the material upon periodic deformation. The glass transition temperature (T_g) was determined from the peak maximum of the tan δ curve. Figure 8 shows the temperature dependence of the tan delta (Figure 8a) and storage modulus (Figure 8b) for the UV cured B-allyl-PETMP and the dual cured pB-allyl-PETMP. Prior to thermal ring-opening polymerization of the benzoxazine, the UV cured B-allyl-PETMP network showed a T_g at 33 °C, which is comparable to the T_g of a pure thiol-ene bisallyl-BPA-PETMP network at 40 °C. The bisallyl-BPA-PETMP network is derived from a structurally similar bisphenol-A based diallyl ether derivative – a derivative that only undergoes radical thiol-ene polymerization and is shown for comparison. The tan δ curve for the B-allyl-PETMP network is broader than that of the bisallyl-BPA-PETMP material due to the thiol-benzoxazine ring-opening reaction as previously discussed. Upon thermal cure of the B-allyl-PETMP network, a broad glass transition was observed at 150 °C from the maximum of the tan δ curve. As expected, the T_g value for pB-allyl-PETMP is much higher than transitions typically reported for pure thiol-ene networks (i.e. bisallyl-BPA-PETMP), but lower than that of the pure, conventional polybenzoxazine

thermosets due to the hybrid composition of the network (i.e. flexible thioether and rigid polybenzoxazine constituents).

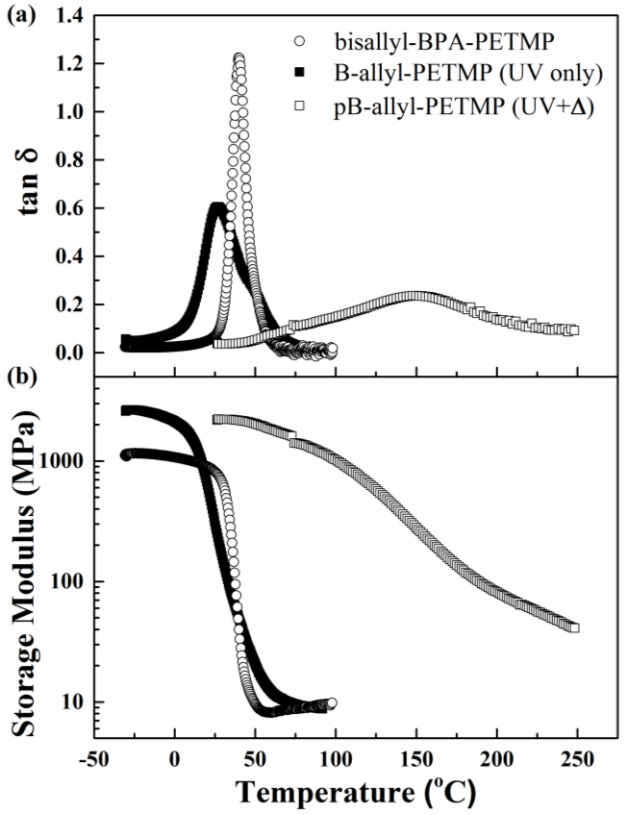

Figure 8. Dynamic mechanical analysis showing (a) tan delta versus temperature and (b) storage modulus versus temperature for the thiol/benzoxazine UV cured B-allyl-PETMP network (■), thiol/benzoxazine dual cured pB-allyl-PETMP network (□), and pure thiol-ene UV cured bisallyl-BPA-PETMP network (○). The bisallyl-BPA-PETMP network is structurally similar to B-allyl-PETMP and is shown for comparative purposes.

For example, the T_g of the thermally cured Araldite® MT-35600 and pB-allyl material have been reported as 180 °C and 322 °C, respectively.[17, 42] The broadness of the thermal transition for pB-allyl-PETMP may be attributed to network heterogeneity which results in a broad distribution of mobilities or relaxation times. The heterogeneity arises from the ring-opening of the benzoxazine with the thiol – a side reaction previously discussed in section 3.2. As shown in Figure 8b, the storage moduli for B-allyl-PETMP and pB-allyl-PETMP are 2.5 GPa (-30 °C) and 2.2 GPa (35 °C). The storage modulus for B-ally-

PETMP decreased sharply at 5 °C and showed a rubbery modulus of 9.4 MPa at 90 °C, similar to that of the pure thiol-ene bisallyl-BPA-PETMP material. The storage modulus for pB-allyl-PETMP showed a gradual decrease from 2.2 GPa at low temperature (ca. 35 °C) to 41 MPa at higher temperature (ca. 250 °C) approaching the rubbery plateau regime. Albeit higher than the UV cured B-allyl-PETMP, the low elastic modulus and hence low cross-linking density is indicative of a more loosely bound network arising from incomplete cross-linking associated with the side reaction of benzoxazine with thiol. The thermomechanical analysis curves for pB-allyl-PETMP and pB-allyl are shown in Figure 9.

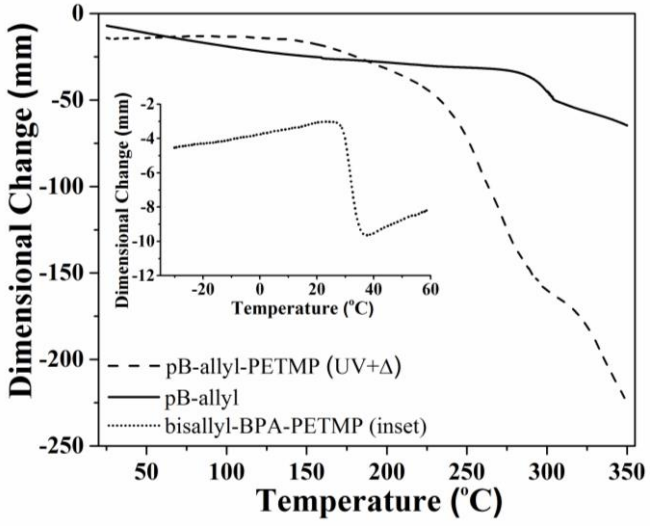

Figure 9. TMA curves of pB-allyl and pB-allyl-PETMP. The inset shows the TMA curve for the bisallyl-BPA-PETMP network.

A slight expansion of the pB-allyl-PETMP film was noted before a negative dimensional change (penetration) occurs at 156 °C; this transition correlates well with the T_g measured with DMA. At higher temperature (240 °C), a second negative dimensional change was observed further indicating the structural heterogeneity of the network. The softening temperature of pB-allyl at 270 °C was much higher than the pB-allyl-PETMP system due to the increased rigidity and cross-linking of the allyl groups and absence of

the flexible PETMP constituent. For comparison, the TMA curve for the bisallyl-BPA-PETMP network is shown in the Figure 9 inset. Bisallyl-BPA-PETMP showed a much lower softening temperature (ca. 29 °C) consistent with DMA analysis and typical for a pure thiol-ene network. TMA of B-allyl-PETMP could be obtained due to thermal curing during the measurement resulting in adhesion of the material to probe.

Conclusions

Hybrid dual-cure polymer networks were synthesized by combining thiol-ene photopolymerization with thermal ring-opening polymerization of benzoxazines. Real-time FTIR conversion studies showed that less than quantitative conversion of thiol and allyl functional groups was achieved during the radical-mediated thiol-ene photopolymerization. Non-stoichiometric consumption of thiol and allyl functional groups results from a competing nucleophilic ring-opening thiol-benzoxazine reaction with the radical-mediated thiol-ene reaction. These competing reactions ultimately yield a heterogeneous polymer network following the sequential thermal ring-opening polymerization the benzoxazines. Nonetheless, thermomechanical analysis of the hybrid networks showed the achievement of a high glass transition temperature (150 °C); one of the highest glass transitions reported to date for a thiol-ene based material. The hybrid polymer networks exhibited good thermal stability and could easily be processed into thin films by spin-coating (Figure A4, Appendix A) the resin prior to the photopolymerization and thermal cure process. Work is underway to reduce the occurrence of the competing thiol reactions, which will lead to more well-defined polymer networks with tunable thermal and mechanical properties.

Acknowledgments

The authors gratefully acknowledge financial support from the National Science Foundation (NSF CAREER DMR-1056817) and the Office of Naval Research (Award N00014-07-1-1057). The authors thank the Thames-Rawlins Research Group (Dr. Pirro Cipi and Dr. Jeremy Swanson) for help with DMA and TMA measurements, and Dr. Chris Comer for assistance with RTIR measurements. The authors thank Huntsman Advanced Materials for the kind donation of Araldite® benzoxazine resins.

References

1. Hoyle, C.; Lee, T.; Roper, T., Thiol-enes: Chemistry of the past with promise for the future. *J. Polym. Sci. A: Polym. Chem.* **2004,** *42* (21), 5301-5338.
2. Hoyle, C. E.; Bowman, C. N., Thiol–Ene Click Chemistry. *Angewandte Chemie International Edition* **2010,** *49* (9), 1540-1573.
3. Hoyle, C. E.; Lowe, A. B.; Bowman, C. N., Thiol-click chemistry: a multifaceted toolbox for small molecule and polymer synthesis. *Chem. Soc. Rev.* **2010,** *39* (4), 1355-1387.
4. Cramer, N. B.; Scott, J. P.; Bowman, C. N., Photopolymerizations of Thiol−Ene Polymers without Photoinitiators. *Macromolecules* **2002,** *35* (14), 5361-5365.
5. Carioscia, J. A.; Schneidewind, L.; O'Brien, C.; Ely, R.; Feeser, C.; Cramer, N.; Bowman, C. N., Thiol-norbornene materials: Approaches to develop high Tg thiol-ene polymers. *J. Polym. Sci. A: Polym. Chem.* **2007,** *45* (23), 5686-5696.
6. Li, Q.; Zhou, H.; Wicks, D.; Hoyle, C., Thiourethane-based thiol-ene high T-g networks: Preparation, thermal, mechanical, and physical properties. *J. Polym. Sci. A: Polym. Chem.* **2007,** *45* (22), 5103-5111.
7. Chan, J. W.; Shin, J.; Hoyle, C. E.; Bowman, C. N.; Lowe, A. B., Synthesis, Thiol−Yne “Click” Photopolymerization, and Physical Properties of Networks Derived from Novel Multifunctional Alkynes. *Macromolecules* **2010,** *43* (11), 4937-4942.
8. Carioscia, J.; Stansbury, J.; Bowman, C., Evaluation and control of thiol-ene/thiol-epoxy hybrid networks. *Polymer* **2007,** *48* (6), 1526-1532.
9. Colucci, G.; Mana, S.; Conzatti, L.; Sangermano, M., Hybrid organic-inorganic

silicate/thiol-ene photocured coatings. *Surf. Coat. Tech.* **2012,** *206* (10), 2719-2724.

10. Schreck, K. M.; Leung, D.; Bowman, C. N., Hybrid Organic/Inorganic Thiol–Ene-Based Photopolymerized Networks. *Macromolecules* **2011,** *44* (19), 7520-7529.
11. Sparks, B. J.; Kuchera, T. J.; Jungman, M. J.; Richardson, A. D.; Savin, D. A.; Hait, S.; Lichtenhan, J.; Striegel, M. F.; Patton, D. L., Cyclic tetravinylsiloxanetetraols as hybrid inorganic-organic thiol-ene networks. *J. Mater. Chem.* **2012,** *22* (9), Thiol-ene materials with a broad range of compositions including hybrid inorganic-organic networks.
12. Ghosh, N.; Kiskan, B.; Yagci, Y., Polybenzoxazines - New high performance thermosetting resins: Synthesis and properties. *Prog. Polym. Sci.* **2007,** *32* (11), 1344-1391.
13. Hatsuo, I.; Tarek, A., *Handbook of Benzoxazine Resins*. Elsevier: Amsterdam, 2011.
14. Takeichi, T.; Kawauchi, T.; Agag, T., High Performance Polybenzoxazines as a Novel Type of Phenolic Resin. *Polymer Journal* **2008,** *40* (12), 1121-1131.
15. Yagci, Y.; Kiskan, B.; Ghosh, N. N., Recent Advancement on Polybenzoxazine-A Newly Developed High Performance Thermoset. *J. Polym. Sci. A: Polym. Chem.* **2009,** *47* (21), 5565-5576.
16. Burke, W. J., *J. Am. Chem. Soc.* **1949,** *71*, 609-612.
17. Agag, T.; Takeichi, T., Synthesis and characterization of novel benzoxazine monomers containing allyl groups and their high performance thermosets.

Macromolecules **2003,** *36* (16), 6010-6017.

18. Aydogan, B.; Sureka, D.; Kiskan, B.; Yagci, Y., Polysiloxane-containing benzoxazine moieties in the main chain. *J. Polym. Sci. A: Polym. Chem.* **2010,** *48* (22), 5156-5162.
19. Huang, K.-W.; Kuo, S.-W., High-performance nanocomposites derived from allyl-terminated benzoxazine and octakis(propylglycidyl ether) polyhedral oligomeric silsesquioxane. *Polym. Compos.* **2011,** *32* (Copyright (C) 2012 American Chemical Society (ACS). All Rights Reserved.), 1086-1094.
20. Chernykh, A.; Agag, T.; Ishida, H., Effect of Polymerizing Diacetylene Groups on the Lowering of Polymerization Temperature of Benzoxazine Groups in the Highly Thermally Stable, Main-Chain-Type Polybenzoxazines. *Macromolecules* **2009,** *42* (14), 5121-5127.
21. Agag, T.; Takeichi, T., Novel benzoxazine monomers containing p-phenyl propargyl ether: Polymerization of monomers and properties of polybenzoxazines. *Macromolecules* **2001,** *34* (21), 7257-7263.
22. Brunovska, Z.; Ishida, H., Thermal study on the copolymers of phthalonitrile and phenylnitrile-functional benzoxazines. *J. Appl. Polym. Sci.* **1999,** *73* (14), 2937-2949.
23. Agag, T.; Takeichi, T., Preparation, characterization, and polymerization of maleimidobenzoxazine monomers as a novel class of thermosetting resins. *J. Polym. Sci. A: Polym. Chem.* **2006,** *44* (4), 1424-1435.
24. Chaisuwan, T.; Ishida, H., High-performance maleimide and nitrile-functionalized benzoxazines with good processibility for advanced composites applications. *J.*

Appl. Polym. Sci. **2006,** *101* (1), 548-558.

25. Ishida, H.; Ohba, S., Synthesis and characterization of maleimide and norbornene functionalized benzoxazines. *Polymer* **2005,** *46* (15), 5588-5595.
26. Jin, L.; Agag, T.; Ishida, H., Bis(benzoxazine-maleimide)s as a novel class of high performance resin: Synthesis and properties. *Eur. Polym. J.* **2010,** *46* (2), 354-363.
27. Jin, L.; Agag, T.; Yagci, Y.; Ishida, H., Methacryloyl-Functional Benzoxazine: Photopolymerization and Thermally Activated Polymerization. *Macromolecules* **2011,** *44* (4), 767-772.
28. Koz, B. K., B.; Yagci, Y., *Polym Bull* **2011,** *66*, 165-174.
29. Kiskan, B.; Aydogan, B.; Yagci, Y., Synthesis, characterization, and thermally activated curing of oligosiloxanes containing benzoxazine moieties in the main chain. *J. Polym. Sci. A: Polym. Chem.* **2009,** *47* (3), 804-811.
30. Chernykh, A.; Agag, T.; Ishida, H., Synthesis of linear polymers containing benzoxazine moieties in the main chain with high molecular design versatility via click reaction. *Polymer* **2009,** *50* (2), 382-390.
31. Nagai, A. K., Y.; Wang, X. S.; Omura, M.; Sudo, A.;; Nishida, H. K., E.; Endo, T. , *J. Polym. Sci. A: Polym. Chem.* **2008,** *46*, 2316-2325.
32. Lu, C.; Su, Y.; Wang, C.; Huang, C.; Sheen, Y.; Chang, F., Thermal properties and surface energy characteristics of interpenetrating polyacrylate and polybenzoxazine networks. *Polymer* **2008,** *49* (22), 4852-4860.
33. Beyazkilic, Z.; Kahveci, M. U.; Aydogan, B.; Kiskan, B.; Yagci, Y., Synthesis of polybenzoxazine precursors using thiols: Simultaneous thiol–ene and ring-

opening reactions. *Journal of Polymer Science Part A: Polymer Chemistry* **2012,** *50* (19), 4029-4036.

34. Gorodisher, I.; DeVoe, R. J.; Webb, R. J., Chapter 11 - Catalytic Opening of Lateral Benzoxazine Rings by Thiols. In *Handbook of Benzoxazine Resins*, Hatsuo, I.; Tarek, A., Eds. Elsevier: Amsterdam, 2011; pp 211-234.

35. Agag, T.; Jin, L.; Ishida, H., A new synthetic approach for difficult benzoxazines: Preparation and polymerization of 4,4'-diaminodiphenyl sulfone-based benzoxazine monomer. *Polymer* **2009,** *50* (25), 5940-5944.

36. Ishida, H. Preparation of benzoxazine compounds in solventless systems. 5543516, 1996.

37. Mollah, M. S. I.; Seo, D. W.; Islam, M. M.; Lim, Y. D.; Cho, S. H.; Shin, K. M. O. O.; Kim, J. H.; Kim, W. G., Synthesis and Characterization of Grafted Silicone Polycarbonates. *J. Macromol. Sci. A* **2011,** *48* (5), 400-408.

38. (a) Andre, S.; Guida-Pietrasanta, F.; Rousseau, A.; Boutevin, B.; Caporiccio, G.; , *J. Polym. Sci., Part A: Polym. Chem.* **2000,** (38), 2993-3003.

39. Low, H. Y.; Ishida, H., *Polymer* **1999,** *40*, 4365-4376.

40. Borah, J.; Lin, G.; Wang, C., Hyperbranched polymers as novel flame retardant material. *Adv. Mat. Res.* **2010,** *87-88*, 271-275.

41. Deng, Y.; Wang, Y.-Z.; Ban, D.-M.; Liu, X.-H.; Zhou, Q., Burning behavior and pyrolysis products of flame-retardant PET containing sulfur-containing aryl polyphosphonate. *J. Anal. Appl. Pyrol.* **2006,** *76* (1–2), 198-202.

42. Ishida, H.; Allen, D. J., Physical and mechanical characterization of near-zero shrinkage polybenzoxazines. *J. Polym. Sci. A: Polym. Phys.* **1996,** *34* (6), 1019-1030.

CHAPTER IV

DEVELOPMENT OF DUAL-CURE HYBRID COVALENTLY CROSSLINKED NETWORKS OF POLYNORBORNENE AND POLYBENZOXAZINES

Introduction

Thermosetting resins have long been in the forefront in development of composites for the fabrication of high-performance aerospace and electrical engineering structural components. Their significance arises from a large number of advantageous properties such as lightweight, high strength, high stiffness, good chemical resistance and good corrosion resistance. With the aforementioned features, the versatility and accessibility of tailor made polymers becomes an added advantage as it broadens the scope of applications. In this aspect, the olefin metathesis chemistry such as Ring Opening Metathesis Polymerization (ROMP) has emerged as a powerful tool towards the synthesis of macromolecules with wide range of complex architectures.[1-3] ROMP follows a catalytically triggered, chain growth mechanistic pathway, which is thermodynamically driven by the relief of ring strain - converting strained cyclic olefins to linear polymers containing olefins in the backbone.[4] Initiation occurs by the formation of metallocyclobutane intermediate via [2+2]-cycloaddition, which is facilitated by the co-ordination between a transition metal alkylidene complex with the cyclic olefin. Subsequent cycloreversion of the intermediate yields a new metal alkylidene centre, which propagates by inserting new monomers, until the polymerization ceases either by the monomer consumption or addition of an external reagent. The degree of ROMP polymerization is determined by several parameters including- monomer composition and functionality, catalyst activity and concentration, experimental conditions – solvent,

temperature and atmospheric conditions (oxygen, moisture). ROMP reactions, initiated by well-defined ruthenium-based Grubbs catalysts are associated with high metathesis activity, functional group tolerance and stability under reaction conditions (solvents, air and moisture).[5-9] The aforementioned advantages of Grubbs catalyst enable access to a wide variety of polymeric and co-polymeric materials with advanced topologies for potential applications. From the material-processing standpoint, ROMP offers several advantages including long shelf life, low monomer viscosity and volatility, fast polymerization, and low shrinkage upon polymerization. A variety of well-defined linear and cross-linked materials, possessing a broad range of tailorable material properties have been developed using ROMP mixtures of monofunctional and bifunctional cyclic olefin monomers.[10,11] ROMP thermosetting materials possessing cyclic olefins in their backbone are associated with numerous advantageous properties including high glass transition, high optical transparency, excellent chemical and electrical resistance, and superior thermal stability (> 400 °C).

Another genre of widely studied and versatile class of non-halogen based thermosetting resins is polybenzoxazines, which offer excellent high performance replacements for conventional phenolic and epoxy resins, while retaining their advantageous properties.[12-15] Polybenzoxazines can undergo thermally activated, ring opening addition reaction under catalyst-free conditions, which renders them excellent processing advantages including no release of volatiles or void formation, limited volumetric shrinkage, and excellent ambient temperature shelf-life stability. However, despite all, they suffer from brittleness, making them difficult to handle and process into mechanically robust thin films.

To date, the incorporation of polybenzoxazines in a dual-curable hybrid system has limitedly been established. The dual-cure hybrid methodology utilizing two or more orthogonal curing mechanisms affords sequentially processable films with an access to a broad range of tailorable material properties. Dual-cure interpenetrating networks (IPNs) incorporating benzoxazine with acrylates[16] or urethane acrylates[17] have been developed *via* sequentially addressable UV photo-polymerization of acrylates and thermally initiated polymerization of benzoxazines. The resulting IPNs possessed an advanced set of hybrid material properties, however were largely dependent on the presence of hydrogen bond forming groups to establish homogeneity between the networks. Unlike IPNs, a covalently cross-linked hybrid network - which is derived from the same monomer bearing both the cross-linkable functionalities offers improved phase homogeneity and reaction kinetics at a molecular level. Sponton et al.[18] developed polybenzoxazine-polysiloxane hybrid network from a dually functional siloxane bearing benzoxazine monomer – first a partial cured polysiloxane network was formed utilizing a sol-gel process, which consists of hydrolysis and condensation, followed by the thermally activated benzoxazine polymerization. The resultant homogenous hybrid materials showcased superior thermo-mechanical properties compared to that of a typical polybenzoxazine. Recently, our group[19] developed a dual-cure hybrid polybenzoxazine network consisting of a primarily formed UV-induced thiol-ene network which templates a secondary polybenzoxazine network. The covalently linked components of low modulus thiol-ene and high modulus polybenzoxazines afforded single, high T_g thiol-ene networks (~150 °C), while the sequential nature of network formation promoted ease of handling and processing of the polybenzoxazine thermosetting resins. In the current work, we have extended the dual-cure hybrid

methodology to combine ROMP and benzoxazine curing chemistries for developing a hybrid polynorbornene-polybenzoxazine network. Tasdelen et al.[20] synthesized linear benzoxazine side-chain functional polyoxnorbornene precursors utilizing ROMP curing technique - which upon subsequent thermally induced oxazine curing resulted in a cross-linked network with superior thermal properties. Although no thermo-mechanical properties were reported, the authors showed the feasibility of developing a dual-cure hybrid system based on ROMP and benzoxazine curing processes.

Our approach, as illustrated in Scheme 8, relies on the use of a multifunctional, dually polymerizable monomer possessing both bis-norbornene and bis-benzoxazine moieties within the same molecule. The two orthogonal cure processes- catalytically triggered ROMP curing of norbornene (25 °C – 160 °C) followed by benzoxazine ring-opening polymerization (~ 200 °C) were systematically addressed on the account of relative differences in the cure chemistry and kinetics. Norbornene functional benzoxazine monomer (Bz-Nor) was separately blended with two co-reactive ROMP monomers- DCPD and ENB at varying concentrations, each differing in their reactivity and cross-linkable functionality. The goal of this study is aimed towards establishing structure-property relationships by studying the effect of a variety of parameters including catalyst concentration, co-monomer type and co-monomer concentration on the network formation, structural composition and thermo-mechanical properties. Dual-cure covalently linked hybrid material derived from polynorbornene and polybenzoxazine networks combine the attributes of ROMP curing chemistry (fast polymerization, self-sustaining, no release of volatiles, excellent heat and chemical resistance, high thermal stability) and polybenzoxazines (catalyst-free polymerization, high glass transition temperature, excellent flame retardancy, low water retention), yielding high T_g materials

with excellent thermal stability for use as - structural matrix composites in aerospace, naval applications, flame retardant materials, and printed circuit boards for electronic applications.

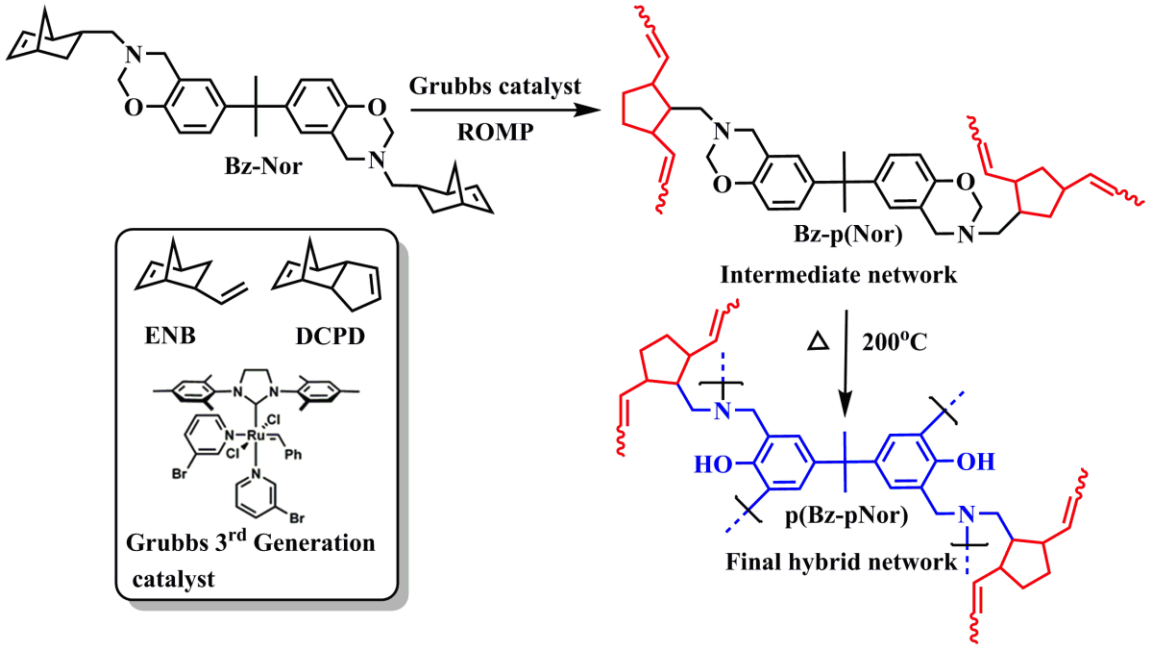

Scheme 8. Schematic representation of the methodology for dual-cure hybrid polynorbornene/polybenzoxazine networks utilizing thermal ROMP curing and thermally activated ring-opening addition reaction of benzoxazines.

Experimental

Materials

All solvents and reagents were purchased at the highest purity available from Sigma Aldrich or Fischer Scientific and were used as received unless otherwise stated. DCPD and 5-norbornene-2-carbonitrile were received as a mixture of exo- and endo-isomers from Sigma Aldrich Company. Araldite MT®-35600 was obtained from Huntsman Advanced Materials as a complimentary sample. Grubbs third generation catalyst was synthesized according to the published procedure reported elsewhere.[21] The abbreviations used in our study are as follows: (1) Bz-Nor and p(Bz-Nor) – norbornyl

functional benzoxazine monomer and corresponding polybenzoxazine network (2) Bz-Nor:DCP / Bz-Nor:ENB – uncured co-monomer mixtures of Bz-Nor and DCPD/ENB (3) p(Bz-pNor:DCP) and p(Bz-pNor:ENB) – the dual-cured hybrid network (thermal ROMP + thermal activated ROP of benzoxazine) of Bz-Nor with DCPD and ENB, respectively. (4) p(DCPD) and p(ENB) – ROMP cured polymers of dicyclopentadiene and ethylidene norbornene, respectively.

Characterization

^{1}H- NMR and ^{13}C-NMR measurements were performed in deuterated chloroform ($CDCl_3$) using a Varian Mercury Plus 300 MHz NMR spectrometer operating at a frequency of 300 MHz with tetramethylsilane as an internal standard. The number of transients for ^{1}H and ^{13}C are 32 and 256, respectively. A relaxation time of 5 s was used for the integrated intensity determination of ^{1}H NMR spectra. FTIR studies were conducted using a Nicolet 8700 FTIR spectrometer with a KBr beam splitter and an MCT/A detector with a 320-500 nm filtered (λ_{max} = 365 nm) ultraviolet light source (Omnicure S1000). The catalyst powder was dissolved in a co-monomer solution of Bz-Nor and DCPD/ENB in dichloromethane (0.2 g/0.2 mL), previously maintained at 0 °C, and the solution was spin coated on a NaCl plate at 1800 rpm for 60 s. All FTIR experiments were carried out under nitrogen atmosphere. Differential scanning calorimetry (DSC) was performed on a TA instruments DSC Q200 differential scanning calorimeter at a heating rate of 10 °C /min and nitrogen flow rate of 50 mL/min. For DSC analysis, the samples were prepared by the addition of catalyst powder to a solution of monomer in dichloromethane (1.0 g/mL) with vigorous stirring over dry ice. A thin layer of solution was applied on a Teflon film to avoid bulk exothermic reaction and

subjected under vacuum for 5 min for solvent removal and to obtain the catalyzed mixture. The catalyzed mixture was crimped in T-zero hermetic aluminum pans with lids. The pans were stored in a vial over a dry ice to avoid premature curing until they were loaded into DSC cell at a standby temperature of 25 °C. Thermogravimetric analysis (TGA) was performed using a TA Instruments Q50 thermogravimetric analyzer with a platinum pan. Samples were heated at 20 °C /min from 25 °C to 800 °C under a nitrogen atmosphere. Dynamic mechanical analysis (DMA) was performed on a TA Instruments Q800 DMA in tension film mode with a heating rate of 2 °C/min from 25 °C to 350 °C at 1 Hz. Samples were prepared using a glass mold and the dimensions of a rectangular specimen were 6.4 x 5.7 x 0.75 mm (Length x Width x Thickness). An average value of three replicates of each sample was taken. Rheological measurements were performed on a strain controlled ARES rheometer (Rheometric Scientific), using a 50.0 mm parallel plate assembly in dynamic oscillation mode. A combined temperature ramp/time sweep experiments were carried out at an angular frequency of 10 rad/s and a controlled strain of 15%. For rheological studies, a catalyst concentration of 0.25 wt% for ENB and 0.5 wt% for DCPD based co-monomer system were employed. The reaction mixture was prepared by the addition of the catalyst powder to the co-monomer solution in dichloromethane (1.0 g/mL), pre-maintained at 0 ^{o}C with vigorous stirring. The sample was immediately loaded onto the plate at room temperature, ramped until 70 ^{o}C at 2 ^{o}C/min for a timeframe of 1000 s. The experimental conditions were chosen in such a way to reduce the effect of solvent evaporation during the curing stage, while getting reliable signal from the curing process. The gap between the plates (or sample thickness) was maintained at 0.5 mm during all the measurements. Gel time (t_{gel}) of the reactive co-

monomer mixtures was roughly determined at the crossover of the shear storage (G′) and loss moduli (G″) in the corresponding rheological curves.

Preparation of dual-cured polymer films

The dual cure hybrid networks were prepared by semi-sequential ring-opening metathesis polymerization of norbornene followed by thermal ring-opening polymerization of benzoxazine. Bz-Nor:DCP and Bz-Nor:ENB co-monomer mixtures were prepared separately at different co-monomer loadings of DCPD and ENB, ranging from 25 to 75 mol%. A catalyst concentration of 1.5 wt% was chosen for all compositions of Bz-Nor:DCP and Bz-Nor:ENB, unless otherwise stated. The co-monomer compositions were dissolved in dichloromethane (1.0 g/mL) and degassed by ultrasonication. To the solution of Bz-Nor:DCP, pre-maintained at 0 °C and Bz-Nor:ENB, pre-maintained in a dry ice bath (-80 °C), a solid catalyst was added with vigorous stirring to ensure complete dissolution of the catalyst and avoid premature gelation. Subsequently, the catalyzed mixture was immediately poured into a glass mold and subjected to a two-stage curing. The samples were cured at 25 °C for 1 h, 35 °C and 50 °C for 0.5 h, each and 70 °C for 2 hrs. At this stage, the partially cured network films possessed enough green strength for easy handling and cutting into desired mold specimens. The intermediate films were subsequently cured step-wise at 100 °C, 120 °C, 140 °C for 1 h each, 160 °C, 180 °C for 2 h each and 200 °C, 220 °C for 1 h each in a programmable nitrogen circulating oven. The samples were then post cured at 240 °C for 1 h in a programmable nitrogen circulating oven. Pure p(DCPD) and p(ENB) were prepared at -40 °C in a dry ice/acetonitrile cooling bath (50/50 w/w) using the cure schedule as follows: 25 °C for 1 h, 35 °C and 50 for 0.5 h each, 70 °C for 2 h, and post

cured at 170 °C for 1.5 h. It should be noted that pristine monomer (Bz-Nor) resin could not be processed into mechanically stable films for DMA characterization due to the foaming nature of monomers at the late curing stage.

Monomer synthesis

Synthesis of exo,endo-5-Norbornene-2-ylmethylamine (NorNH$_2$). Synthesis of 5-norbornene-2-methylamine was carried out using lithium aluminum hydride reduction method.[22] Lithium aluminum hydride (7.20 g, 0.189 mol) was weighed in a 500 mL round bottom flask inside a nitrogen-filled glove box, sealed and removed from the box. To this, 300.0 mL of anhydrous diethyl ether was added *via* a two-way cannula transfer and maintained at 0 ^{o}C, followed by a slow drop-wise addition of 5-norbornene-2-carbonitrile (15.00 mL, 0.126 mol) for a period of 20-30 minutes. The septum was removed and the reaction mixture was quenched by successive addition of 5 mL of deionized H_2O, 4.0 mL of 20% NaOH and 15.0 mL of deionized H_2O with stirring and continuous cooling, converting aluminium hydroxide to a water-soluble sodium aluminate residue. The ether solution was decanted from the white, granular sodium aluminate residue and residue was washed thrice with ether. The solution was dried over $MgSO_4$, filtered and the solvent was distilled out under reduced pressure to afford a colorless liquid (15.19 g, 98 %). ^{1}H-NMR (300 MHz, $CDCl_3$): δ (ppm) = 5.92-6.10 (m, 2H, -CH=CH-, **H$_2$ and H$_3$**), 2.63-2.88, 2.10 (m, 3H, -CH_2NH_2, **H$_7$**, -CH, **H$_4$**), 2.36, 1.81 (m, 1H, -CH **H$_1$**), 1.06-1.47 (m, 5H, -CH_2 **H$_5$, H$_8$**, CH **H$_6$**).

Synthesis of norbornenyl functionalized bis-benzoxazine (abbreviated as Bz-Nor). 5-norbornene-2-methylamine ($NorNH_2$) (15.20 g, 0.123 mol), bisphenol-A (14.1 g, 0.062 mol) and paraformaldehyde (7.41 g, 0.247 mol) were taken in a 250 mL round bottom

flask. The mixture was heated at 120 ^{o}C for 20 minutes and cooled to room temperature. The product was dissolved in diethyl ether (150 mL), extracted with 3N NaOH (3 × 150 mL) to remove phenolic impurities and finally washed with distilled water (3 × 150 mL). The organic layer was stirred over anhydrous magnesium sulfate, filtered over basic alumina to further remove phenolic impurities and the solvent was distilled under reduced pressure to afford a creamish solid. The product was dried under vacuum at 35 °C overnight (28.0 g, 84%). ^{1}H-NMR (300 MHz, $CDCl_3$), ppm: δ = 6.59-7.10 (m, 6H, **Aromatic-H**), 5.83-6.32 (4H, m, -CH=CH-, **H_2** and **H_3**), 4.85 (4H, s, -N-CH_2-O-, **H_{10}**), 3.95 (4H, s, -Ar-CH_2-N-, **H_9**), 1.59 (s, 6H, -CH_3, **H_{11}**).

^{13}C-NMR ($CDCl_3$) : δ = 152.03, 142.82, 126.24, 126.17, 125.47, 119.46, 115.81, 115.77 (12C, **Aromatic-C**), 137.23, 136.75, 136.67, 132.52 (4C, -CH=CH-, **C_2 and C_3)**, 82.68, 82.62 (2C, -N-CH_2-O-, **C_{10}**), 57.26 (2C, -Ar-CH_2-N-, **C_9**), 55.70 (2C, -CH_2-N, **C_7**), 50.941, 50.84 (2C, -CH_2, **C_8**), 49.53 (2C, -CH, **C_1**), 45.31 (1C, -C $(CH_3)_2$, **C_{12}**), 44.69 (2C, -$(CH_3)_2$, **C_{11}**), 42.43, 41.94, 41.71, 41.62 (2C, -CH, **C_4**), 37.44, 37.33 (2C, -CH, **C_6**), 31.49, 31.20, 30.85 (2C, -CH_2, **C_5**).

Results and Discussion

Norbornenyl functional bis-benzoxazine (Bz-Nor) cross-linker was synthesized using the Mannich condensation of Bis-phenol-A, 5-norbornene-2-methylamine and paraformaldehyde in 1:2:4 molar ratio using Ishida's solventless synthesis in melt state[23] as depicted in Scheme 9.

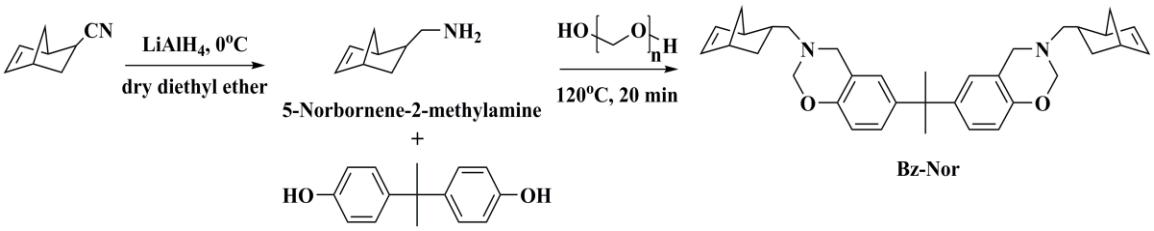

Scheme 9. Schematic representation of the synthesis of Bz-Nor.

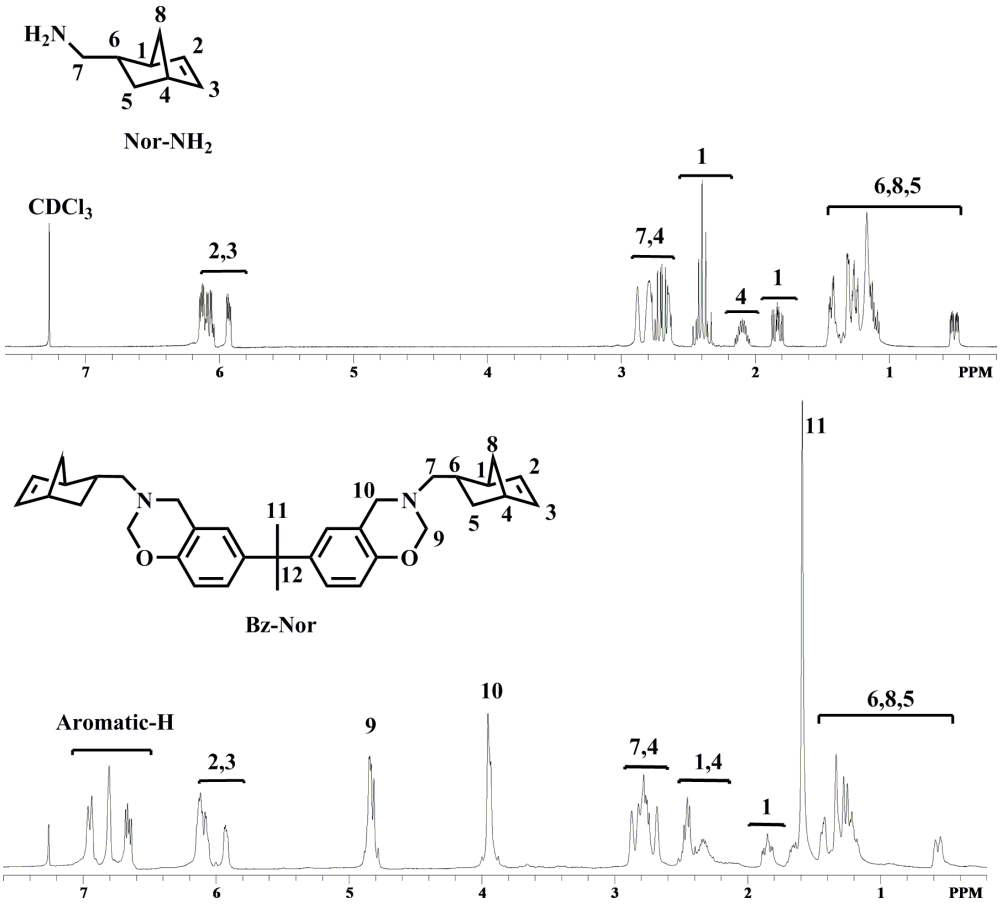

Figure 10. ^{1}H-NMR spectrum of 5-norbornene-2-methylamine (Nor-NH_2) and norbornenyl functional bis-benzoxazine (Bz-Nor).

The melt synthetic route employed afforded Bz-Nor monomer with high yield (84%) within short reaction time (20 min). The structure of the monomer was confirmed using ^{1}H-NMR analysis, as depicted in Figure 10. The formation of benzoxazine monomer was confirmed by the occurrence of two characteristics peaks corresponding to methylene

protons of the oxazine ring, -N-CH_2-O- at 4.85 ppm and Ar-CH_2-N- at 3.95 ppm. The characteristic olefin protons attached to the norbornene ring appeared as a multiplet between 5-6 ppm.

For ROMP copolymerization, commercially available DCPD and ENB comonomers were chosen due to their distinct curing kinetics and mode of polymerization. Scheme 10 illustrates the formation of intermediate ROMP cured network of Bz-Nor cross-linker blended with DCPD/ENB using Grubbs 3rd generation catalyst.

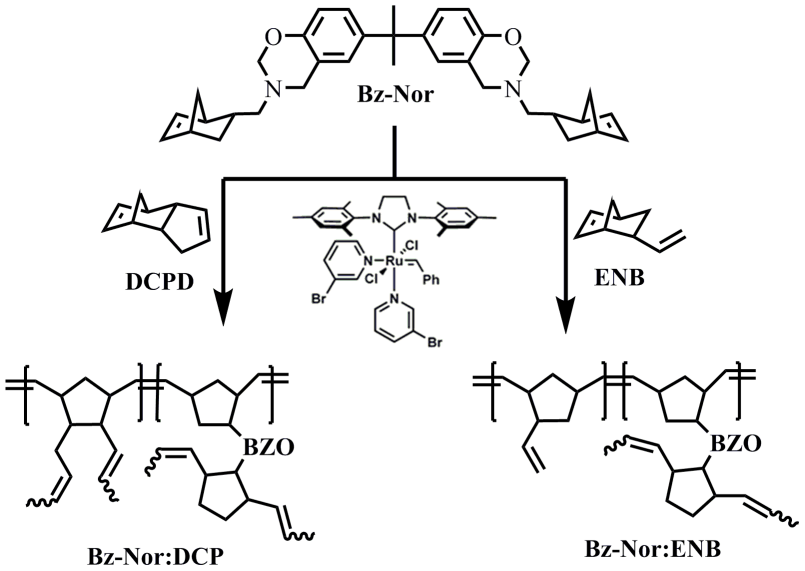

Scheme 10. Schematic representation of formation of intermediate ROMP cured network of Bz-Nor:DCP and Bz-Nor:ENB using Grubbs 3rd generation catalyst.

Dicylopentadiene (DCPD) is capable of forming highly cross-linked structure with high toughness, excellent impact strength resistance, and corrosion resistance properties.[24] The additional cyclopentene bond in DCPD is known to subsequently impart crosslinking either by olefin metathesis or olefin addition.[25] On the other hand, 5-ethylidene-2-norbornene (ENB) has much higher ROMP activity than DCPD and forms a linear polymer through ROMP.[26] These attractive features, along with their low cost and

ease of fabrication influenced our choice of co-monomers employed in this study. Our preliminary DSC studies on ROMP curing of Bz-Nor cross-linker showed that a higher extent of Bz-Nor crosslinking was favored at a much higher catalyst concentration as compared to that typically employed for DCPD and ENB monomers in literature studies.[27,28,29] Due to relatively large differences in the co-monomer reactivity and high metathesis activity of Grubbs 3rd generation catalyst, an intermediate catalyst concentration (1.5 wt%) for all compositions were chosen for this study. The reason for the choice of the aforementioned concentration was to allow time for sufficient interaction between the co-monomers to minimize the possibility of reaction induced phase separation arising due to differences in the ROMP reactivity of Bz-Nor and DCPD/ENB co-monomers. Moreover, due to the exothermic nature and rapid reaction kinetics, ROMP polymerizations are often associated with premature gelation, accompanied with incomplete catalyst dissolution; hence, the moderate use of a catalyst would facilitate a better process control either during the film fabrication process or while performing cure kinetic studies. During film formulation, the catalyst and the monomer solution were vigorously mixed so as to facilitate short initial mixing time to prevent unwanted premature exothermic reaction, particularly in the ENB or ENB-rich systems.

Thermal rheological curing studies

The time evolution of viscoelastic behavior during the ring-opening metathesis polymerization of Bz-Nor:DCP and Bz-Nor:ENB blends were investigated using parallel plate oscillatory rheometer. Lower catalyst concentrations were chosen for rheological studies so as to allow enough induction time for evaluating viscoelastic properties under the experimental conditions. Figure 11 shows the time dependence of shear storage

modulus (G') and shear loss modulus (G'') and Figure 12 shows the comparison curves of G' and Tan delta vs. time for various co-monomer mixtures of Bz-Nor:DCP. Gelation time marks the transition from viscous liquid to elastic solid with a three-dimensional (3-D) network formation, and is an important processing parameter for thermosetting resins. Gelation time for all the samples was measured as the crossover point of storage shear modulus (G') and loss shear modulus (G''). The samples containing 100% Bz-Nor monomers showed no change in the rheological values over the timescale of the experimental conditions, suggesting that the combination of longer curing time and higher temperature is needed to establish viscoelastic behavior for low reactive systems. As seen in Figure 11, in the beginning of the cure time, the initial phase of both G' and G'' is associated with low S/N ratio because of solvent evaporation, which is then followed by a gradual steady increase with time and temperature as the polymerization proceeds. The onset of gelation time was marked by the crossover of G' and G'', where tan δ equals 1, beyond which the shear storage modulus levels off upon reaching the plateau regime indicating the formation of a glassy polymer network. Although the gelation time is a frequency dependent parameter in rheological experiments, however in this study the observed gelation times are specific at the frequency used for the experiment. Nevertheless, the rheological experiments were used to study the gelation kinetics, and evaluate final plateau value of the storage modulus, which is an indication of the degree of crosslinking in the final cured film.

A drastic decrease in the gelation time from 702 to 171 s was observed with an increasing fraction of DCPD from 25 to 75 mol%, respectively. Furthermore, this trend was accompanied by faster and superior development of mechanical properties, as

observed from the slope of the shear modulus curve and limiting shear modulus value in the vitrification regime (Figure 12).

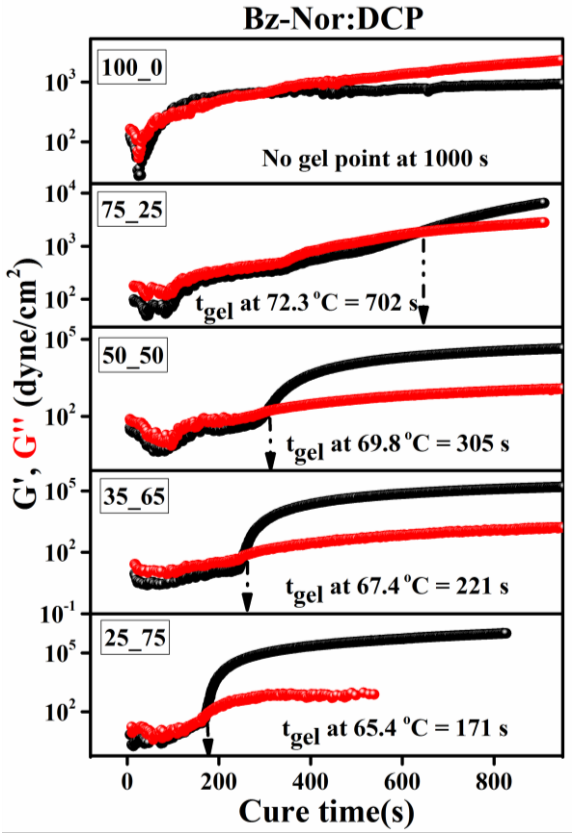

Figure 11. Rheological time-sweep experiments for ROMP curing of Bz-Nor:DCP blends using Grubbs 3rd generation initiator (0.5 wt%) ramped to 70 °C at the rate of 2 °C/min for 1000 s.

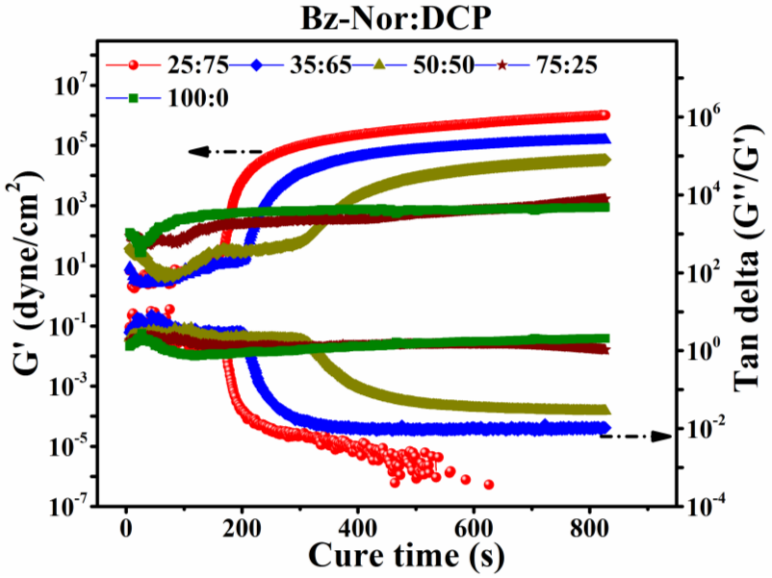

Figure 12. Comparison curves of G' and Tan delta vs. cure time for ROMP curing of Bz-Nor:DCP blends.

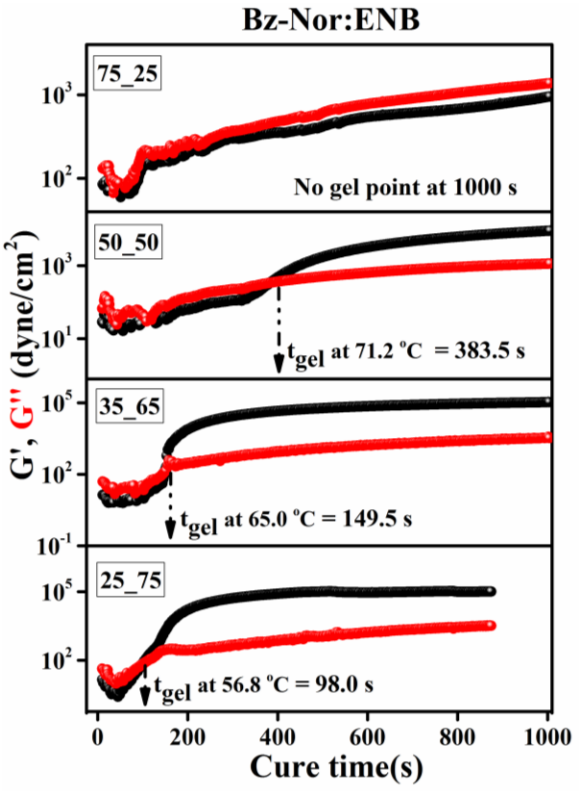

Figure 13. Rheological time-sweep experiments for ROMP curing of Bz-Nor:ENB samples using Grubbs 3rd generation initiator (0.25 wt%) ramped to 70 ^{o}C at the rate of 2 ^{o}C/min for 1000 s.

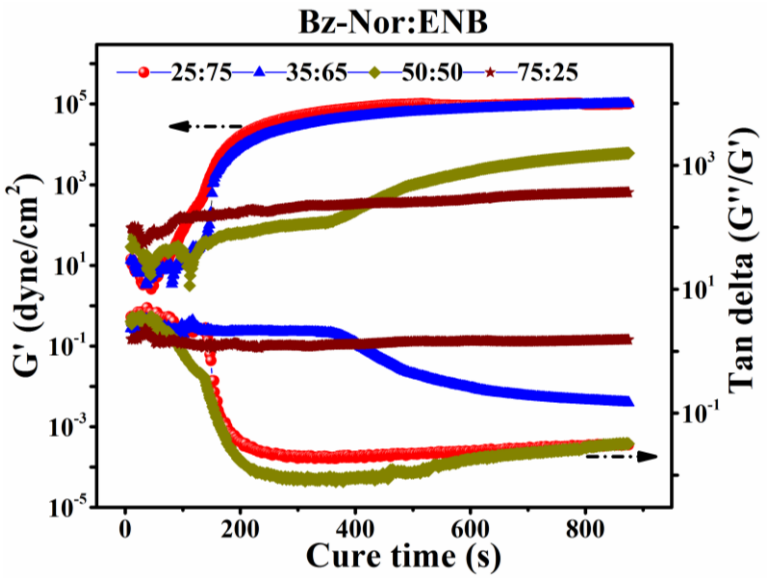

Figure 14. Comparative plots of G' and Tan delta vs. cure time for ROMP curing of Bz-Nor:ENB samples.

Dicyclopentadiene is a low viscous monomer, which can instantaneously undergo ROMP reaction with the Grubbs catalyst at room temperature. Moreover, DCPD is capable of forming a cross-linked polymer through the ROMP reaction of initial norbornene ring (more strained and active), followed by the reaction of additional crosslinking site (less strained) at a higher temperature - which aids in the network formation with more pronounced viscoelastic properties. The reactivity of DCPD plays a dominant role in determining the gelation behavior irrespective of their low crosslinkable functionality in relative to the Bz-Nor crosslinker. Bz-Nor:DCPD copolymer possessing high concentration of DCPD (75 mol%) displayed highest shear modulus value in the glassy region (~10^5 dyne/cm^2), suggesting the occurrence of greater extent of crosslinking.

Figure 13 shows the time dependence of shear storage modulus (G') and shear loss modulus (G'') and Figure 14 shows the comparison curves of G' and Tan delta vs. cure time for various co-monomer mixtures of Bz-Nor:ENB. In comparison to Bz-Nor:DCP, Bz-Nor:ENB blends possessing higher concentrations of ENB (above 50

mol%) showed rather fast gelation kinetics even at lower amount of catalyst concentration. Unlike DCPD, ENB polymerizes *via* the formation of a linear polymer, and have studied to exhibit faster cure kinetics.[29] Liu et al. reported that the inclusion of ENB in the blends of DCPD and ENB had an accelerating effect on the polymerization kinetics, even at low catalyst loadings, with increasing ENB content.[28] As seen from Figure 13, the Bz-Nor:ENB samples containing 75 mol% of Bz-Nor showed no change in viscoelastic properties under the experimental conditions employed. However, the addition of ENB co-monomer exhibited an accelerating effect on the curing behavior of Bz-Nor:ENB blends, as the gelation drastically reduced from 383.5s to 98s with an increasing ENB concentration from 50 to 75 mol%, respectively. The highest shear modulus values in the plateau regime were shown by Bz-Nor:ENB blends at 65 and 75 mol% of ENB concentration (~10^4 dyne/cm^2), implying the rigidity of the glassy viscoelastic network.

Step-curing studies: FT-IR and DSC

The dual-cure hybrid films were cured using stepped cure procedure in a nitrogen atmosphere. The polynorbornene backbone is susceptible to oxidation on the account of high density of alkenes in the polymer backbone,[30] because of which curing was conducted under inert atmospheric conditions. The step - cure method was employed so as to ensure complete removal of volatiles, and establish a good balance between low and high temperature cure, as lower stress will be induced due to the slower formation of cross-links, while a higher level of network formation will be attained as the higher temperature is reached. Based on the FT-IR and DSC step-cure curing studies, an

optimum cure schedule was designed so as to achieve the best ultimate network properties.

FTIR studies: Structural elucidation

The structure of Bz-Nor monomer was confirmed using FT-IR analysis, as shown in Figure B3 in Appendix B. The absorption peaks centered at 1230 cm^{-1} and 1030 cm^{-1}, and 1121 cm^{-1} and 864 cm^{-1} correspond to the asymmetric and symmetric stretching vibrations of C-O-C and C-N-C, respectively. The peak centered at 1322 cm^{-1} is ascribed to $–CH_2$ wagging mode of the oxazine ring. The characteristic benzoxazine peaks at 935 cm^{-1} and 1498 cm^{-1} corresponds to the out-of-plane and in-plane bending modes of C-H vibration of the benzene ring attached to the oxazine ring, respectively. Additionally, the peak at 822 cm^{-1} is due to out-of-plane C-H bending mode of tri-substituted benzene ring. The absence of bands corresponding to hydroxyl stretching frequency suggests high purity of Bz-Nor resin. The characteristic bands of the norbornene skeleton at 720 cm^{-1} with a shoulder at 714 cm^{-1}, and 1569 cm^{-1} is designated to the out-of-plane deformation of the -CH=CH- moiety and C=C stretching vibrations of the norbornene ring, respectively.

FT-IR thermal cure studies of Bz-Nor monomer was performed in an air-circulating oven using the aforementioned cure cycle and the structural evolution after each stage of cure was qualitatively monitored, as illustrated in Figure 15.

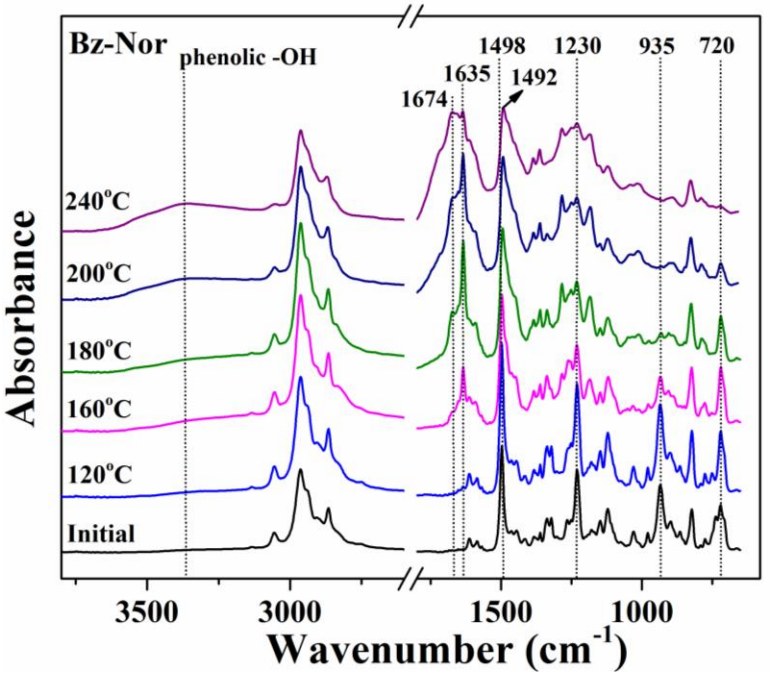

Figure 15. FT-IR spectra of thermal cure of Bz-Nor after each stage of oxidative cure.

During thermal step-cure of Bz-Nor, as the cure temperature increased, the characteristic benzoxazine peaks assigned to the tri-substituted benzene ring at 935 cm^{-1} (out-of-plane C-H bending) and 1498 cm^{-1} (in-plane C-H bending) started to decrease in intensity at 120 ^{o}C, and completely disappeared at 240 ^{o}C, indicating consumption of closed oxazine ring of benzoxazine. Furthermore, in conjunction with this decrease, the appearance of a new absorption band at 1493 cm^{-1} corresponding to the tetra substituted benzene ring, and a broad band around 3300 cm^{-1} assigned to –OH stretching vibrations of phenolic hydroxyl groups formed during oxazine ring-opening polymerization, confirmed the completion of the polymerization. Interestingly, beginning at 160 ^{o}C two new bands originated at 1636 cm^{-1} and 1674 cm^{-1} and increased in intensity as a function of cure temperature. The observed bands were previously assigned in literature as the carbonyl peaks of the substituted benzoquinones- a major oxidation product formed during UV oxidative degradation of bisphenol-A based polybenzoxazines.[31]

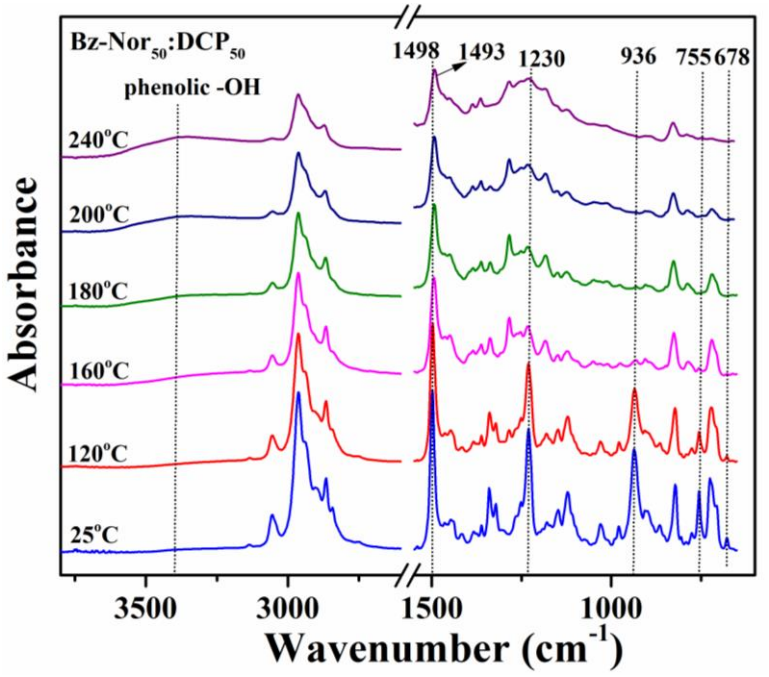

Figure 16. FT-IR spectra of dual-cure of Bz-Nor_{50}:DCP_{50} after each stage of oxidative cure.

FT-IR spectra of thermally induced two-stage crosslinking of Bz-Nor_{50}:DCP_{50} and Bz-Nor_{50}:ENB_{50} blends after each stage of oxidative cure are shown in Figure 16 and 17, respectively. The extent of ROMP polymerization of Bz-Nor and DCPD was monitored using the characteristic IR peaks of norbornene skeleton of Bz-Nor (714 cm^{-1} and 720 cm^{-1}) and DCPD (678 cm^{-1}, 708 cm^{-1} and 755 cm^{-1}), corresponding to the out-of-plane =C-H bending vibration.

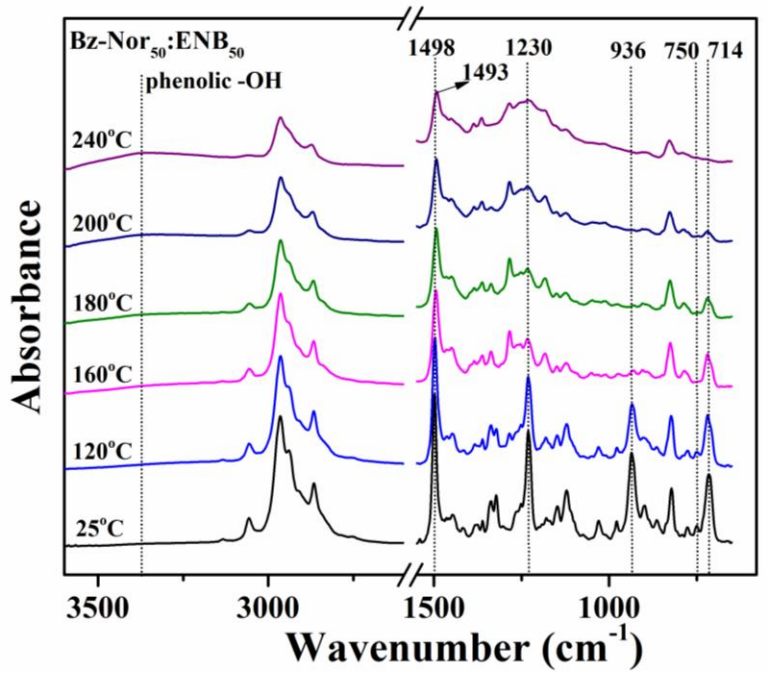

Figure 17. FT-IR spectra of dual-cure of Bz-Nor$_{50}$:ENB$_{50}$ after each stage of oxidative cure.

Similarly, for Bz-Nor:ENB blends, changes in the IR intensities of Bz-Nor and ENB (714 cm^{-1} and 750 cm^{-1}) corresponding to bending mode of =CH of norbornene ring were monitored during the thermal step-cure. As the cure stage progressed from room temperature to 180 °C, the characteristic IR bands of corresponding to C-H deformation of norbornene started to decrease in intensity, and disappeared by end of 180 °C cure cycle, confirming the formation of metathesis product. A broad peak at 720 cm^{-1} characteristic for the cis isomer of the =CH bending vibrations of polynorbornene for both Bz-Nor:DCP and Bz-Nor:ENB blends was observed.

During the second stage cure involving thermally induced ring opening polymerization of benzoxazine in Bz-Nor$_{50}$:DCP$_{50}$ and Bz-Nor$_{50}$:ENB$_{50}$ blends, the previously assigned (Figure 15) absorption peaks associated with the closed oxazine ring

completely disappeared by end of cure at 240 °C, while a new absorption peak appeared at 1493 cm^{-1}, signifying the formation of polybenzoxazine network.

DSC studies: Thermal step-curing

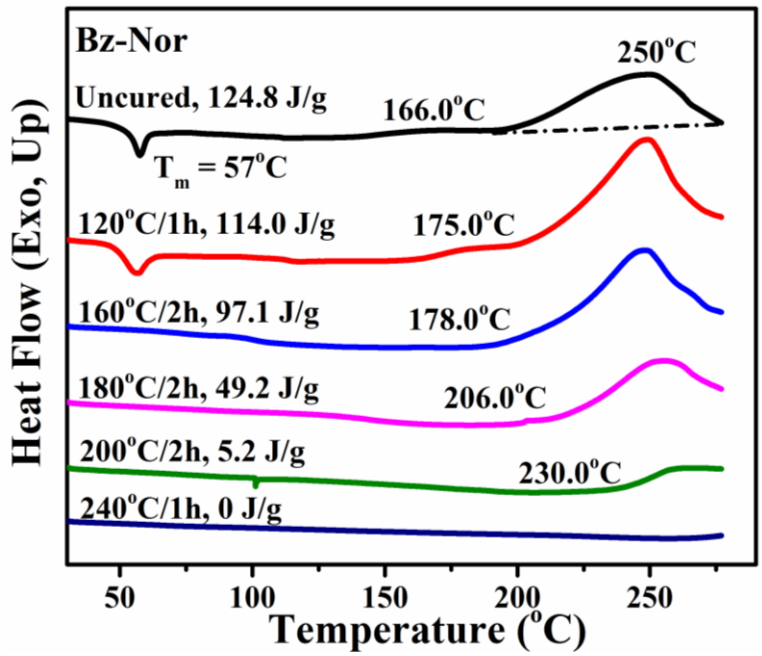

Figure 18. DSC cure studies of thermally activated ring opening polymerization of pristine Bz-Nor monomer at each stage of cure.

Figure 18 shows DSC thermal cure profile of the pristine Bz-Nor monomer at each stage of cure. Uncured Bz-Nor monomer demonstrated a typical cure exotherm corresponding to thermally activated ring-opening polymerization of benzoxazines with the onset and peak maxima at 166 °C and 250 °C, respectively. Bz-Nor showed a melting endotherm at 57 °C, and a wide gap (c.a. 110 °C) between the melting point of Bz-Nor (57 °C) and the onset of ring opening polymerization of Bz-Nor (250 °C) is an indicative of an excellent processing advantage for practical applications. A broad and asymmetric exotherm in Bz-Nor can be attributed to the fact that the presence of a small amount of phenolic oligomer impurities in the monomer resin may initiate thermally accelerated cationic ring-opening polymerization of benzoxazines at a lower temperature. Moreover,

the presence of mixtures of endo and exo-isomers of Bz-Nor, each differing in their reactivity could varyingly affect the rate of the benzoxazine polymerization.[32] The total heat of reaction for Bz-Nor, 124.8.0 J/g was comparatively lower than the typical range exhibited by polybenzoxazines in literature (150-600 J/g).[33] As seen from Figure 18, when heated above ca. 275 °C, DSC exothermic processes were flanked by baseline noise interruptions that may have resulted from evaporation of volatile cycloaliphatic amines of the cured Bz-Nor, and is clearly evidenced by TGA analysis of thermally cured p(Bz-Nor) described in the following discussion (Figure 26). Thus, the lower cure exotherm recorded for the polymerization of Bz-Nor could be a result of the interference of thermal data acquisition process by the early Mannich base degradation of p(Bz-Nor).

DSC step-cure studies showed a gradual decrease in the total heat of enthalpy (ΔH) until about 160 °C, followed by a substantial decrease at 180 °C -200 °C, until it finally disappeared after post cure at 240 °C, thereby indicating completion of cure. The total heat of polymerization of Bz-Nor reduced from 125 J/g for the uncured resin to 5.0 J/g at 200 ^{o}C.

Figures 19 and 20 represents DSC step-cure profile of thermal dual-cure processes of Bz-Nor$_{50}$:DCP$_{50}$ and Bz-Nor$_{50}$:ENB$_{50}$ blends, respectively. After initial ambient temperature cure, DSC thermogram of Bz-Nor:DCP showed two exotherms. The first exotherm with the onset at 67 ^{o}C and peak maxima at 124 ^{o}C can be primarily attributed to ROMP co-curing of the cyclic olefin units appended to the co-monomers. The 1st exotherm diminishes rapidly and disappears by the end of curing at 120 ^{o}C (1 h). The broad nature of exotherm could be attributed to the unequal reactivity of the co-monomers and their related endo- and exo-isomers. Rule and Moore [32] showed that the

kinetics of ROMP curing of exo-DCPD isomer was much faster than endo-DCPD and occurred at relatively lower temperature, primarily for steric reasons. The second exotherm – predominantly attributed to the ring-opening polymerization of benzoxazine in addition to the residual ROMP reaction appeared at a much higher temperature with the onset at 172 °C and peak maxima at 235 °C. A bimodal trend was observed in the second exotherm by the end of 70 °C cure cycle, which suggested the presence of at least two reactions in this temperature range. DSC ROMP curing studies of exo- and endo isomers of DCPD showed the occurrence of two distinct exothermic peaks for exo-DCPD, and one broad peak for endo-DCPD, wherein the first peak was attributed to ring-opening of norbornene ring (more strained) and the second peak at a higher temperature was related to metathesis of additional cyclopentene ring (less strained).[26] Thus, the existence of a bimodal curve can be related to the additional crosslinking of the cyclopentene units in DCPD occurring alongside benzoxazine polymerization. The total heat of reaction of the second exotherm gradually decreased with increase in the cure temperature, as the first peak of the bimodal curve disappeared by the end of cure at 180 °C, followed by the complete disappearance of the second peak at 240 °C, thereby confirming the completion of the polymerization.

In Figure 20, initial DSC curing of Bz-Nor_{50}:ENB_{50} blends at 25 °C revealed two distinct exothermic peaks: the first exotherm with lower onset of exotherm at 60 °C and peak maxima at 104 °C can be assigned to the ROMP co-curing of Bz-Nor and ENB, and the second exotherm, around 250 °C is ascribed to benzoxazine polymerization.

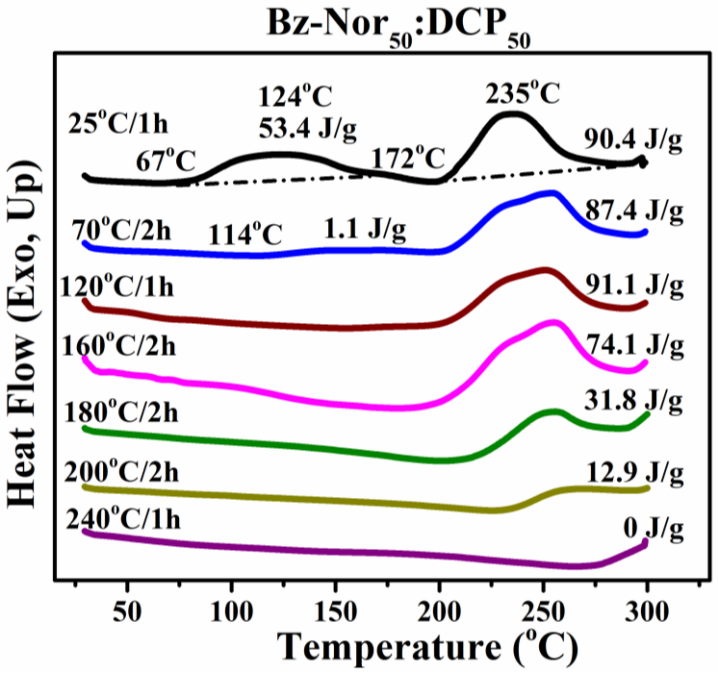

Figure 19. DSC of thermal dual-cure processes of Bz-Nor$_{50}$:DCP$_{50}$ blends at each stage of cure.

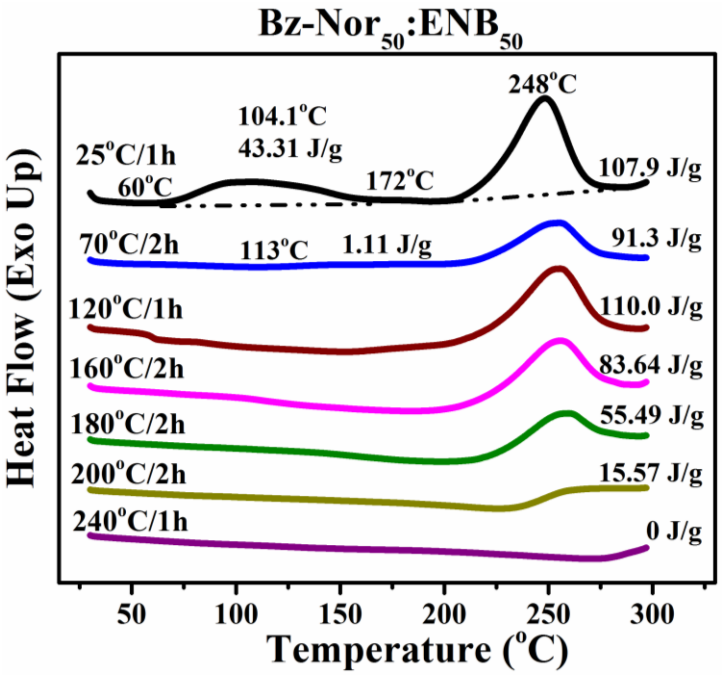

Figure 20. DSC of thermal dual-cure processes of Bz-Nor$_{50}$:ENB$_{50}$ blends at each stage of cure.

Unlike Bz-Nor:DCP blends, the appearance of a singular second exotherm in Bz-Nor:ENB can be attributed to the absence of additional crosslinking in ENB, as it possesses only one strained, active double bond. The first exotherm disappeared by end of cure at 120 °C, while the second exotherm decreased gradually until 180 °C curing cycle, followed by the complete disappearance at 240 °C, suggesting cure completion.

DSC curing studies: Effect of catalyst concentration

Figure 21 shows DSC thermograms of Bz-Nor after 10 min of cure at room temperature, and the related thermal data are shown in Table 2. Bz-Nor monomer with no catalyst exhibited a melting endotherm at 57 °C and exotherm at 250 °C, corresponding to the previously assigned thermally activated ring-opening polymerization of benzoxazine, At 0.5 wt% catalyst concentration, a small exotherm with ΔH = 8.0 J/g appeared with maxima at 137 °C corresponding to the ring-opening metathesis polymerization of norbornene. As the catalyst concentration increased, the appearance of first exotherm became more distinct with an expected rise in total heat of polymerization from 8.0 J/g (0.5 wt%) to 68 J/g (4.5 wt%), while both the onset and peak of exotherm shifted to a lower temperature. However, the extent of ROMP polymerization reached a maximum at 4.5wt% catalyst concentration, above which there was only a minimal change in the total heat of reaction. As the monomer was converted to a relatively stable polymer, the masking of benzoxazine exotherm at ca. 275 °C (as previously observed in Figure 18) was reduced.

On the other hand, the second exotherm exhibited a lower shift in the onset and peak exotherm temperature, wherein the total heat of exotherm gradually increased from 124.8 J/g (0 wt%) to 157 J/g (3.5 wt%). These observations could be attributed to the

ROMP crosslinking of residual norbornene units occurring alongside benzoxazine polymerization, which additionally contributes to the overall heat of reaction. As a higher extent of ROMP crosslinking was attained above 3.5 wt% catalyst loading, the concentration of unreacted ROMP entities reduced, thus leading to a decrease in the overall heat of reaction of the second exotherm.

DSC curing studies: Effect of catalyst concentration

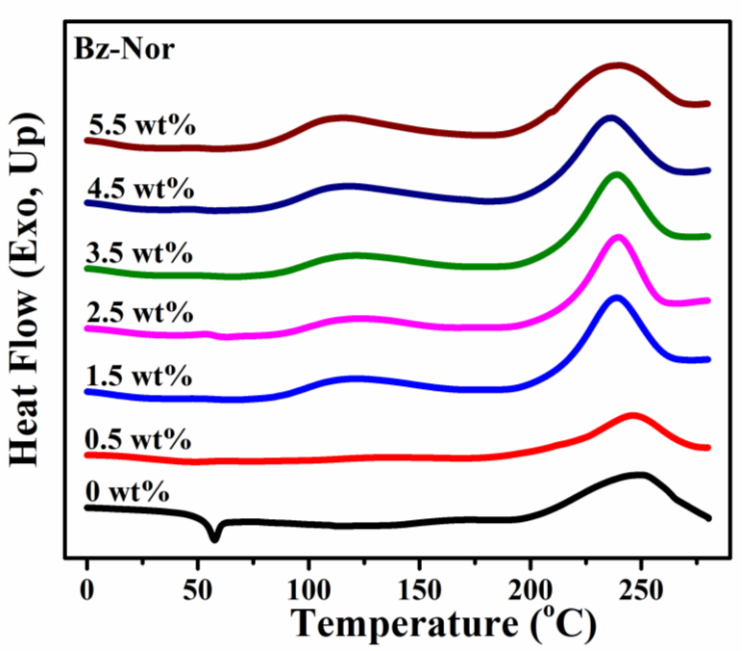

Figure 21. DSC thermal studies showing the effect of catalyst concentration on the dual-cure behavior of Bz-Nor after 10 min of cure at room temperature.

Table 2

Results of DSC thermal data of ROMP curing of Bz-Nor monomer using different catalyst loadings

	1st exotherm			2nd exotherm		
Catalyst loading (wt%)	**Onset of exotherm (°C)**	**Peak of exotherm (°C)**	**Total heat of enthalpy (ΔH, J/g)**	**Onset of exotherm (°C)**	**Peak of exotherm (°C)**	**Total heat of enthalpy (ΔH, J/g)**
0	-	-	-	166.0	249.6	124.8
0.5	76.4	136.6	8.0	172.0	246.3	125.4
1.5	71.9	124.9	19.6	184.4	240.5	139.5
2.5	71.2	123.3	41.2	184.6	239.6	149.3
3.5	69.5	120.9	52.2	180.3	239.0	157.4
4.5	67.3	116.9	68.3	179.1	236.7	146.6
5.5	61.2	115.0	74.4	176.8	239.3	132.0

DSC studies: Effect of co-monomer composition

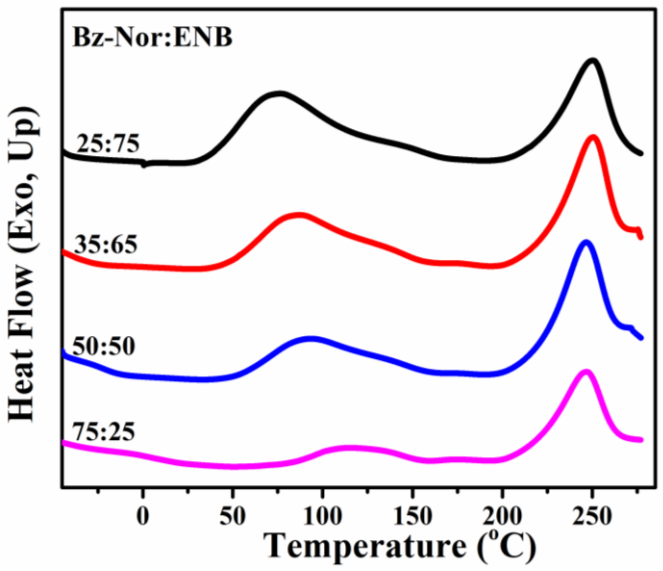

Figure 22. DSC thermograms of dual-cure of Bz-Nor:ENB samples cured for 5 mins at room temperature.

Table 3

Summary of DSC thermal data of dual-cure compositions of Bz-Nor:ENB

Sample	**1st exotherm**			**2nd exotherm**		
BzNor: ENB	**Onset of exotherm (°C)**	**Peak of exotherm (°C)**	**Total heat of enthalpy (ΔH, J/g)**	**Onset of exotherm (°C)**	**Peak of exotherm (°C)**	**Total heat of enthalpy (ΔH, J/g)**
75:25	54.4	115.6	38.5	176.1	247.0	109.8
50:50	37.7	93.5	80.3	177.4	246.6	99.6
35:65	31.2	86.6	101.6	177.6	250.4	96.3
25:75	23.3	75.7	110.9	181.2	250.4	95.9

DSC cure profiles of dual cure processes of varying compositions of Bz-Nor:ENB blends after 5 min cure at room temperature using 1.5 wt% catalyst loading are shown in Figure 22 and the corresponding DSC thermal data are summarized in Table 3. All blends of Bz-Nor:ENB exhibited two distinct exotherm - the first exotherm previously assigned to the ring-opening cross-metathesis polymerization of norbornene monomers is driven by the relief of ring strain associated with the norbornene ring. The incorporation of highly reactive ENB co-monomer led to an overall increase in the co-monomer reactivity– as both the onset and peak exotherm were shifted to a lower temperature with an increase in the total heat of reaction from 20 J/g (0% ENB) to 111 J/g (75% ENB). The second exotherm – primarily attributed to the thermal ring opening polymerization of benzoxazine and residual ROMP crosslinking – showed a slight increase in the onset of exotherm and peak maxima owing to the rigidity incurred by the primary polynorbornene crosslinks. The total heat of polymerization for the benzoxazine polymerization

decreased from 140 J/g (0% ENB) to 96 J/g (75% ENB) in relation to the reduction in the benzoxazine mole content.

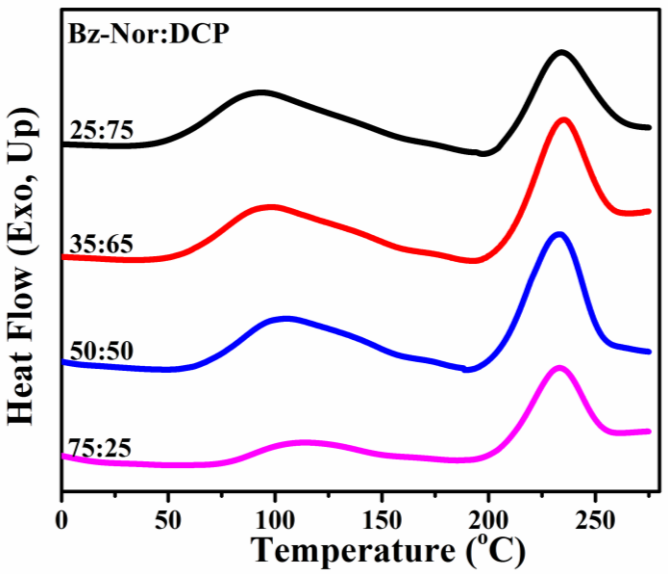

Figure 23. DSC thermograms of dual-cure of Bz-Nor:DCP samples cured for 5 min at room temperature.

Table 4

Summary of DSC thermal data of dual-cure compositions of Bz-Nor:DCP

Sample	**1st exotherm**			**2nd exotherm**		
BzNor: DCP	**Onset of exotherm (°C)**	**Peak of exotherm (°C)**	**Total heat of enthalpy (ΔH, J/g)**	**Onset of exotherm (°C)**	**Peak of exotherm (°C)**	**Total heat of enthalpy (ΔH, J/g)**
75:25	65.2	113.1	41.5	169.2	233.6	119.0
50:50	51.4	105.9	76.3	174.5	232.3	112.1
35:65	36.2	98.0	101.8	176.4	235.5	108.5
25:75	32.0	93.9	125.1	176.1	234.1	102.9

Likewise, Bz-Nor:DCP blends displayed a similar qualitative trend in the DSC cure behavior, as shown in Figure 23. The corresponding thermal data are tabulated in Table 4. The addition of DCPD led to a systematic decrease in the onset and peak

temperature of ROMP exotherm, while the total heat of enthalpy increased from 20 J/g (0% DCPD) to 125 J/g (75% DCPD). For the second exotherm - the rigidity, originating from the formation of primary ROMP crosslinks, led to a shift in the onset and peak maxima to a higher temperature, whereby the total heat of enthalpy decreased from 140 J /g (0% DCPD) to 102.9 J/g (100% DCPD) with a relative decrease in the benzoxazine mole content.

Thermal stability studies: TGA

Thermal stability of the cured compositions was investigated by TGA under nitrogen. To elucidate the effect of catalyst concentration on thermo-mechanical properties, the dual cure hybrid networks of Bz-Nor:DCP(1.5) and Bz-Nor:DCP(3) were prepared using two different catalyst concentrations at 1.5 wt% and 3.0 wt%, respectively. TGA curves of dually cured Bz-Nor:DCP(1.5) and Bz-Nor:DCP(3) are shown in Figure 24 and 25, respectively, and the corresponding data are summarized in Table 5 and 6, respectively. All thermosets exhibited superior thermal stability with high initial degradation temperature above 300 °C. The dual-cured p(Bz-pNor) network exhibited higher initial degradation temperatures (T_5 and T_{10}) compared to the pure analogue p(Bz-Nor), and commercially available p(Araldite 35600) (Figure 26 and Table 7). The enhanced thermal stability of the dual-cured thermosets can be attributed to the formation of rigid crosslinks that prevents the early Mannich base degradation, which is shown to occur during the initial degradation step of bisphenol-A based polybenzoxazines derived from aliphatic amines (260–300 °C).[34] A systematic increment in the initial weight loss temperatures (T_5 and T_{10}) was observed with the incorporation of DCPD concentration.

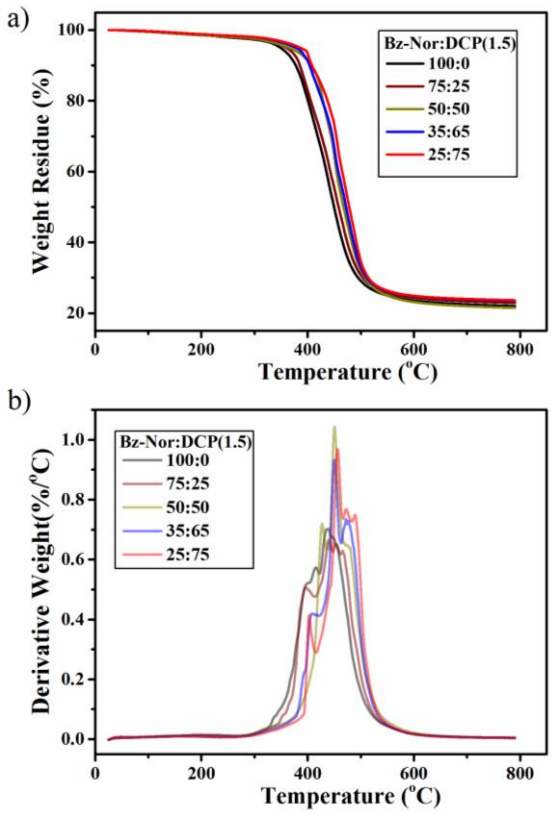

Figure 24. a) TGA degradation profiles and b) derivatives of compositions of dual cure hybrid network p(Bz-pNor:DCP-1.5).

Table 5

Summary of the thermal stability data of the samples of dual cured hybrid network p(Bz-pNor:DCP-1.5) under N_2

p(Bz-pNor:DCP-1.5)	$T_{5\%}$ (°C)[a]	$T_{10\%}$ (°C)[b]	Char Yield (800 °C)
100:0	349	378	22.0
75:25	360	385	22.9
50:50	364	404	21.5
35:65	378	407	23.5
25:75	386	408	23.6

[a] Temperature at which 5% weight loss occurs; [b] Temperature at which 10% weight loss occurs

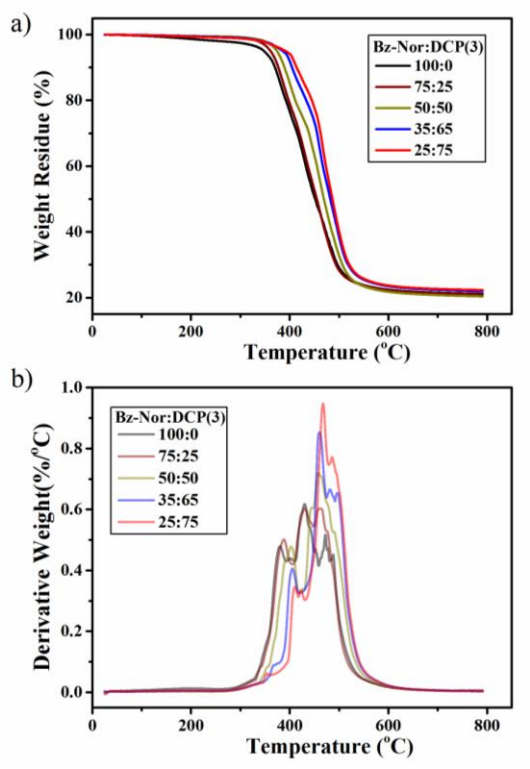

Figure 25. a) TGA degradation profiles and b) derivatives of compositions of dual cure hybrid network p(Bz-pNor:DCP-3).

Table 6

Summary of thermal stability data of the samples of dual cured hybrid network p(Bz-pNor:DCP-3)

p(Bz-pNor:DCP-3)	$T_{5\%}$ (°C)[a]	$T_{10\%}$ (°C)[b]	Char Yield (800 °C)
100:0	348	370	21.2
75:25	361	377	20.9
50:50	374	389	20.4
35:65	386	405	21.9
25:75	391	414	22.3

[a] Temperature at which 5% weight loss occurs; [b] Temperature at which 10% weight loss occurs

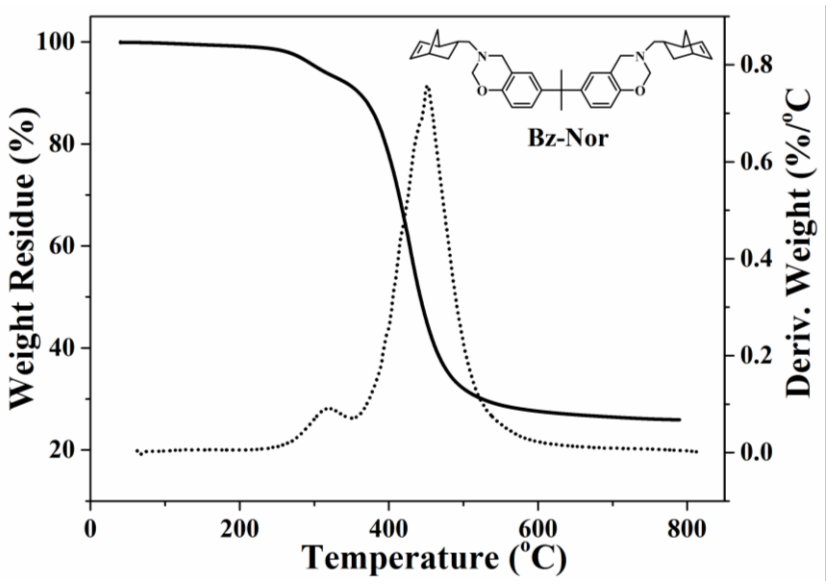

Figure 26. TGA degradation profile and derivative of thermally cured p(Bz-Nor).

Table 7

Summary of the TGA results of the ROMP cured pDCPD and pENB, thermally cured pristine p(Bz-Nor) and Araldite-35600 under N_2

Sample	$T_{5\%}$ (°C)[a]	$T_{10\%}$ (°C)[b]	Char Yield (800 °C)
p(Bz-Nor)	303	360	25.9
p(Araldite-35600)[c]	330	362	38.0
p(ENB)[d]	410	432	7.9
p(DCPD)[d]	483	493	16.4

[a] Temperature at which 5% weight loss occurs; [b] Temperature at which 10% weight loss occurs; [c] Ref.[19]; [d] Figure B4 in Appendix B

Pure pDCPD network possess superior thermal stability with relatively high initial weight loss temperature at 483.52 °C ($T_{5\%}$) and 493.37 °C ($T_{10\%}$) (Figure B4, Appendix B), on the account of stable, unsaturated cycloaliphatic crosslinks, and show the absence of early degradation events that are prevalent in polybenzoxazines as mentioned earlier. Additionally, the higher reactivity of DCPD in relative to Bz-Nor co-monomer facilitates

effective crosslinking, and minimizes the amount of loose chain-ends and unreacted monomer residues, thereby preventing early degradation.

All the hybrid compositions of Bz-Nor:DCP(1.5) showed a marginal difference in char yield at 800 °C with a slight increase relative to DCPD content. As seen from Table 5 and 7, the char yield at 800 °C of p(Bz-Nor) (26%) and Araldite 35600 (38%) were higher than that of dual-cure hybrid networks of Bz-Nor:DCP(1.5) (22%) and ROMP cured p(DCPD) (16%). The char yield of polybenzoxazines is determined by several factors including the cure atmosphere, structure of the polymer backbone and nature of the phenol/amine substituents, molecular weight, and degree of crosslinking. Polybenzoxazines typically possess an excellent char yield due to stable aromatic composition, and the presence of hydrogen bonding interactions between the Mannich base and phenolic –OH groups have been shown to contribute to the network structure and influence their thermo-mechanical properties.[35-36] Consequently, the char yield of p(Bz-Nor:DCP-1.5) was lowered with the addition of relatively less stable cycloaliphatic units within the polybenzoxazine matrix.

A similar qualitative trend was observed for Bz-Nor:DCP(3) blends (Figure 25 and Table 6). A systematic increase in the initial weight loss temperatures ($T_{5\%}$ and $T_{10\%}$) was observed with an increase in DCPD content, accompanied by a slight variation in the char yield at 800 °C. The effect of catalyst concentration on thermal stability was reflected in the initial weight loss temperatures of the hybrid networks. The initial weight loss temperature ($T_{5\%}$) for all compositions of p(Bz-pNor:DCP-3) were higher than that of p(Bz-pNor:DCP-1.5). This could be explained by the fact that the higher catalyst concentration enhances the rate of polymerization and final conversion, subsequently

minimizing the amount of unreacted molecules and loose chain ends/ branches responsible for early degradation.

Figure 27 and Table 8 shows the TGA profile and the corresponding thermal data of dual-cured p(Bz-pNor:ENB) thermosets, respectively. The thermosets displayed an increase in initial weight loss temperatures ($T_{5\%}$ and $T_{10\%}$) with the addition of ENB. The increase in T_5 and T_{10} can be attributed to the combination of the inherent thermal stability of p(ENB), which possess a significantly high initial weight loss temperatures $T_{5\%}$ (410 °C) and $T_{10\%}$ (432 °C) (Figure B4, Appendix B), and the formation of effective crosslinks due to high reactivity of ENB. These results can be correlated to viscoelastic measurements (Figure 13), which showed a decrease in gel fraction time, and increase in extent of crosslinking with the addition of ENB co-monomer. Overall, the char yield at 800 °C of p(Bz-pNor:ENB) thermosets showed a decrease with the addition of p(ENB) segments for the reasons discussed previously. The observed trend in the char yield explains the resultant effect of both the network composition and degree of crosslinking in p(Bz-pNor:ENB) thermosets.

As compared to p(Bz-pNor:DCP), p(Bz-Nor:ENB) system exhibited higher initial degradation temperature values and lower char yield, and can be attributed to the differences in the reactivity and network composition of ENB and DCPD co-monomers. The ability of DCPD to form rigid crosslinks leads to higher char yield in p(Bz-pNor:DCP), while the higher reactivity of ENB accelerates the conversion and shifts the onset of degradation to a higher temperature in p(Bz-pNor:ENB) thermosets.

To better understand the thermal stability, the derivative weight loss curves of thermosets were systematically evaluated. Figure 26 shows the TGA thermogram and

derivative curve of thermally cured p(Bz-Nor). The derivative curve of p(Bz-Nor) revealed two well-resolved degradation events, which is a typical of bisphenol-A based polybenzoxazines shown in literature.[34] The first degradation stage between 220-320 °C represents a slow decline and corresponds to the loss of volatile amine fragments, while the second stage (320–600 °C) centered at 430 °C is assigned to the degradation of different substituted phenolic moieties. Finally, the final degradation stage above 600 °C can be associated with oxidation of residual char. In comparison with p(Bz-Nor), the derivative curve of p(DCPD and p(ENB) showed high degradation resistance between 400-600 °C for the decomposition of main-chain polynorbornene units (cleavage of C=C bonds).

The degradation events in dual-cure hybrid thermosets p(Bz-pNor:DCP-1.5), p(Bz-pNor:DCP-3) and p(Bz-pNor:ENB) (Figure 24b, 25b and 27b, respectively) occurred in three successive stages. The first stage between 300–400 °C may be correlated to the decomposition of lightly cross-linked chain segments or branches, including volatization of amines in polybenzoxazines as discussed previously. The second stage ranging between 400–500 °C corresponds to the degradation of main-chain polynorbornene units and phenolic derivatives of polybenzoxazines. The final stage, which extends above 650 °C can be attributed to the oxidation of residual char. A systematic shift in the onset of degradation events to a higher temperature was observed with the rise in DCPD/ENB content.

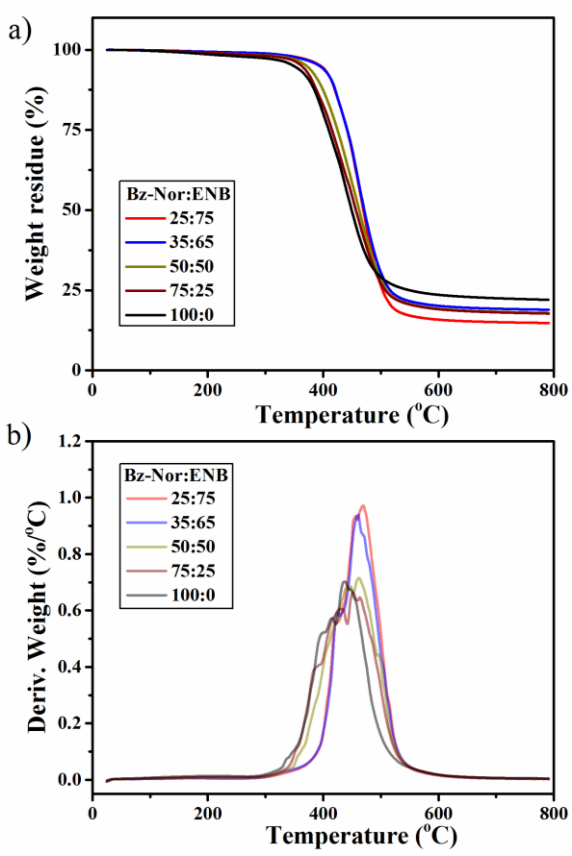

Figure 27. a) TGA degradation profiles and b) derivatives of all compositions of dual cure hybrid network p(Bz-pNor:ENB).

Table 8

Summary of the thermal stability data for samples of the dual cured hybrid network p(Bz-pNor:ENB)

p(Bz-pNor:ENB)	$T_{5\%}$ (°C)[a]	$T_{10\%}$ (°C)[b]	Char Yield (800 °C)
100:0	348	378	22.0
75:25	363	382	17.7
50:50	371	393	17.9
35:65	394	416	18.9
25:75	395	415	14.8

[a] Temperature at which 5% weight loss occurs; [b] Temperature at which 10% weight loss occurs

Dynamic Mechanical Analysis

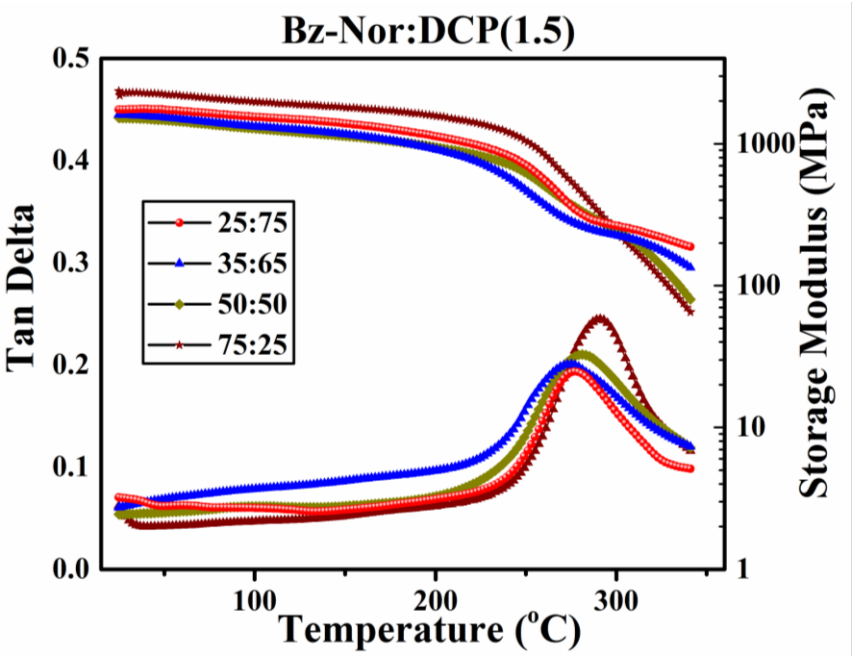

Figure 28. Plots of temperature dependence of storage modulus and tan delta of dual cross-linked Bz-Nor:DCP(1.5) compositions.

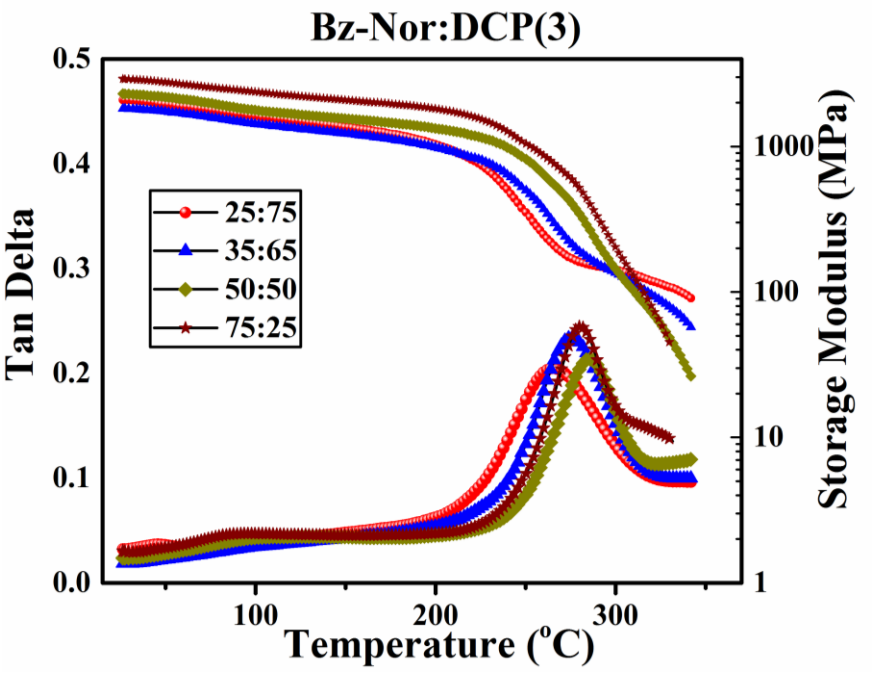

Figure 29. Plots of temperature dependence of storage modulus and tan delta of dual cross-linked Bz-Nor:DCP(3) compositions,

Table 9

Summary of the thermo-mechanical analysis data for samples of the dual cured hybrid network p(Bz-pNor:DCP-1.5) and p(Bz-pNor:DCP-3)

Sample p(Bz-pNor:DCP-1.5)	**T_g (°C)**	**Peak tandelta value**	**E' at 30 °C [MPa]**
75:25	291	0.24	2292
50:50	287	0.22	1742
35:65	275	0.20	1591
25:75	276	0.16	1638
p(Bz-pNor:DCP-3)			
75:25	279	0.24	2901
50:50	285	0.21	2291
35:65	274	0.23	1806
25:75	265	0.20	2087

Thermo-mechanical properties of the copolymers were investigated by dynamic mechanical analysis (DMA). The storage modulus relates to the ability of materials to store energy, while the loss modulus is attributed to dissipative and viscous losses in the materials. The ratio of E'' to E' is the mechanical damping (tan δ). The peak of tan δ was used to mark the glass transition temperature (T_g).

All compositions of Bz-Nor:DCP (1.5) and Bz-Nor:DCP (3) were optically transparent and showed a single T_g, indicating no phase separation. Figure 28 and 29 represent DMA plots of dual-cured Bz-Nor:DCP(1.5) and Bz-Nor: DCP(3) blends, respectively. The related thermo-mechanical analysis data are tabulated in Table 9. The storage modulus of a solid sample in the glassy state - an indicative of material's stiffness under shear deformation decreases with increasing DCPD content of the Bz-Nor:DCP(1.5). The storage modulus for all the compositions maintained constant until a high temperature around 250 °C, which is an indicative of high rigidity and degree of

crosslinking. The sample containing 75 mol% Bz-Nor exhibited a glassy storage modulus of 2.3 GPa at 30 °C, and this value was close to that observed for most of the commonly studied polybenzoxazines, B-a (2.2 GPa).[37] The glassy storage modulus values of thermosets reduced as a function of increasing DCPD content owing to the inclusion of lesser rigid cycloaliphatic crosslinks. A decrease in the peak height was observed with the addition of DCPD. Peak tan delta is the ratio of viscous to elastic components and a suppression in peak height suggests a reduction in segmental mobility and hence, an indication of increase in the degree of crosslinking in Bz-Nor:DCP (1.5) blends. The addition of DCPD (above 50%) resulted in a stable plateau modulus regime, which is an indicative of higher extent of crosslinking and the resultant high thermal stability. As evidenced by the DSC and rheological curing studies, both the rate and degree of ROMP curing were greatly enhanced with the inclusion of highly reactive DCPD co-monomer, which thereby minimizes the amount of unreacted molecules and dangling chain ends leading to a greater stabilization of a rubbery plateau modulus. Also, the improvement in thermal stability of p(Bz-pNor:DCP-1.5) was further supported by TGA analysis (Figure 24) , which showed a systematic increase in the onset of degradation temperature with the addition of DCPD.

According to the statistical theory of rubbery elasticity[38] the crosslinking density can be derived from the plateau modulus using $v_c = G_e/3RT_e$, where G_e is the plateau modulus at T_g+40 °C, R is the gas constant, and T_e is the temperature at T_g+40 ^oC. The equation is only valid for lightly cross-linked materials possessing a stable rubbery plateau regime. For highly cross-linked materials employed in our studies, the values were used for the purpose of qualitative comparison. The analysis of crosslinking

densities for Bz-Nor:DCP(1.5) blends was complicated by the thermal degradation immediately following the glass transition temperature. Hence, the plateau modulus values were unobtainable due to the absence of a stable rubbery plateau regime on the account of degradation, which is generally the case for polybenzoxazines owing to their high glass transition characteristics. Generally, the crosslinking often increases the T_g by reducing chain mobility. Conversely, the addition of DCPD showed a systematic decrease in glass transition temperature, which suggested a rather dominant effect of the composition of the network structure irrespective of the trend observed in peak tan delta values. DCPD is a known to form a lightly cross-linked network through the metathesis reaction of 20% of the less strained cyclopentene bond at high temperature.[25] The reported glass transition temperature of pure pDCPD is in the range of 150-160 ^{o}C.[39] The lowering of the glass transition temperature can be attributed to the incorporation of a relatively lesser rigid cycloaliphatic units of p(DCPD), and the non-planar structure of DCPD facilitates less efficient molecular packing, aiding in an increase in free volume. Furthermore, the formation of pDCPD can possibly affect the extent of hydrogen bonding interactions in polybenzoxazines, which are known to contribute to their high glass transition characteristics.[35]

The width of tan delta peak increases in relative to the DCPD content, which is a result of increasing network heterogeneity - arising from a broad distribution of relaxation times, as would be expected from copolymerization. Thus, the incorporation of DCPD component in the brittle polybenzoxazine matrix could potentially act as a stress concentration site, aiding in energy damping characteristics towards better impact resistant properties in polybenzoxazines.

On the other hand, Bz-Nor:DCP(3) blends exhibited a similar qualitative trend in the glass storage modulus values and glass transition temperature relative to DCPD modification, as shown in Figure 29. Blends containing 25% DCPD exhibited the highest glassy storage modulus at room temperature (2.9 GPa at 30 °C), and showed a systematic decrease in glass transition temperature with a rise in DCPD content. The increase in glass transition temperature for blends containing 50% DCPD can be attributed to the initial rise in degree of crosslinking and rigidity offered by the bulky co-monomer structures. All compositions of p(Bz-pNor:DCP-3) showed a lower T_g in comparison to that of p(Bz-Nor:DCP-1.5). The catalyst concentration is shown to have a prominent effect on the rate and degree of network formation in a way that higher catalyst concentration leads to an increase in ROMP curing rate and final conversion.[26] Moreover, the catalyst concentration can likely affect the molecular weight distribution and the resultant distribution of crosslinks. One possible explanation for Bz-Nor:DCP(3) exhibiting lower viscoelastic properties is that the high catalyst concentration and unequal reactivity of co-monomers may result in broadening of crosslink distribution. Misra et al.[40] demonstrated that for a given average of crosslinking density, a wide distribution of crosslinks lowers the T_g as a result of increase in the length between the crosslinks as compared to those with narrow distribution. Moreover, an excess of catalyst concentration can act as a plasticizer and influence the viscoelastic properties of the cured thermosets.

Figure 30 shows the dynamic mechanical analysis curves of dual-cured compositions of Bz-Nor:ENB, and the corresponding results are highlighted in Table 10. The storage modulus curves were maintained stable up to a high temperature (250 °C),

indicating high rigidity and thermo-mechanical stability. A systematic decrease in glassy storage modulus values was observed in direct proportion to the ENB content, and can be related to reduction in stiffness arising from the incorporation of the mobile linear poly(ENB) network chains.

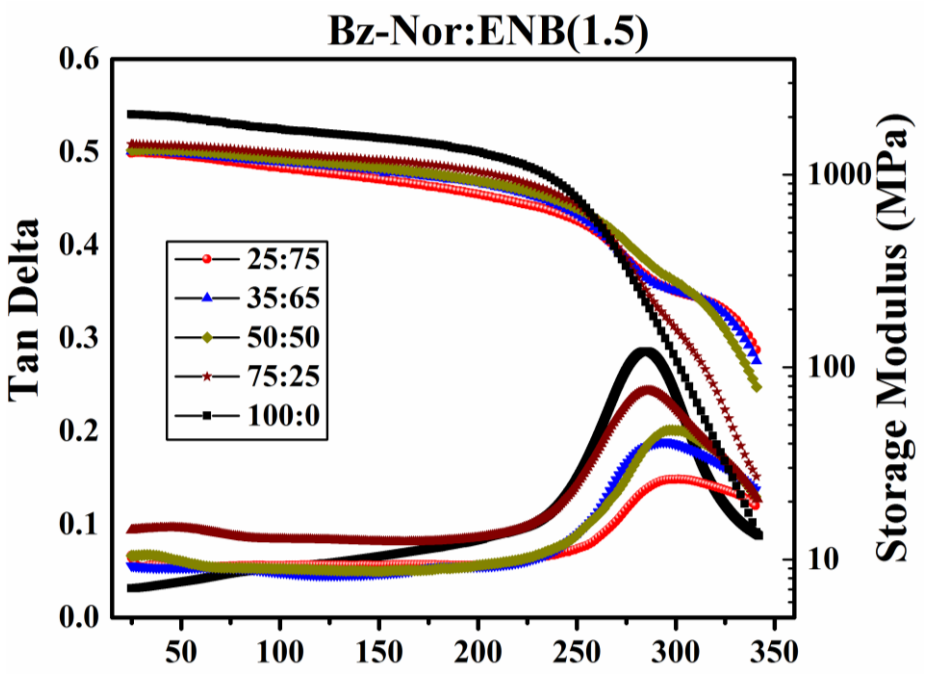

Figure 30. Plots of temperature dependence of storage modulus and tan delta of dual-crosslinked p(Bz-pNor:ENB) compositions.

Table 10

Summary of the thermo-mechanical analysis data for samples of the dual cured hybrid network p(Bz-pNor:ENB)

Sample p(Bz-pNor:ENB)	**T_g (°C)**	**Peak tandelta value**	**E' at 25 °C [MPa]**
100:0	285	0.28	2056
75:25	286	0.24	1443
50:50	299	0.20	1345
35:65	294	0.19	1323
25:75	301	0.15	1300

A decrease in peak tan delta values was observed with the increasing ENB concentration. Similar to DCPD-based system, the thermal stabilities of rubbery plateau modulus regime of p(Bz-Nor:ENB) thermosets were enhanced with the addition of ENB content, and was further supported by TGA studies. Again, in the view of a short-term stability of rubbery plateau regime, the measurements for crosslinking densities of p(Bz-Nor:ENB) could not be estimated. The glass transition temperature of p(Bz-Nor:ENB) thermosets showed an increase from 0 mol% (285 °C) to 75 mol% (301 °C) of ENB concentration. This trend can be attributed to the fact that the high reactivity of ENB enables increase in the extent of network formation and thereby, decreasing the amount of loose dangling chain-ends and small molecules that act as a plasticizer and reduce the glass transition temperature. This is further supported by rheological curing studies, which showed an accelerating effect of ENB on gelation kinetics, wherein the compositions containing 75% ENB exhibited the highest limiting shear modulus value in short reaction time.

In comparison to p(Bz-Nor:DCP) thermosets, the high glass transition temperatures of p(Bz-Nor:ENB) thermosets can be related to the reactivity differences of

DCPD and ENB co-monomers, which could varyingly influence the extent of network formation before the reaction becomes diffusion-controlled. Moreover, high conversion associated with ENB-based systems reduces the concentration of unreacted molecules and dangling chain-ends that induce plasticization and enable mobility of the chain segments. Another possible reason for this difference can be attributed to the extent of hydrogen bonding network formation in polybenzoxazines, which may vary for different co-monomer compositions. Kim and Ishida[41] showed that in addition to the basicity, the steric aspect of the amine substituents has a profound effect on the extent of hydrogen bonding network formation, which in turn was correlated to the compactness of the network structure and glass transition temperature. Moreover, it was demonstrated that the bulkier amine substituents interfere with the extent of benzoxazine crosslinking because of extensive degradation processes during the polymerization of benzoxazines in addition to the steric effect, resulting in lowered T_g. Different compositions of Bz-Nor:DCP and Bz-Nor:ENB vary in the extent of ROMP crosslinking and rigidity of the network attached to the nitrogen, which may interfere with the degree of oxazine polymerization and extent of hydrogen bond formation in polybenzoxazines, and varyingly affect the thermo-mechanical properties of the fully cured resin.

Albeit the thermal curing of the studied films were performed in N_2 atmosphere to prevent unwanted reactions, depending upon the purity of N_2 gas, it could be expected that small amount of oxygen may participate during the cure process of polybenzoxazines. FT-IR curing studies of dual-cure compositions showed a strong carbonyl band at 1637 cm^{-1} related to the substituted benzoquinone, which has been previously assigned as the oxidation product of UV thermal degradation of

polybenzoxazines.[31] Furthermore, the presence of oxidation products has been shown to vary the crosslinking density and distribution of hydrogen bonding interactions in influencing the final thermo-mechanical properties.[42,43] Therefore, the effect of the formation of undesirable oxidation products during thermal cure on the final thermo-mechanical properties of the cured thermosets could be taken into consideration.

Conclusions

A novel class of dual cross-linked hybrid network was developed incorporating both norbornyl and benzoxazine based polymer networks. The dual cross-linked hybrid networks were synthesized combining two independent curing mechanisms: thermally induced ROMP polymerization (25 °C to 180 °C) followed by ring opening addition polymerization of benzoxazines. Benzoxazine containing bisfunctional norbornene cross-linker (Nor-BZO) was synthesized and blended separately with two different reactive comonomers – 5-ethylidene-2-norbornene (ENB) and dicyclopentadiene (DCPD) at varying concentrations. The addition of DCPD and ENB exhibited an accelerating effect on the viscoelastic properties of blends, among which ENB-based systems showed faster gelation kinetics due to the low viscosity and high reactivity of ENB co-monomer. On the other hand, no gel point was obtained for 100% Bz-Nor blends under the conditions investigated, suggesting low reactivity of Bz-Nor monomer and the use of a longer curing time and higher temperature for achieving viscoelastic transitions. DSC cure studies showed that a high catalyst concentration (> 3.5 wt%) was required to conduct an efficient ROMP reaction of Bz-Nor monomer. The onset and peak of exotherm of ROMP curing of Bz-Nor:DCP and Bz-Nor:ENB blends were shifted to a lower temperature in relative to the rise in DCPD and ENB content, respectively. The rigidity incurred by the

formation of primary polynorbornene crosslinks resulted in a higher temperature shift of the onset and peak maxima of oxazine polymerization.

Albeit the flammability characteristics (char yield) of the dual cross-linked hybrid thermosets were lowered compared to that of the pristine p(Bz-Nor) due to reduction in aromatic content, a systematic increment in the initial weight loss temperatures was observed with increasing DCPD/ENB content. Dual-cure networks based on ENB-based blends showed higher initial degradation temperatures and lower char yield than that of DCPD-based blends. The incorporation of less rigid cycloaliphatic crosslinks of DCPD exhibited a relative decrease in stiffness and glass transition temperatures in addition to the enhancement of the thermal stability of rubbery plateau modulus. For ENB-based systems, a systematic reduction in stiffness was observed in direct proportion to the ENB content, while on the other hand the glass transition temperatures increased, and was relatively higher than that of DCPD-based networks.

Irrespective of the semi-sequential nature of network formation, easily moldable partially cured polynorbornene films were obtained, which were then subjected to thermal step-cure to obtain final hybrid thermosets. Thus, the dual-cure hybrid approach offered a versatile platform to overcome the brittleness of polybenzoxazines with an access to a wide range of tailorable material properties within the same system.

Acknowledgments

The authors gratefully acknowledge financial support from the National Science Foundation (NSF CAREER DMR-1056817) and the Office of Naval Research (Award N00014-07-1-1057). The authors thank the Thames-Rawlins Research Group (Steve Wand and David Delatte) for help with DMA and TGA measurements, and Otaigbe Research group (Dr. Joshua U. Otaigbe and Shahab K. Rahimi) for assistance with rheological measurements. The authors thank Huntsman Advanced Materials for the kind donation of Araldite® benzoxazine resins.

References

1. Grubbs, R. H., *Handbook of Metathesis*. Wiley-VCH: Weinheim, Germany, 2003.

2. Bielawski, C. W.; Grubbs, R. H., Living ring-opening metathesis polymerization. *Progress in Polymer Science* 2007, *32* (1), 1-29.

3. Leitgeb, A.; Wappel, J.; Slugovc, C., The ROMP toolbox upgraded. *Polymer* 2010, *51* (14), 2927-2946.

4. Jean-Louis Hérisson, P.; Chauvin, Y., Catalyse de transformation des oléfines par les complexes du tungstène. II. Télomérisation des oléfines cycliques en présence d'oléfines acycliques. *Die Makromolekulare Chemie* 1971, *141* (1), 161-176.

5. Wu, Z.; Benedicto, A. D.; Grubbs, R. H., Living ring-opening metathesis polymerization of bicyclo[3.2.0]heptene catalyzed by a ruthenium alkylidene complex. *Macromolecules* 1993, *26* (18), 4975-4977.

6. Schwab, P.; Grubbs, R. H.; Ziller, J. W., Synthesis and Applications of RuCl2(CHR‘)(PR3)2: The Influence of the Alkylidene Moiety on Metathesis Activity. *Journal of the American Chemical Society* 1996, *118* (1), 100-110.

7. Grubbs, R. H.; Chang, S., Recent advances in olefin metathesis and its application in organic synthesis. *Tetrahedron* 1998, *54* (18), 4413-4450.

8. Bielawski, C. W.; Grubbs, R. H., Highly Efficient Ring-Opening Metathesis Polymerization (ROMP) Using New Ruthenium Catalysts Containing N-Heterocyclic Carbene Ligands. *Angewandte Chemie International Edition* 2000, *39* (16), 2903-2906.

9. Scholl, M.; Ding, S.; Lee, C. W.; Grubbs, R. H., Synthesis and Activity of a New Generation of Ruthenium-Based Olefin Metathesis Catalysts Coordinated with

1,3-Dimesityl-4,5-dihydroimidazol-2-ylidene Ligands. *Organic Letters* 1999, *1* (6), 953-956.

10. Khosravi, E., Well-defined crosslinked materials via ring opening metathesis polymerisation. *Macromolecular Symposia* 2002, *183* (1), 121-126.
11. Hine, P. J.; Leejarkpai, T.; Khosravi, E.; Duckett, R. A.; Feast, W. J., Structure property relationships in linear and cross-linked poly(imidonorbornenes) prepared using ring opening metathesis polymerisation (ROMP). *Polymer* 2001, *42* (23), 9413-9422.
12. Yagci, Y.; Kiskan, B.; Ghosh, N. N., Recent Advancement on Polybenzoxazine-A Newly Developed High Performance Thermoset. *J. Polym. Sci. A: Polym. Chem.* 2009, *47* (21), 5565-5576.
13. Ghosh, N.; Kiskan, B.; Yagci, Y., Polybenzoxazines - New high performance thermosetting resins: Synthesis and properties. *Prog. Polym. Sci.* 2007, *32* (11), 1344-1391.
14. Takeichi, T.; Kawauchi, T.; Agag, T., High Performance Polybenzoxazines as a Novel Type of Phenolic Resin. *Polym. J* 2008, *40* (12), 1121-1131.
15. Hatsuo, I.; Tarek, A., *Handbook of Benzoxazine Resins*. Elsevier: Amsterdam, 2011.
16. Lu, C.-H.; Su, Y.-C.; Wang, C.-F.; Huang, C.-F.; Sheen, Y.-C.; Chang, F.-C., Thermal properties and surface energy characteristics of interpenetrating polyacrylate and polybenzoxazine networks. *Polymer* 2008, *49* (22), 4852-4860.
17. Okhawilai, M.; Pudhom, K.; Rimdusit, S., Synthesis and characterization of sequential interpenetrating polymer networks of polyurethane acrylate and

polybenzoxazine. *Polymer Engineering & Science* 2014, *54* (5), 1151-1161.

18. Spontón, M.; Estenoz, D.; Lligadas, G.; Ronda, J. C.; Galià, M.; Cádiz, V., Synthesis and characterization of a hybrid material based on a trimethoxysilane functionalized benzoxazine. *Journal of Applied Polymer Science* 2012, *126* (4), 1369-1376.

19. Narayanan, J.; Jungman, M. J.; Patton, D. L., Hybrid dual-cure polymer networks via sequential thiol–ene photopolymerization and thermal ring-opening polymerization of benzoxazines. *Reactive and Functional Polymers* 2012, *72* (11), 799-806.

20. Tasdelen, M. A.; Durmaz, H., Thermally Curable Polyoxanorbornene by Ring Opening Metathesis Polymerization. *Macromolecular Chemistry and Physics* 2011, *212* (19), 2121-2126.

21. Love, J. A.; Morgan, J. P.; Trnka, T. M.; Grubbs, R. H., A Practical and Highly Active Ruthenium-Based Catalyst that Effects the Cross Metathesis of Acrylonitrile. *Angewandte Chemie International Edition* 2002, *41* (21), 4035-4037.

22. Amundsen, L. H.; Nelson, L. S., Reduction of Nitriles to Primary Amines with Lithium Aluminum Hydride1. *Journal of the American Chemical Society* 1951, *73* (1), 242-244.

23. Ishida, H. U.S. Pat. 5,543,516, assigned to Edison Polymer Innovation Corporation.

24. Mol, J. C., Industrial applications of olefin metathesis. *Journal of Molecular Catalysis A: Chemical* 2004, *213* (1), 39-45.

25. Davidson, T. A.; Wagener, K. B., The polymerization of dicyclopentadiene: an investigation of mechanism. *Journal of Molecular Catalysis A: Chemical* 1998, *133* (1–2), 67-74.

26. Kessler, M. R.; Larin, G. E.; Bernklau, N., Cure characterization and viscosity development of ring-opening metathesis polymerized resins. *J Therm Anal Calorim* 2006, *85* (1), 7-12.

27. Lee, J. K.; Hong, S. J.; Liu, X.; Yoon, S. H., Characterization of dicyclopentadiene and 5-ethylidene-2-norbornene as self-healing agents for polymer composite and its microcapsules. *Macromolecular Research* 2004, *12* (5), 478-483.

28. Liu, X.; Lee, J. K.; Yoon, S. H.; Kessler, M. R., Characterization of diene monomers as healing agents for autonomic damage repair. *Journal of Applied Polymer Science* 2006, *101* (3), 1266-1272.

29. Kessler, M.; Larin, G.; Bernklau, N., Cure characterization and viscosity development of ring-opening metathesis polymerized resins. *J Therm Anal Calorim* 2005, *85* (1), 7-12.

30. Hayano, S.; Takeyama, Y.; Tsunogae, Y.; Igarashi, I., Hydrogenated Ring-Opened Poly(endo-dicyclopentadiene)s Made via Stereoselective ROMP Catalyzed by Tungsten Complexes: Crystalline Tactic Polymers and Amorphous Atactic Polymer. *Macromolecules* 2006, *39* (14), 4663-4670.

31. Macko, J. A.; Ishida, H., Behavior of a bisphenol- A- based polybenzoxazine exposed to ultraviolet radiation. *Journal of Polymer Science Part B: Polymer Physics* 2000, *38* (20), 2687-2701.

32. Rule, J. D.; Moore, J. S., ROMP Reactivity of endo- and exo-Dicyclopentadiene. *Macromolecules* 2002, *35* (21), 7878-7882.

33. Ishida, H.; Agag, T., *Handbook of benzoxazine resins*. Elsevier: 2011.

34. Low, H. Y.; Ishida, H., Mechanistic study on the thermal decomposition of polybenzoxazines: Effects of aliphatic amines. *Journal of Polymer Science Part B: Polymer Physics* 1998, *36* (11), 1935-1946.

35. Kim, H.-D.; Ishida, H., A study on hydrogen-bonded network structure of polybenzoxazines. *The Journal of Physical Chemistry A* 2002, *106* (14), 3271-3280.

36. Ishida, H.; Allen, D. J., Physical and mechanical characterization of near-zero shrinkage polybenzoxazines. *Journal of Polymer Science Part B: Polymer Physics* 1996, *34* (6), 1019-1030.

37. Ishida, H.; Allen, D. J., Physical and mechanical characterization of near-zero shrinkage polybenzoxazines. *J. Polym. Sci. A: Polym. Phys.* 1996, *34* (6), 1019-1030.

38. Ferry, J. D., *Viscoelastic Properties of Polymers; Wiley: New York*., 1980.

39. Vidavsky, Y.; Navon, Y.; Ginzburg, Y.; Gottlieb, M.; Lemcoff, N. G., Thermal properties of ruthenium alkylidene-polymerized dicyclopentadiene. *Beilstein Journal of Organic Chemistry* 2015, *11*, 1469-1474.

40. Misra, S. C.; Manson, J. A.; Sperling, L. H., Effects of Crosslink Density Distribution on Properties of Epoxies. Abstracts of Papers of the American Chemical Society. 1978, *176* (Sep), p. 32- 32.

41. Kim, H.-D.; Ishida, H., Model compounds study on the network structure of

polybenzoxazines. *Macromolecules* 2003, *36* (22), 8320-8329.

42. Allen, D. J.; Ishida, H., Polymerization of linear aliphatic diamine-based benzoxazine resins under inert and oxidative environments. *Polymer* 2007, *48* (23), 6763-6772.

43. Velez-Herrera, P.; Doyama, K.; Abe, H.; Ishida, H., Synthesis and Characterization of Highly Fluorinated Polymer with the Benzoxazine Moiety in the Main Chain. *Macromolecules* 2008, *41* (24), 9704-9714.

CHAPTER V

TUNABLE NETWORK PROPERTIES BASED ON DUAL-CURE HYBRID POLY(METHACRYLATE) AND POLYBENZOXAZINE NETWORKS

Introduction

Polybenzoxazines - a class of non-halogen based thermosetting resins serve as a potential contender in overcoming the limitations of traditional phenolic resins, yet retaining their advantageous properties.[1-3] Polybenzoxazines undergo ring opening addition polymerization by thermal activation (180 °C–220 °C) in the absence of catalyst, which renders them with excellent processing advantages including no release of volatiles, ambient temperature storage stability, low viscosity and near-zero volumetric shrinkage. However, the practical use of polybenzoxazines suffer from common limitations of thermosetting resins including high brittleness and difficulty to be processed into mechanically robust thin films on the account of rigidity incurred by bulky backbone structure and short molecular weight between the crosslinks.

Photo-crosslinked materials represent state-of-the-art technology, which have found a myriad of applications in the areas of printing inks, graphic arts, adhesives and photolithiography.[4-5] High-energy efficiency, low VOC, high productivity, and cost-effectiveness are the major highlights of a photo curing technology. UV curable materials based on methacrylates/acrylates are widely used due to their rapid reaction kinetics, low viscosity, ambient temperature cure and solvent free formulations. Moreover, the wide choice of commercially available monomers/oligomers with different structural compositions, viscosities and functionalities provide an opportunity to tailor a variety of design constituents such as viscosity, cure rate and conversion, network formation.

In contrast to rapid kinetics observed in photo-initiated polymerization, thermally curable benzoxazine chemistry exhibit a slow rate of polymerization, which makes the combination of the two network chemistries rather appealing. Moreover, the high UV resistance of benzoxazine resins compared to epoxies further broadens the scope of applications.[6] To date, few photo-polymerizable groups have been studied with the benzoxazine system, mostly focusing on the synthesis of linear polymers bearing pendant thermo-labile benzoxazine groups. Some of the examples include radical mediated polymerization of styrene-co-maleimide[7], methacrylate-co-styrene[8], and methacrylate[9] based benzoxazine polymer systems. Additionally, the photo-initiated cationic polymerization and free-radical promoted cationic polymerization of benzoxazine monomer[10], and its application as hydrogen donors for conducting free radical photo-polymerization of vinyl-based compounds[11] have been documented.

The selective and independent nature of cure chemistries (UV or moisture) can be sequentially addressed in conjunction with thermally activated ring-opening addition polymerization to develop dual-cure hybrid networks. Dual-cure hybrid networks render thermosets with processing advantages and offer a platform to access a broad range of tailorable material properties. To date, there are only limited examples based on dual-cure hybrid systems incorporating polybenzoxazine network. Sequential interpenetrating networks of polyacrylate/polybenzoxazine[12] and polyurethane acrylate/polybenzoxazines[13] have been developed *via* UV initiated free-radical polymerization of acrylates and thermally activated polymerization of benzoxazines. As opposed to IPNs and blends, a covalently cross-linked hybrid network derived from the same molecule bearing both the cross-linkable functionalities offers improved phase

homogeneity and network formation. Sponton et al.[14] designed a dual-cure hybrid network based on polysiloxane-polybenzoxazine network, combining primary sol-gel chemistry (hydrolysis followed by condensation) involving siloxane groups followed by thermally activated polymerization of benzoxazines. The resultant hybrid materials were homogenous, and possessed superior thermal stability and dynamic-mechanical properties compared to that of conventional polybenzoxazines. Recently, our group[15] developed dual-cure hybrid polybenzoxazine network based on sequential UV induced thiol-ene polymerization and thermally activated polymerization of benzoxazines. The covalently linked components of low modulus thiol-ene and high modulus polybenzoxazine afforded a single, high T_g thiol-ene materials (~ 150 °C), while the ease of resin application, and high machinability of thiol-ene films allowed improved processability of polybenzoxazines. Lin et al.[9] developed a dual-cure system based on methacryoyl functional benzoxazine to investigate the cure behavior of sequential photopolymerization of methacrylate functionality and thermally activated polymerization of benzoxazine. Although no thermo-mechanical properties were investigated, authors showed the feasibility of combining UV curable methacrylate chemistry with the thermally curable polymerization of benzoxazines.

As an extension to our previous work, the current work is directed towards furthering the development of dual-cure hybrid polybenzoxazine networks by incorporating sequential UV curable methacrylate and thermally curable benzoxazine chemistries. For this study, the methacrylate functional bis-benzoxazine was synthesized and co-polymerized with different amounts of mono-functional butyl acrylate monomer to target a broad range of tailorable material properties. The independent cure processes

(UV and thermal) were serially employed to develop stable, easy to handle polymeth(acrylate) films after primary UV-cure process, followed by thermal-step cure curing to obtain the final hybrid form. The goal of this study was aimed at establishing a structure-processing-property relationship by evaluating the effect of different co-monomer compositions on conversion, viscosity, network formation and thermo-mechanical properties. With the advantages of photopolymerization combined with catalyst free thermal polymerization, the meth(acrylate) and benzoxazine chemistries offers enormous molecular design flexibility.

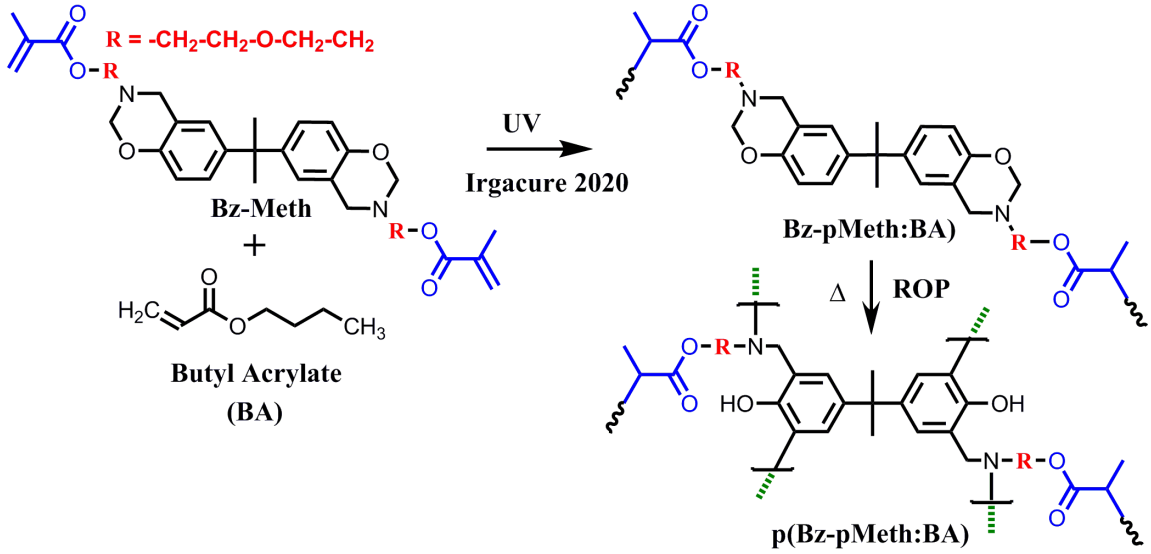

Figure 31. Schematic representation of dual-cure hybrid methodology based on UV co-polymerization of Bz-Meth:BA, followed by thermally activated polymerization of benzoxazines.

Materials

All the solvents and reagents were obtained at the highest purity available from Aldrich Chemical Company or Fisher Scientific and were used as received unless otherwise specified. Methacryloyl chloride was purified by distillation under reduced pressure (67 °C, 450 mm) and dichloromethane was distilled over anhydrous calcium

chloride before use. The abbreviations used for this study are as follows: Bz-Meth – methacrylate functional benzoxazine monomer, p(Bz-Meth) – thermally cured network of Bz-Meth, Bz-pMeth:BA – UV cured co-polymer network of Bz-Meth and BA, and p(Bz-pMeth:BA) – dually cured (UV+thermal) network of Bz-Meth:BA.

Characterization and Measurements

^{1}H- NMR and ^{13}C-NMR measurements were performed in deuterated chloroform ($CDCl_3$) using a Varian Mercury Plus 300 MHz NMR spectrometer operating at a frequency of 300 MHz with tetramethylsilane as an internal standard. The number of transients for ^{1}H and ^{13}C are 32 and 256, respectively. A relaxation time of 5 s was used for the integrated intensity determination of ^{1}H NMR spectra. Kinetic analysis was conducted using real-time FTIR spectroscopy to determine the conversions of methacrylate functional group. FTIR studies were conducted using a Nicolet 8700 FTIR spectrometer with a KBr beam splitter and an MCT/A detector with a 320-500 nm filtered (λ_{max} = 365 nm) ultraviolet light source (Omnicure S1000). Solvent-free formulations of co-monomer mixtures of Bz-Meth and BA, containing 3 wt% Irgacure 2020 photoinitiator were spin coated on a NaCl plate at 1800 rpm for 60 s and exposed to UV light with an intensity of 20.0 mW/cm^2 using a liquid light guide. Series scans were recorded, where spectra were recorded approximately 4 scans/s, each with a resolution of 4 cm^{-1}. All FTIR experiments were carried out under nitrogen atmosphere. Plots shown are representative data of a repeatable process. Differential scanning calorimetry (DSC) was performed on a TA instruments DSC Q200 differential scanning calorimeter at a heating rate of 10 °C/min and nitrogen flow rate of 50 mL/min. Samples were crimped in hermetic aluminum pans with lids. Thermogravimetric analysis (TGA) was performed

using a TA Instruments Q50 thermogravimetric analyzer with a platinum pan. Samples were heated at 20 °C /min from 25 °C to 800 °C under a nitrogen atmosphere. Dynamic mechanical analysis (DMA) was performed on a TA Instruments Q800 DMA in tension film mode with a heating rate of 2 °C/min at 1Hz from -40 °C to 150 °C for the UV cured films and -40.0 °C to 250 °C for the fully cured films. Samples were prepared using a silicone rubber mold and the dimensions of a rectangular specimen were 6.2 x 4.9 x 1.5 mm (Length x Width x Thickness). Rheological characterization was performed using a Paar Physica MCR501 strain controlled rheometer equipped with parallel plate geometry (0.3 mm gap) and Peltier set up with glass bottom window for the purpose of transmission of UV light. An optical fiber connected to ultraviolet light source (Omnicure S1000) was used to illuminate the sample through the glass window, and a UV light intensity of 0.1 mW/cm^2 was used. After 30 seconds of pre-equilibration stage, the UV light was switched on and a dynamic oscillatory time sweep test was performed using 0.7% strain and a frequency of 1 Hz and the evolution of storage and loss modulus of the network development process was monitored over time.

Preparation of dual-cured polymer films

The dual cure hybrid networks were developed by sequential UV initiated polymerization of meth(acrylates), followed by thermal ring-opening of benzoxazine, as represented in Figure 31. The methacrylate functional bis-benzoxazine (Bz-Meth) monomer was blended with different amounts of butyl acrylate at concentrations ranging from 25 mol% to 75 mol%. The mixture was homogenously mixed using a vortex stirrer, both before and after the addition of 3 wt % of Irgacure 2020 photoinitiator. The UV curable mixture was then casted onto a silicone mold and vacuumed for 10 min to

remove air bubbles. The casted reaction mixture was exposed to UV light for 20 min on one side first, followed by 10 min on the other side of the films. The resultant UV cured films were yellow transparent and tack-free (film thickness 1.5 mm), and were used for DSC analysis to study the thermal curing behavior and for DMA analysis for evaluating thermo-mechanical properties. UV cured films were subsequently cured step-wise at 100 °C, 140 °C for 1 h each, 160 °C, 180 °C, 200 °C for 2 h each and 220 °C for 2 h in an air-circulating oven.

Monomer Synthesis

Synthesis of hydroxyl functional bis-benzoxazine monomer (Bz-OH). Synthesis of Bz-OH was carried out using the modified literature procedure reported elsewhere.[8] Bisphenol-A (12.0 g, 0.05 mol), paraformaldehyde (6.4 g, 0.2 mol) and 2-(2-Aminoethoxy) ethanol (11.0 g, 0.1 mol) were dissolved in 120 mL of xylene and heated in open for 20 min in a 250 mL round bottom flask. The crude reaction mixture was cooled, transferred to a 250 mL conical flask, and stirred overnight with N_2 purge to remove the solvent. The concentrated reaction mixture was dissolved in 120 mL of chloroform, extracted with 3N NaOH (3 × 120 mL) to remove the phenolic impurities and finally washed with distilled water (3 × 120 mL). The organic mixture was stirred over anhydrous magnesium sulfate and the solvent was removed under reduced pressure to afford viscous colorless oil (16.3 g, 62.5%). ^{1}H-NMR (300 MHz, $CDCl_3$): δ (ppm) = 6.65-6.96 (m, 6H, **Ar-H**), 3.99 (s, 4H, -N-CH_2-O-, $\mathbf{H_b}$), 4.86 (s, 6H, Ar-CH_2-N-, $\mathbf{H_b}$), 3.66-3.72 (t, 8H, -CH_2-O-, $\mathbf{H_e}$ **and** $\mathbf{H_f}$), 3.51 (t, 4H, -CH_2-OH, $\mathbf{H_g}$), 3.00 **(t,** -N-CH_2-, $\mathbf{H_d}$), 1.57 (s, 6H, $\mathbf{H_a}$).

Synthesis of methacrylate functional bis-benzoxazine (Bz-Meth). Bz-OH (16.0 g, 0.03 mol) was dissolved in 110 mL dry dichloromethane under N_2 purge and maintained at 0 °C. To this solution, triethyl amine (9.0 mL, 0.06mol) was added, followed by a drop-wise addition of methacryloyl chloride with continuous stirring. After the addition, the reaction mixture was slowly warmed to room temperature and stirred overnight. The crude reaction mixture was filtered to remove the white triethylamine hydrochloride salt and washed with minimal amount of cold dichloromethane. The mixture was extracted with 0.5 N NaOH (3 × 120 mL) to remove the phenolic impurities and unreacted methacryloyl chloride, followed by washings with distilled water (3 x 120 mL) and finally with brine solution. The mixture was concentrated by distilling off dichloromethane under reduced pressure. The concentrated mixture was treated to remove the residual salt by re-dissolving the mixture in diethyl ether (120 mL), and washed with distilled water (2 × 120 mL), finally with brine solution. The organic extract was dried over dry magnesium sulfate, filtered and the solvent was distilled off under reduced pressure to afford yellow viscous oil (18.7 g, 90%). The product was dried under high vacuum and immediately stored in a deep freezer to avoid premature gelation. A 0.01 wt% of BHT inhibitor was added before the distillation step to prevent unwanted radical-mediated polymerization reaction. ^{1}H-NMR (300 MHz, $CDCl_3$): δ (ppm) = 6.62-6.93 (m, 6H, **Ar-H**), 6.10, 5.55 (s, 4H, -CH=CH_2, **H_h and H_i**), 4.83 (s, 4H, -N-CH_2-O-, **H_b**), 4.27 (t, 4H, -CH_2-O-CO, **H_g**), 3.98 (s, 6H, Ar-CH_2-N-, **H_c**), 3.64-3.72 (t, 8H, -CH_2-O-, **H_e and H_f**), 2.96 **(t,** -CH_2-N-, **H_d**), 1.92 (s, 6H, CH_3-CH=CH_2, **H_j**), 1.55 (s, 6H, -CH_3, **H_a**) (Figure C1 in Appendix C).

^{13}C-NMR ($CDCl_3$) : δ = 161.11 (2C, -**C**=O-), 151.83, 142.82, 126.15, 125.68, 125.29, 119.20, 115.81, 115.75 (12C, Aromatic-**C**), 136.07 (4C, -**C**H=**C**H**)**, 82.68 (2C, -N-**C**H_2-O-), 69.83 (2C,-O-**C**H_2-CH_2), 68.91 (2C, -CH_2-**C**H_2-O), 63.70 (2C, -**C**H_2-O-C=O-), 51.03 (2C, -Ar-**C**H_2-N-), 50.93 (2C, -**C**H_2-N), 41.58 (1C, -**C**-), 31.00 (6C, -**C**H_3), 18.28 (6C, -**C**H_3-CH=CH_2) (Figure C2 in Appendix C)

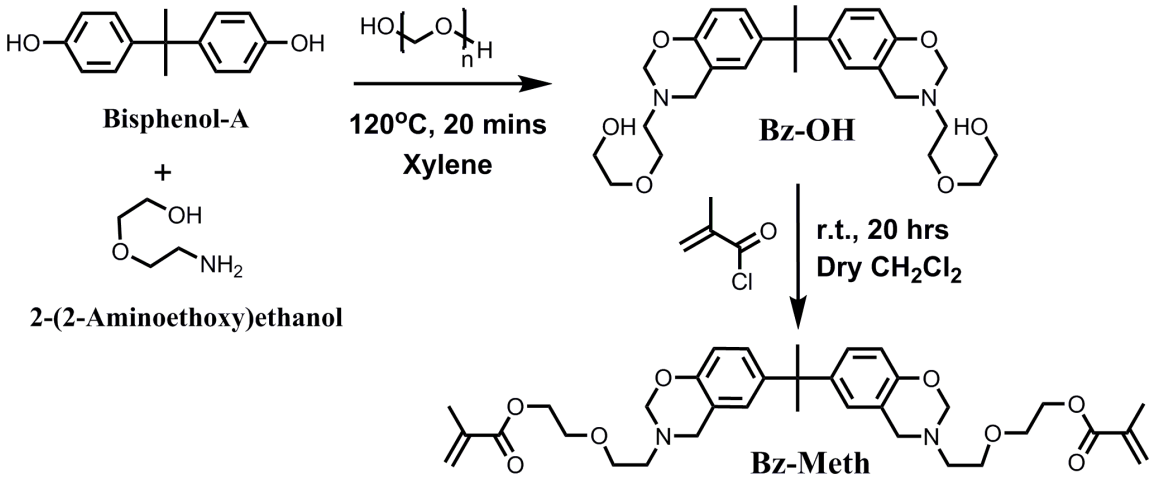

Scheme 11. Schematic representation of synthesis of methacrylate functional bis-benzoxazine monomer (Bz-Meth).

Results and Discussion

Monomer synthesis

Scheme 11 shows the overall synthetic scheme for the synthesis of Bz-Meth monomer used in this study. The synthesis of Bz-OH was performed in xylene, and the reaction conditions (120 °C, 20min) were optimized to achieve best conversion (62%). The polarity of the solvent used in benzoxazine synthesis is known to play a crucial role in determining the stability and yield of the benzoxazine ring.[16] Nonpolar solvents including 1,4-dioxane and chloroform favor the oxazine ring formation as compared to polar solvents – i.e. water and alcohol – which allow side-reactions and initiate ring-opening reaction of benzoxazines. Additionally, solvents with low dielectric constant are

known to favor the ring-closure and improve the yield of benzoxazine formation.[17] Xylene is a nonpolar solvent with a low dielectric constant, and has been previously shown to aid in an efficient synthesis of benzoxazines.[18,15] The high boiling point of xylene allows improved solubility of the reaction components at high temperature, and drives the equilibrium towards ring-closure by removing the water- a chief condensation byproduct formed during the reaction.

Methacrylate functional bis-benzoxazine monomer (Bz-Meth) was synthesized by esterification reaction of Bz-OH and methacryloyl chloride using triethyl amine as a base catalyst. A two-step extraction process was carried out, first using dichloromethane, followed by diethyl ether. Triethylamine hydrochloride salt – a byproduct in the esterification reaction – is quite soluble in dichloromethane, but is insoluble in diethyl ether. Following the extractions using dichloromethane, the product was concentrated and re-dissolved in diethyl ether to remove the residual salt. The structural elucidation of Bz-OH and Bz-Meth monomers using ^{1}H-NMR analysis (Figure C1 in Appendix C) confirmed the formation of the benzoxazine ring with the appearance of the characteristic benzoxazine peaks at 4.8 ppm and 3.9 ppm, assigned to protons of –N-CH_2-O- and Ar-CH_2-N-, respectively.

Real-time FTIR kinetics

In-situ UV cure studies of Bz-Meth:BA compositions were carried out using real-time FT-IR analysis (RTIR). Figure 32 shows the real-time FT-IR conversion plots of compositions of Bz-Meth:BA, and the corresponding data are tabulated in Table 11. The photo-curable compositions of Bz-Meth:BA were spin coated on a NaCl plate at 1800 rpm for 60 s and irradiated with UV light (320-500 nm) using a light intensity of 20 mW/cm^2. The characteristic absorption peak of methacrylate group at 1637 cm^{-1},

corresponding to C=C vinyl double bond stretching was used to determine the conversion. The conversion was calculated based on the ratios of the relative areas of the peak at time t=0 and at any given time t during the polymerization. The changes in benzoxazine ring peak during UV cure was monitored using the characteristic benzoxazine peak at 945 cm^{-1} corresponding to the out-of-plane C-H vibration of benzene ring attached to the oxazine ring.

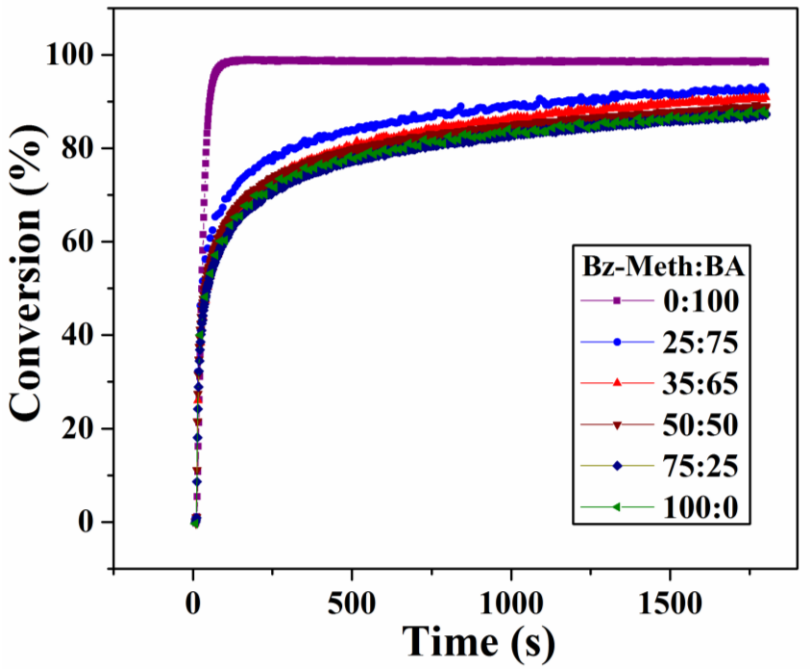

Figure 32. Double-bond (1637 cm^{-1}) conversion plots for Bz-Meth:BA formulations containing 3 wt% Irgacure 2020, irradiated with UV light (320-500 nm) for 1800 s using a light intensity of 20 mW/cm^2 at ambient temperature.

Pure BA exhibited higher extent of conversion (98%) relative to Bz-Meth monomer (87%). The copolymerization of BA and Bz-Meth resulted in an increase of final extent of conversion with the inclusion of BA mole content. During the early stages of polymerization, both the viscosity and the chemical structure have a profound effect on the segmental mobility of macro-radicals, affecting the rate of polymerization and final extent of conversion before diffusional limitations occur. Bz-Meth monomer represents a

bulky, hindered molecule with relatively high viscosity, and the incorporation of butyl acrylate co-monomer lowers the viscosity and enhances the polymerization rate before the mobility becomes restricted due to network formation.

The nature of the kinetic plot represents a characteristic chain-growth polymerization reaction, exhibiting a rapid increase in polymerization rate at a low conversion. Initially, both rates of propagation and termination are chemically controlled. In the early stages of polymerization, as the viscosity increases, the mobility of macro-radicals become restricted, which presents diffusional limitations to the termination kinetics (also referred as auto-acceleration effect), and increases the macro-radical concentration. During the course of the polymerization, as more cross-links are formed and the mobility of radicals continue to decrease; the propagation rate becomes diffusion-limited (auto-deacceleration). Finally, the maximum rate of polymerization or limiting conversion is reached due to vitrification (solidification) and additional crosslinking, and the transformation takes place from the rubbery state to glassy state.

FTIR: Thermal step-cure studies

FT-IR spectra of dual-cure of Bz-Meth:BA (50:50) after each stage of thermal cure is shown in Figure 33. After UV cure for 30 min, the representative peaks of the methacrylate double bond at 1637 cm^{-1} (in-plane C-H) and 3090 cm^{-1} (sp^2 C-H stretching) significantly decreased. The shift in the carbonyl band from 1718 cm^{-1} to 1720 cm^{-1} accompanied with a decrease in intensity after UV cure that suggested the loss of conjugation due to the formation of a saturated polymer. The characteristic benzoxazine-related band at 937 cm^{-1} showed a decrease in intensity after UV cure (1800 s), indicating the occurrence of ring opening of benzoxazine during UV cure. Moreover, the

benzoxazine conversion values for the compositions varied from 26-31%, wherein the compositions with a higher amount of BA co-monomer presented slightly higher oxazine ring-opening (Figure C3 in Appendix C, Table 11). Conventional benzoxazines are known to exhibit high UV stability for the timescale used in this study.[6]

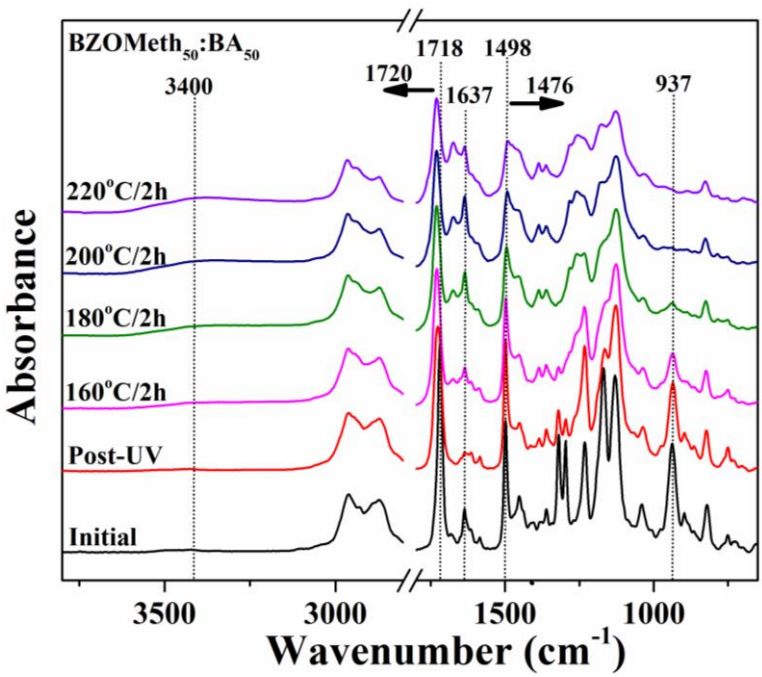

*Figure 33***.** FT-IR spectra of UV and thermal cure of Bz-Meth:BA (50:50) after each cure stage of oxidative cure.

Since the RTIR studies were conducted in an inert atmosphere, there was a limited possibility for the oxidative degradation to occur, which was confirmed by the absence of the main oxidation product at 1655 cm^{-1} related to the formation of benzoquinone in benzoxazines.[6] In addition, the absence of a broad band in the range 3400-3600 cm^{-1}, corresponding to the stretching vibration of the phenolic hydroxyl peak, excludes the possibility of the ring-opening polymerization to take place. Another possibility is that the closed ring is opening in a non-oxidative manner, which could likely form either radicals or other intermediate species, participating in the hydrogen abstraction or internal

reactions. Also, the exothermic heat from the methacrylate polymerization and the energy input from the UV curing light may promote ring opening of benzoxazine.

The extent of benzoxazine polymerization was monitored using the characteristic benzoxazine-related bands at 937 cm^{-1} (out-of-plane C-H bending vibration) and 1495 cm^{-1} (in-plane C-H bending vibration) of the benzene ring attached to the oxazine ring. As the cure temperature increased, the characteristic oxazine peaks gradually decreased and disappeared at 200 °C, suggesting the consumption of the oxazine ring. Correspondingly, a new peak appeared at 1476 cm^{-1} assigned to the formation of tetra-substituted benzene ring appeared and a broad peak at 3400-3600 cm^{-1} assigned to the phenolic –OH stretching vibration, indicating the completion of benzoxazine polymerization. Beginning at 160 °C, two new bands originated at 1636 cm^{-1} and 1675 cm^{-1} and increased in intensity as a function of cure temperature. The observed bands were previously assigned as the carbonyl peaks of the substituted benzoquinones- a major oxidation product formed during UV oxidative degradation of bisphenol-A based polybenzoxazines.[6]

Rheological studies

In combination with Real-time FTIR, in-situ rheological experiments were performed to monitor the cure kinetics of compositions of Bz-Meth:BA co-monomer blends. Gel time – an important processing parameter for thermosetting resins – marks the transition from viscous liquid to solid state. For this study, the gel point is taken as the value of the crossover of storage modulus (G”) and loss modulus (G’), where the loss factor no longer depends on the frequency (tan delta = G”/G’=1). Figure 4 describes the time evolution behavior of viscous and elastic moduli during the photo-curing of Bz-

Meth:BA samples containing different amounts of butyl acrylate. The UV irradiation was started after 30 seconds of stabilization. During the initial stages of reaction, the elastic modulus (G') was lower than viscous modulus, indicating the sample was still a viscous liquid. As the chain-growth polymerization proceeds, both elastic and viscous modulus increases with reaction time and eventually a point is reached where the crossover of elastic modulus and viscous modulus occurs, beyond which G' becomes larger than G". After the gelation regime, the modulus reaches a limiting shear modulus plateau indicating the formation of a highly cross-linked material. The vitrification occurred gradually extending over a wide range of conversion – a trend typically observed in a chain-growth systems such as meth(acrylates)/acrylates.

The initial viscosity, chemical structure, functionality and relative reactivity of the co-monomers are all important parameters affecting the overall development of the visco-elastic properties. As shown in Figure 4, the highest gel time was observed for pure Bz-Meth system (117.0 s), and can be related to the high viscosity and mobility restrictions of a hindered Bz-Meth monomer, which negatively affects the propagation rate during the early stages of polymerization. The corresponding gel time of the Bz-Meth:BA blends decreased with the inclusion of BA co-monomer, wherein the lowest gel time was observed for the intermediate compositions of Bz-Meth:BA at 50 and 65 mol% BA concentrations. The presence of Bz-Meth in the co-monomer mixture restricts the mobility of reaction species, which significantly decreases the rate of termination during the early stages of polymerization. Subsequently, restricted termination allows for an enhanced auto-acceleration effect, which facilitates relatively rapid polymerization kinetics compared to the pure systems. On the other hand, BA is a non-viscous liquid

with a low T_g, and the initial rate of termination is high due to the segmental diffusion of monomer molecules, which lowers the rate of propagation. Additionally, the number of reactive functional groups in a monomer also affects the extent of network formation and the gelation kinetics. Higher functionality of a bifunctional crosslinker Bz-Meth would allow faster network formation and attainment of earlier gelation. The relatively lower gelation time observed for the intermediate compositions of Bz-Nor:BA (50:50 and 35:65) can be ascribed to the interplay of higher functionality with an accelerated onset of reaction diffusion limited termination kinetics for Bz-Meth, in coherence with the higher mobility of propagating radicals facilitated by a more mobile BA.

Figure 35a and 35b represent the logarithmic time dependence plots of shear moduli and complex viscosity during UV curing of Bz-Meth:BA co-monomer mixtures. The initial complex viscosity values of the Bz-Meth:BA co-monomer mixtures presented a systematic decrease in relative to the addition of BA content. It was inferred from the slope of G' that pure Bz-Meth monomer showed slower reaction kinetics with the limiting shear modulus value of 0.8×10^5 Pa. This can be attributed to the retarded mobility of propagating chains arising from the high viscosity and diffusional limitations during vitrification. The polymerization reactivity of Bz-Meth was improved in the presence of BA monomer, where $Bz\text{-}Meth_{35}$:BA_{65} system exhibited fastest polymerization kinetics due to the reasons previously discussed. The limiting shear storage modulus showed an initial increase, until it reached a maximum for the $Bz\text{-}Meth_{50}$:BA_{50} system, which thereafter decreased because of lower degree of network formation based on the lower functionality of BA co-monomer.

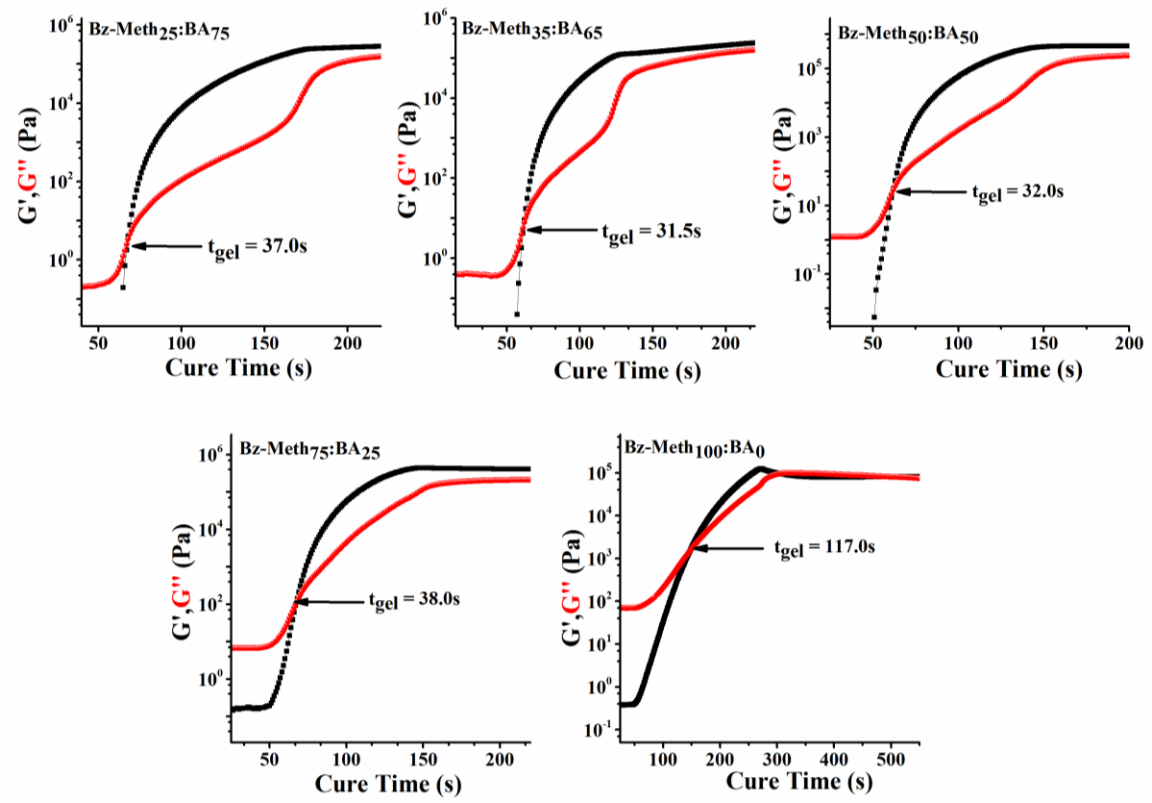

Figure 34. Plots of G' and G" vs. UV exposure time of compositions of Bz-Meth:BA blends using frequency at 1Hz, strain at 7% and 0.3 mm gap thickness. UV light (0.1 mW/cm^2) was turned on after 30 seconds.

Table 11

Real-time FT-IR conversion and rheological data of UV cure of Bz-Meth:BA compositions

Sample Bz-Meth:BA	**RTIR (%) 1637 cm^{-1}**	**RTIR (%) 945 cm^{-1}**	**Gel time (s)**	**Initial complex viscosity (Pa.s)**	**Shear G' (10^5 Pa)**
100:0	87.1	26.6	117.0	11.0	0.8
75:25	87.4	28.0	38.0	1.07	4.4
50:50	88.7	29.0	32.0	0.19	4.5
35:65	90.9	29.2	31.5	0.06	3.9
25:75	92.4	31.7	37.0	0.02	2.6

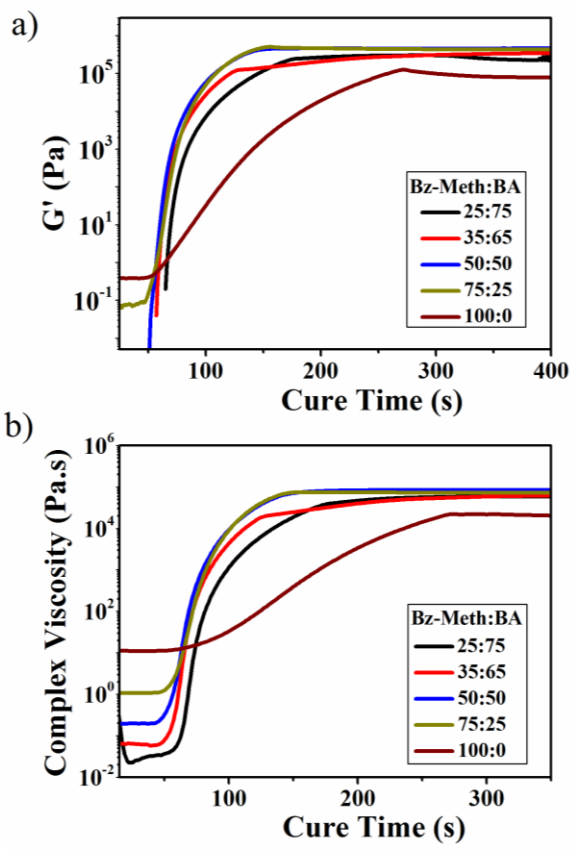

Figure 35. Comparison plots of a) G' and b) Complex viscosity vs. cure time for Bz-Meth:BA samples using frequency at 1 Hz, strain at 7% and 0.3 mm gap thickness.

DSC curing studies

DSC thermogram of pristine Bz-Meth monomer is depicted in Figure 36, which presents two distinct exotherms. The first exotherm occurring at a lower temperature with onset at 113 °C and peak maxima at 155 °C can be attributed to thermal self-initiation polymerization of methacrylate group, which are known to undergo spontaneous thermal polymerization in the absence of extraneous initiating species.[19] The higher temperature exotherm with the respective onset and peak maxima at 184 °C and 238 °C, can be attributed to thermally accelerated ring-opening addition polymerization of benzoxazines. The appearance of a shoulder at around 256 °C is a result of early degradation events of poly(methacrylate) structure, which is further supported by TGA analysis (Figure 39),

described in the following discussion. The analysis of total heat of reaction for the benzoxazine polymerization was complicated by the peak overlap with the onset of degradation at 256 °C.

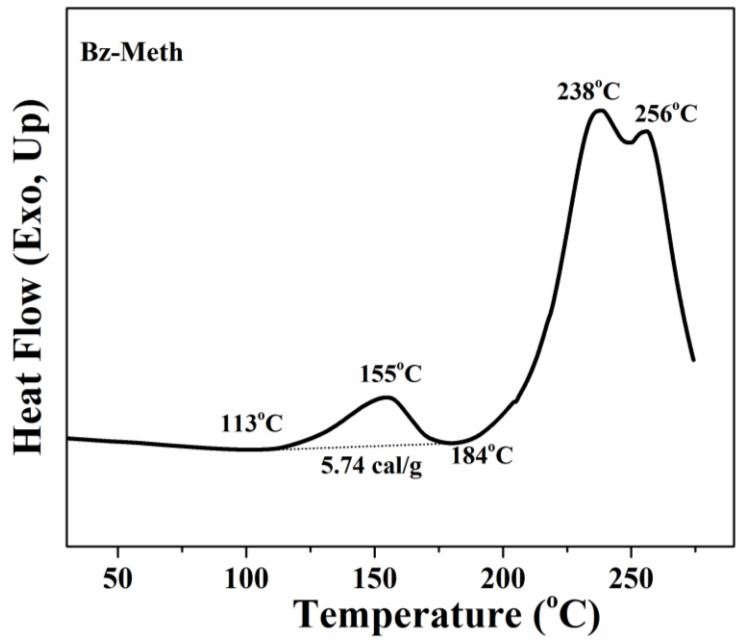

Figure 36. DSC thermogram of pristine Bz-Meth resin.

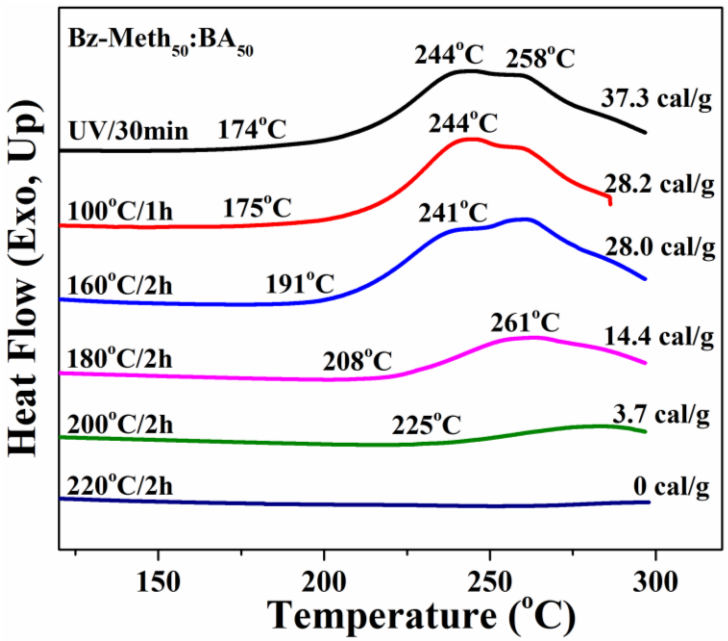

Figure 37. DSC thermal step-cure of Bz-Meth$_{50}$:BA$_{50}$ after each curing stage.

DSC thermal step-cure studies of Bz-Meth:BA (50:50) are shown in Figure 37. With the increase in the cure temperature, the exotherm corresponding to ring-addition polymerization of benzoxazines gradually decreased, followed by a significant decrease at 180 °C, finally disappearing at 220 °C, thus confirming the completion of polymerization.

Figure 38 shows the effect of co-monomer composition on the thermal-cure behavior of UV cured compositions of Bz-Meth:BA. The UV-cured composition of Bz-Meth exhibited a lower onset of exotherm at 168 °C with peak maxima at 233 °C and a shoulder at a higher temperature. The lower onset of exotherm can be attributed to the thermal self-addition polymerization of residual methacrylate groups from the previous UV stage cure. The appearance of a shoulder at a higher temperature arises from the early degradation of structures of poly(methacrylate) and polybenzoxazines occurring in the range 250-300 °C, wherein the intensity decreases with the inclusion of BA, as evidenced from TGA analysis (Figure 39). A systematic increase in both onset and peak of exotherm was observed in relative to the BA mole content. One of the reasons for the observed shift can be related to the increase in the extent of methacrylate polymerization, which is facilitated by the inclusion of low viscous and more mobile BA, as previously inferred from RTIR and rheological studies. Expectedly, the resulting rigidity in the surrounding environment incurred by the primary poly(methacrylate) cross-links shifts the second exotherm to a higher temperature.

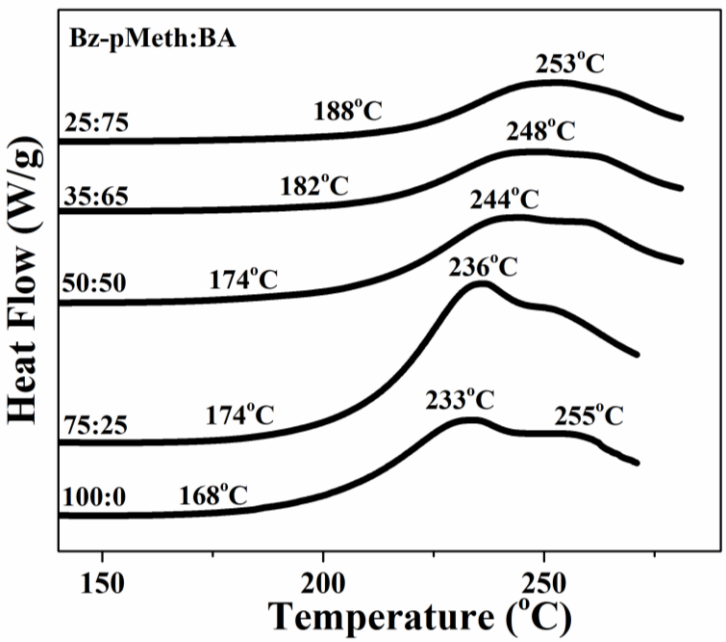

Figure 38. DSC thermal-cure analysis of UV cured Bz-pMeth:BA compositions.

TGA Analysis

TGA degradation profile of fully cured compositions of Bz-Meth:BA are shown in Figure 39, and the corresponding thermal data are summarized in Table 12. The initial degradation temperatures ($T_{5\%}$ and $T_{10\%}$) decreased in direct proportion to the butyl acrylate mole percentage in the co-monomer network. This trend could be attributed to different degradation mechanisms of polymer backbones involving poly(methacrylate), poly(butyl acrylate) and polybenzoxazine, which would vary depending upon the composition of the copolymer. The degradation mechanisms of poly(methyl methacrylate) and poly(butyl acrylate) have been extensively documented in literature, where poly(methyl methacrylate) degrades through a two-step mechanism involving random chain-scission and main-chain scission,[20] and thermal degradation of poly(butyl acrylate) occurs predominantly via a one-step mechanism - random-chain scission.[21]

Table 12

Thermal stability data of dual cured compositions of Bz-Meth:BA and pristine Bz-Meth

p(Bz-pMeth:BA)	$T_{2\%}$ (°C)[a]	$T_{5\%}$ (°C)[b]	$T_{10\%}$ (°C)[c]	Char Yield (800 °C)
100:0	272	292	318	20.9
75:25	268	298	317	20.6
50:50	272	303	328	19.9
35:65	272	311	336	18.3
25:75	273	318	353	17.5
p(Bz-Meth)	269	296	329	20.2

[a] Temperature at which 2% weight loss occurs; [b] Temperature at which 5% weight loss occurs; [c] Temperature at which 10% weight loss occurs.

In case of bisphenol-A based polybenzoxazines derived from aliphatic amines, the early degradation is known to occur by Mannich base cleavage in the range of 260-300 °C.[22] Therefore, the increasing BA amount in the copolymer offsets the occurrence of early degradation events of poly(methacrylate) (chain-scission event) and that of polybenzoxazines, thereby enhancing thermal stability of the co-polymer network. Another possible reason is that the increasing BA content in the blends permits higher conversion during UV curing of Bz-Meth (Figure 32), thereby reducing the amount of unreacted monomer and loose dangling chain-ends that are often responsible for early degradation. The char yield of the thermosets showed a relative decrease with the rise in BA mole content, and can be attributed to the incorporation of relatively less stable aliphatic crosslinks and reduction in rigidity.

Degradation profile of the fully cured compositions of Bz-Meth:BA in Figure 39b, showed a two-step degradation event. The first-stage degradation event around 250-350 °C corresponds to volatile loss of amine arising from Mannich base cleavage, which is known to be the initial degradation step during polybenzoxazine degradation.

Additionally, this temperature range has also been previously assigned to the degradation of poly(methyl methacrylate) in literature.[20] The intensity of first stage degradation declined with the incorporation of p(BA) backbone for the reasons previously been discussed. The second stage corresponds to the main-stage degradation occurring around 400-600 °C, which can be attributed to the degradation of main-chain polymer chains and different substituted phenolic units.

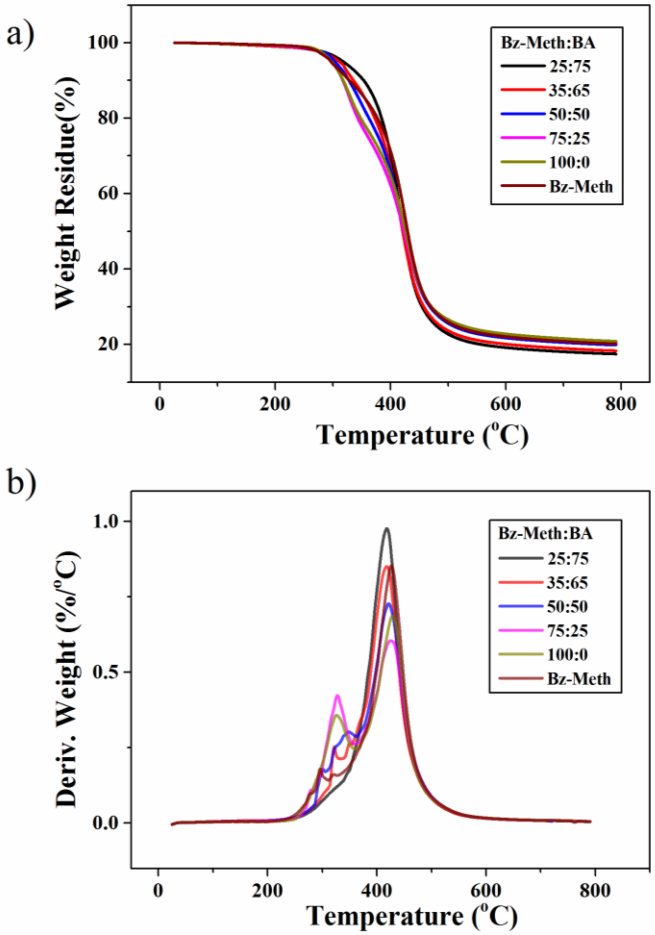

Figure 39. TGA degradation profiles and b) derivatives of all compositions of dual cured hybrid network p(Bz-pMeth:BA) and pristine p(Bz-Meth).

DMA Analysis

Thermo-mechanical properties of both UV cured and fully cured compositions of Bz-Meth:BA were evaluated as shown in Figure 40, and the corresponding thermo-mechanical data are tabulated in Table 13. The storage modulus measures the ability of material to store energy, and relates to the stiffness of the material. The storage modulus for all the compositions showed a gradual decrease over a wide range of temperature in correspondence with their glass transition temperatures. The effect of co-monomer composition on glassy storage modulus demonstrated an initial increase until Bz-$Meth_{50}$:BA_{50} (2.8 GPa), which then reduced with further rise in BA mole content. The observed trend can be very well correlated with the rheological measurements, wherein the highest limiting shear modulus value was obtained for Bz-$Meth_{50}$:BA_{50}, attributed to the balanced effect of higher functionality of Bz-Meth and greater mobility of BA co-monomer leading to an increase in the overall conversion and degree of network formation.

The glass transition temperature, measured as the peak of tan δ peak and heterogeneity, taken as the breadth of the tan δ were studied. For all compositions, a single T_g was observed, indicating the presence of a homogenous amorphous phase, which is typical for random co-polymers. The dependence of glass transition temperature on the co-monomer composition was observed as the glass transition temperature exhibited a systematic decrease in direct proportion to the BA mole content. The Fox equation is a simplistic empirical model used to predict the glass transition temperatures in random or statistical co-polymer mixtures, involving little or no specific interactions.[23]

The T_g of a pure p(Bz-Meth) was measured as 104.7 °C and the T_g for p(BA) was taken as -55.0 °C, previously reported in literature.[24]

The T_g's of the co-monomer mixtures were calculated based on the following Fox equation[23] and compared with the experimental values, tabulated in Table 13.

$$\mathbf{1/T_g = w_1/T_{g1} + w_2/T_{g2}}$$

where T_{g1} and T_{g2} are the glass transition temperatures of p(Bz-Meth) and p(BA), respectively (both in Kelvin), and w_1 and w_2 are the corresponding weight fractions. All co-monomers presented lower theoretical values compared to experimental T_g's, except for $Bz\text{-}Meth_{75}$:BA_{25} system, which showed a higher glass transition temperature. Moreover, there were inconsistent differences in the glass transition temperatures across the compositions. Glass transition temperature of a cross-linked polymer is affected by numerous parameters including the extent of crosslinking and conversion, chemical structure of cross-links, presence of inter- and intra- molecular interactions, amount of dangling-chain ends, and co-monomer sequence distribution. The discrepancy in the T_g values can be attributed to the different chemical structures of the co-monomers and the sequence distribution of the monomer units, and their effect on the mobility of the polymer chain, which was not accounted by Fox equation.[25] The peak and width of tan delta denotes the sound and vibration damping characteristics of the material. In terms of peak height, the highest tan δ peak value was obtained for the pure Bz-Meth system, which after a first initial decrease for 25 mol% BA remained constant for all other compositions. This suggests that the degree of crosslinking of Bz-Meth system is elevated with the inclusion of a more mobile BA component, which aids in overcoming the diffusional limitations of Bz-Meth and achieving higher final extent of conversion.

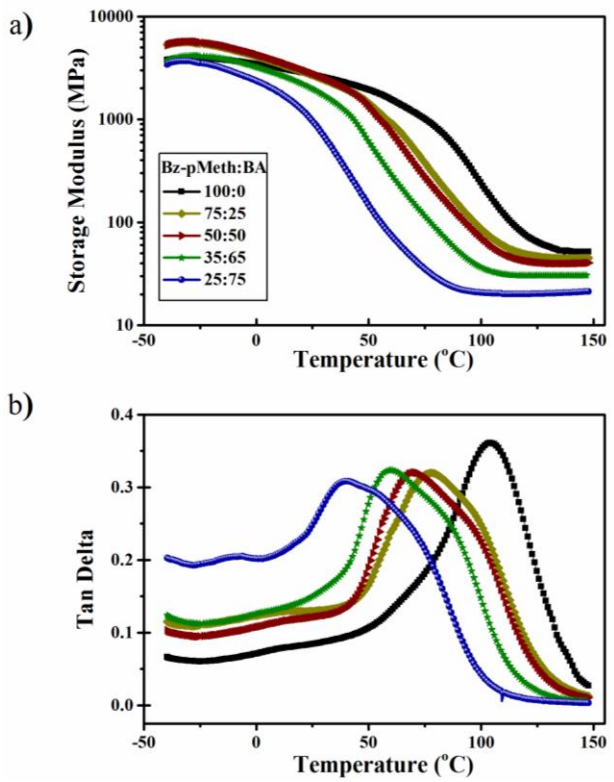

*Figure 40***.** DMA plots of time dependence of a) storage modulus b) tan delta of UV-cured compositions of Bz-Meth:BA.

The full width at half height (FWHH) of the tan delta peak broadened until Bz-$Meth_{50}$:BA_{50} composition and decreased thereafter with the addition of BA. The observed glass transition broadening can be related to the structural heterogeneity of the network.[26] The glass transition temperature of a pure p(Bz-Meth) and p(BA) are 104.7 °C and -54 °C respectively. The composition dependence of the tan δ peak is perceived as a common indicator to establish miscibility in the co-monomers.[27] The glass transition temperatures of the Bz-Meth:BA compositions showed single main-chain relaxation processes spanning between the effective T_g's of the pure components, indicating miscibility in the co-monomers. The transition peak broadening can be related to the existence of a broad spectrum of glass transition temperatures in the material.

Table 13

Thermo-mechanical data of UV cured and dually cured compositions of Bz-Meth:BA

Only UV Bz-pMeth:BA	**$^{1}T_{gexp}$ (°C)**	**$^{2}T_{gtheo}$ (°C)**	**E' at 25 °C [MPa]**	**FWHH (°C)**	**E' at T_g+40 °C [MPa]**	**$^{3}v_e$ (mol/cm^3)**
100:0	104.7	104.7	2653	41.5	55	5.90×10^{-3}
75:25	77.5	86.7	2706	48.1	50	5.80×10^{-3}
50:50	70.6	63.5	2802	51.2	49	5.77×10^{-3}
35:65	60.6	41.2	1995	47.2	36	5.31×10^{-3}
25:75	39.5	23.3	924	41.9	29	4.99×10^{-3}
UV+Thermal p(Bz-pMeth:BA)	**T_g (°C)**		**E' at 25 °C [MPa]**	**FWHH (°C)**	**E' at 175 °C [MPa]**	
p(Bz-Meth)	177.0		2470	64.5	303	-
100:0	183.8		4618	100.4	368	-
75:25	172.1		5789	129.2	252	-
50:50	163.0		4000	133.4	199	-
35:65	152.3		2000	144.3	146	7.10×10^{-3}
25:75	120.0		1833	119.4	93	6.84×10^{-3}

[1] Experimental T_g value; [2] Theoretical T_g by Fox equation; The T_g of poly(butyl acrylate) homopolymer was taken as -54 °C.[3] Values calculated using Nielson equation.[28]

The high level of heterogeneity in dimethacrylate network stems from the complex nature of radical-mediated chain-growth crosslinking polymerization, which has been studied to occur by the formation of high T_g micro-gel clusters during the initial stages of polymerization, co-existing with micro-gels of a lower T_g.[29-31] The presence of a small low-temperature shoulder of the loss tangent maximum could be a result of juxtaposition of the relaxation processes corresponding to the components with high and low crosslinking density that are responsible for the high and low temperature transitions, respectively.[32] Additionally, the low-temperature transitions (-50-40 °C) could be related to the β-relaxation processes of poly(methacrylate) structure due to the hindered side-chain motion of carboxyl side groups around the C-C bond connecting the side groups to

the main-chain backbone, and which is comparable to that of pure PMMA backbone of similar nature.[33]

All compositions exhibited a stable rubbery plateau regime, suggesting the fact that the maximum cure conversion is attained, despite the presence of residual amount of unreacted monomers. The cross-link density of Bz-pMeth:BA materials were estimated using the following Nielson equation[26, 34], designed for highly cross-linked materials.

$$\text{Log } G_e = 7 + 293\ (\rho/M_c)$$

where, G_e (dyne/cm^2) - storage modulus in the rubbery plateau regime at T_g+40 °C, ρ - density of the material at room temperature (g/cm^3), M_c- molecular weight between the crosslinks (g/mole) and $v_e = \rho/M_c$ - crosslinking density (mol/cm^3). The cross-linking density for all the compositions presented a systematic reduction with the increase of BA mole content, which was in direct coherence with the trend observed for glass transition temperatures. Glass transition temperature of a polymeric material can be related to its crosslinking density, where an increase in the crosslinking density results in tighter packing and restricts the segmental motion of the polymer chains, thereby increasing the glass transition temperature.

Figure 41 shows the temperature dependence plots of storage modulus and tan delta of fully cured compositions of Bz-Meth:BA. A storage modulus of around 2.47 GPa was observed for the thermally cured pristine p(Bz-Meth), this value was close to that observed for most of the commonly studied polybenzoxazines, B-a (2.2 GPa).[35] The storage modulus values for all the dual-cured compositions (1.8–4.6 GPa) were relatively higher than their corresponding UV cured network, which is expected as a result of combined rigidity imposed by the polymethacrylate and polybenzoxazines crosslinks.

The glass transition temperatures of the fully cured specimens presented similar trend as that of primary UV cured network, and decreased linearly upon addition of BA. Additionally, for all the compositions including the pristine p(Bz-Meth) network, a broad transition (40–90 °C) centered at ca. 70 °C presenting a partial overlap with the main-chain α-relaxation peak appeared. This range appears to be very close to the β-transition zone observed for a wide variety of bisphenol and diamine-based polybenzoxazines,[36] and is associated with the movement within Mannich bridge. Furthermore, the position of β-relaxation peak relatively shifted to a lower temperature with the incorporation of p(BA) segments. It can be postulated that the relative increase in chain flexibility with the addition of BA enhances the short-chain motion of the atoms associated with the Mannich bridge, and shifts the secondary tan delta peak to a lower temperature. Low temperature shift of the β-relaxation peak was a result of higher degree of flexibility with the inclusion of flexible p(BA) segments.

The height and area of tan δ peak is associated with the degree of crosslinking.[37] A depression in the damping peak with the incorporation of BA, suggested a relative increase in the degree of crosslinking, which can be ascribed to increased mobility and the offset of degradation process affecting the extent of benzoxazine polymerization, as previously suggested by DSC and TGA analysis. The magnitude of the tan δ peak for the fully cured specimens were lower than that of UV cured network, suggesting higher crosslink density. Similar to UV cured network, the peak width at half height at the α-transition broadened with the incorporation of BA, which is a result of increased network heterogeneity in the co-monomer mixture. In comparison to the blends, the pristine Bz-Meth showed relatively a sharper damping behavior. Polybenzoxazines are known to

exhibit low crosslinking density, yet possess a high glass transition temperature resulting in a sharper damping peak.[35]

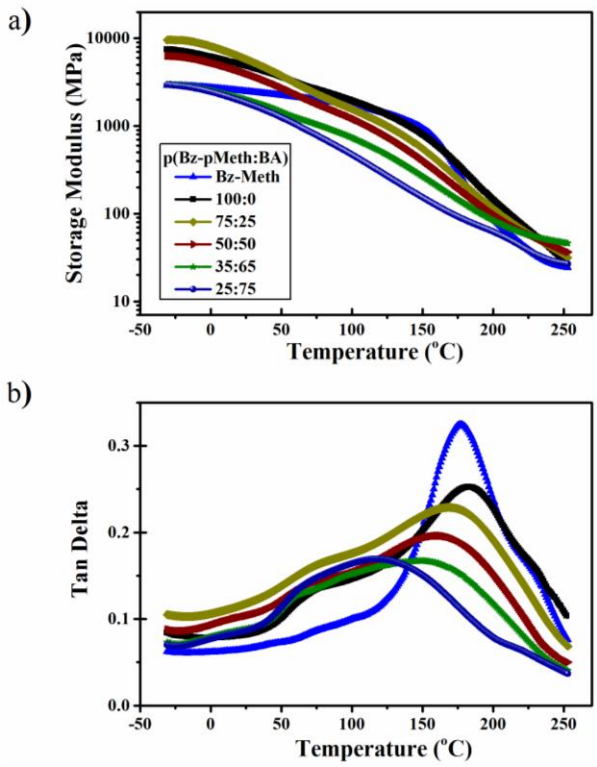

Figure 41. DMA plots of time dependence of a) storage modulus b) Tan delta of dually cured (UV + thermal) compositions of Bz-Meth:BA.

The crosslinking densities were calculated from the storage modulus in the rubbery plateau regime using the Nielson equation, as described above. Analysis of crosslink densities for the dual-cured compositions of Bz-Meth:BA were complicated by thermal degradation immediately following the glass transition temperature. These results can be correlated with the DSC and TGA studies, which showed that the extent of benzoxazine polymerization was interrupted due to the immediate overlap of the early degradation process. On the basis of lower glass transition temperature and higher onset of degradation temperatures, the Bz-Meth$_{35}$-BA$_{65}$ and Bz-Meth$_{25}$-BA$_{75}$ systems showed

relatively stable rubbery plateau regime. The calculated crosslinking densities of Bz-$Meth_{35}$:BA_{65} (7.10×10^{-3} mol/cm^3) and Bz-$Meth_{25}$:BA_{75} (6.84×10^{-3} mol/cm^3) were relatively higher compared to their corresponding UV cured network (Table 13).

Conclusions

Sequentially addressable hybrid polybenzoxazine networks were developed involving UV photopolymerization of meth(acrylates), followed by thermally activated polymerization of benzoxazines. Butyl acrylate (BA) was used as a reactive diluent in UV polymerization of methacrylate functional benzoxazine (Bz-Meth). Structure-property relationships of the formation of hybrid networks were established by relating the effect of co-monomer composition with the time evolution of visco-elastic properties, nature of cure exotherm and thermo-mechanical properties.

UV cure kinetics of Bz-Meth:BA blends showed faster and superior development of visco-elastic properties with the inclusion of BA diluent. The lower viscosity and higher mobility of the propagating radicals prior to the vitrification stage with the subsequent delayed vitrification led to the attainment of higher final extent of conversion. The highest limiting shear storage modulus value was obtained for equal weight mixtures of Bz-Meth and BA, which was a result of the superior network formation with faster diffusion-controlled termination kinetics in Bz-Meth in combination with higher extent of polymerization due to the presence of a more mobile BA. The progressive addition of BA diluent reduced the viscosity of the Bz-Meth monomer, rendering them highly processable. The initial degradation stability of the fully cured networks was improved with the addition of BA because of the absence of early degradation processes in p(BA) as compared to poly(methylacrylate) and polybenzoxazine structures. On the other hand,

the char yield of the hybrid networks systematically reduced with the BA mole content because of the reduction in aromatic content and degree of rigidity with the inclusion of relatively less stable aliphatic crosslinks. The glass transition temperatures and crosslinking densities of UV cured compositions of Bz-Meth:BA showed a systematic reduction in relative to the BA content, indicating enhanced flexibility. Likewise, the glass transition temperatures of the dually cured networks reduced with the incorporation of BA content.

The dual-cure methodology offers an ease of handling of the otherwise brittle polybenzoxazine films via the formation of stable, moldable intermediate networks prior to the full final cure. Moreover, the sequential of network synthesis allowed systematic study of network formation and properties of the individual polymer networks. Future studies will be directed towards utilizing a library of structurally distinct acrylate/methacrylate monomers to target a broad range of tailorable material properties, and establish a strong fundamental understanding of structure-processing-property relationships.

Acknowledgments

The authors gratefully acknowledge financial support from the National Science Foundation (NSF CAREER DMR-1056817). The authors thank the Otaigbe Research group (Dr. Joshua U. Otaigbe and Shahab K. Rahimi) for assistance with rheological measurements.

References

1. Ghosh, N.; Kiskan, B.; Yagci, Y., Polybenzoxazines - New high performance thermosetting resins: Synthesis and properties. *Prog. Polym. Sci.* 2007, *32* (11), 1344-1391.

2. Takeichi, T.; Kawauchi, T.; Agag, T., High Performance Polybenzoxazines as a Novel Type of Phenolic Resin. *Polym. J* 2008, *40* (12), 1121-1131.

3. Yagci, Y.; Kiskan, B.; Ghosh, N. N., Recent advancement on polybenzoxazine—A newly developed high performance thermoset. *Journal of Polymer Science Part A: Polymer Chemistry* 2009, *47* (21), 5565-5576.

4. Fouassier, J. P., In *Photoinitiation, Photopolymerization, and Photocuring: Fundamentals and Applications*, Hanser/Gardner Publications: Munich, 1995.

5. Yagci, Y.; Jockusch, S.; Turro, N. J., Photoinitiated polymerization: advances, challenges, and opportunities. *Macromolecules* 2010, *43* (15), 6245-6260.

6. Macko, J. A.; Ishida, H., Behavior of a bisphenol- A- based polybenzoxazine exposed to ultraviolet radiation. *Journal of Polymer Science Part B: Polymer Physics* 2000, *38* (20), 2687-2701.

7. Gacal, B.; Cianga, L.; Agag, T.; Takeichi, T.; Yagci, Y., Synthesis and characterization of maleimide (Co)polymers with pendant benzoxazine groups by photoinduced radical polymerization and their thermal curing. *Journal of Polymer Science Part A: Polymer Chemistry* 2007, *45* (13), 2774-2786.

8. Koz, B.; Kiskan, B.; Yagci, Y., A novel benzoxazine monomer with methacrylate functionality and its thermally curable (co)polymers. *Polym. Bull.* 2011, *66* (2), 165-174.

9. Jin, L.; Agag, T.; Yagci, Y.; Ishida, H., Methacryloyl-Functional Benzoxazine: Photopolymerization and Thermally Activated Polymerization. *Macromolecules* 2011, *44* (4), 767-772.

10. Kasapoglu, F.; Cianga, I.; Yagci, Y.; Takeichi, T., Photoinitiated cationic polymerization of monofunctional benzoxazine. *Journal of Polymer Science Part A: Polymer Chemistry* 2003, *41* (21), 3320-3328.

11. Tasdelen, M. A.; Kiskan, B.; Yagci, Y., Photoinitiated free radical polymerization using benzoxazines as hydrogen donors. *Macromolecular rapid communications* 2006, *27* (18), 1539-1544.

12. Lu, C.-H.; Su, Y.-C.; Wang, C.-F.; Huang, C.-F.; Sheen, Y.-C.; Chang, F.-C., Thermal properties and surface energy characteristics of interpenetrating polyacrylate and polybenzoxazine networks. *Polymer* 2008, *49* (22), 4852-4860.

13. Okhawilai, M.; Pudhom, K.; Rimdusit, S., Synthesis and characterization of sequential interpenetrating polymer networks of polyurethane acrylate and polybenzoxazine. *Polymer Engineering & Science* 2014, *54* (5), 1151-1161.

14. Spontón, M.; Estenoz, D.; Lligadas, G.; Ronda, J. C.; Galià, M.; Cádiz, V., Synthesis and characterization of a hybrid material based on a trimethoxysilane functionalized benzoxazine. *Journal of Applied Polymer Science* 2012, *126* (4), 1369-1376.

15. Narayanan, J.; Jungman, M. J.; Patton, D. L., Hybrid dual-cure polymer networks via sequential thiol–ene photopolymerization and thermal ring-opening polymerization of benzoxazines. *Reactive and Functional Polymers* 2012, *72* (11), 799-806.

16. Ning, X.; Ishida, H., Phenolic materials via ring-opening polymerization: Synthesis and characterization of bisphenol-A based benzoxazines and their polymers. *Journal of Polymer Science Part A: Polymer Chemistry* 1994, *32* (6), 1121-1129.

17. Liu, J. Synthesis, characterization, reaction mechanism and kinetics of 3,4-dihydro-2H-1,3-benzoxazine and its polymer, Ph.D. Thesis. Case Western Reserve University, Cleveland, OH, May 1995.

18. Agag, T.; Jin, L.; Ishida, H., A new synthetic approach for difficult benzoxazines: Preparation and polymerization of 4,4′-diaminodiphenyl sulfone-based benzoxazine monomer. *Polymer* 2009, *50* (25), 5940-5944.

19. Srinivasan, S.; Lee, M. W.; Grady, M. C.; Soroush, M.; Rappe, A. M., Self-initiation mechanism in spontaneous thermal polymerization of ethyl and n-butyl acrylate: A theoretical study. *The Journal of Physical Chemistry A* 2010, *114* (30), 7975-7983.

20. MacCallum, J. R., The thermal degradation of poly(methyl methacrylate). *Die Makromolekulare Chemie* 1965, *83* (1), 137-147.

21. Haken, J. K.; Tan, L., Mechanism of thermal degradation of poly(alkyl acrylate)s using pyrolysis gas chromatography mass spectrometry. *Journal of Polymer Science Part A: Polymer Chemistry* 1988, *26* (5), 1315-1322.

22. Low, H. Y.; Ishida, H., Mechanistic study on the thermal decomposition of polybenzoxazines: Effects of aliphatic amines. *Journal of Polymer Science Part B: Polymer Physics* 1998, *36* (11), 1935-1946.

23. Fox, T. G., Influence of diluent and copolymer composition on the glass

temperature of a polymer system. *Bull. Am. Phys. Soc.* 1956, *1*, 123.

24. Kine, B.; Novak, R., Acrylic and methacrylic ester polymers. *Wiley-Interscience, Encyclopedia of Polymer Science and Engineering.* 1985, *1*, 234-286.

25. Fernández–García, M.; Cuervo–Rodriguez, R.; Madruga, E. L., Glass transition temperatures of butyl acrylate–methyl methacrylate copolymers. *Journal of Polymer Science Part B: Polymer Physics* 1999, *37* (17), 2512-2520.

26. Nielsen, L. E., Cross-linking–effect on physical properties of polymers. 1969.

27. Olagoke, O.; Lloyd, M. R.; Montgomery, T. S., *Methods for determining polymer-polymer miscibility. Polymer-Polymer Miscibility*. Academic Press, New York: 1979.

28. Nielsen, L. E., Cross-Linking–Effect on Physical Properties of Polymers. *Journal of Macromolecular Science, Part C* 1969, *3* (1), 69-103.

29. Guo, Z.; Browne, E.; Compton, J.; Sautereau, H.; Kranbuehl, D., Dielectric, dynamic mechanical and DSC evidence for a spatial and dynamic heterogeneity in a single phase polymer system. *Journal of Non-Crystalline Solids* 2006, *352* (42–49), 5025-5028.

30. Krzeminski, M.; Molinari, M.; Troyon, M.; Coqueret, X., Characterization by atomic force microscopy of the nanoheterogeneities produced by the radiation-induced cross-linking polymerization of aromatic diacrylates. *Macromolecules* 2010, *43* (19), 8121-8127.

31. Rey, L.; Galy, J.; Sautereau, H.; Simon, G. P.; Cook, W. D., PALS free volume and mechanical properties in dimethacrylate-based thermosets. *Polymer International* 2004, *53* (5), 557-568.

32. Simon, G. P.; Allen, P. E. M.; Williams, D. R. G., Properties of dimethacrylate copolymers of varying crosslink density. *Polymer* 1991, *32* (14), 2577-2587.

33. Espadero Berzosa, A.; Gómez Ribelles, J. L.; Kripotou, S.; Pissis, P., Relaxation Spectrum of Polymer Networks Formed from Butyl Acrylate and Methyl Methacrylate Monomeric Units. *Macromolecules* 2004, *37* (17), 6472-6479.

34. Nielsen, L. E., Mechanical behavior of some lightly crosslinked rubbers. *Journal of Applied Polymer Science* 1964, *8* (1), 511-520.

35. Ishida, H.; Allen, D. J., Physical and mechanical characterization of near-zero shrinkage polybenzoxazines. *J. Polym. Sci. A: Polym. Phys.* 1996, *34* (6), 1019-1030.

36. Ning, X.; Ishida, H., Phenolic materials via ring-opening polymerization of benzoxazines: Effect of molecular structure on mechanical and dynamic mechanical properties. *Journal of Polymer Science Part B: Polymer Physics* 1994, *32* (5), 921-927.

37. Nielsen, L. E., Mechanical Properties of Polymers and Composites. Marcel Dekker: New York, 1974; Vol. I, pp 174-181.

CHAPTER VI

CONCLUSIONS AND FUTURE DIRECTIONS

In this dissertation, dual-cure hybrid polybenzoxazine thermosets have been developed with an aim to improve the processability and showcase a broad range of tailorable material properties attainable within the same system. The versatility of the work has been demonstrated with the study of different orthogonal cure chemistries in combination with thermally activated polymerization of benzoxazines, These cure chemistries included - rapid UV curable thiol-ene click chemistry, thermally curable ring-opening metathesis polymerization of norbornene, and free radical photo-polymerization of meth(acrylate) functionalities. A strong fundamental understanding of structure-property relationships with respect to network structure, kinetics, processing control and material properties of the hybrid networks was evaluated.

In the first study, orthogonal UV mediated thiol-click and thermally activated benzoxazine chemistries were combined to develop sequentially processable network. Less than quantitative conversion of thiol and allyl functional groups was achieved during the radical-mediated thiol-ene photopolymerization as a result of competing nucleophilic ring-opening thiol-benzoxazine reaction with the radical-mediated thiol-ene reaction. These competing reactions ultimately yield a heterogeneous polymer network following the sequential thermal ring-opening polymerization the benzoxazines. Nonetheless, thermomechanical analysis of the hybrid networks showed the achievement of a high glass transition temperature (150 °C); one of the highest glass transitions reported to date for a thiol-ene based material. The hybrid polymer network exhibited

good thermal stability and could easily be processed into thin films by spin-coating the resin prior to the photopolymerization and thermal cure process.

Future work in the first study will be based on investigating mechanical properties of the hybrid network, and quantitatively evaluate the relative effect of intermediate network formation on the cure kinetics of benzoxazine polymerization. Future area of interest will focus on establishing optimum conditions for reducing the occurrence of the competing thiol reactions, which will lead to more well-defined polymer networks with tunable thermal and mechanical properties. In this direction, structure-property relationship will be studied by taking into account various parameters, including the choice of thiols and enes monomers with different chemical structure, reactivity, acidity and functionality, and curing conditions – cure time and temperature, source of trigger, light intensity type and concentration of the initiator.

In the second study, dual cross-linked hybrid networks were synthesized by combining two independent curing mechanisms – thermally induced ROMP polymerization (25 ^{o}C to 180 ^{o}C) followed by ring opening addition polymerization of benzoxazines. Benzoxazine containing bisfunctional norbornene cross-linker (Nor-BZO) was synthesized and blended separately with two different reactive comonomers – 5-ethylidene-2-norbornene (ENB) and dicyclopentadiene (DCPD) at varying concentrations. The addition of DCPD and ENB exhibited an accelerating effect on the viscoelastic properties of blends, among which ENB-based systems showed faster gelation kinetics due to the low viscosity and high reactivity of ENB co-monomer. The onset and peak of exotherm of ROMP curing of Bz-Nor:DCP and Bz-Nor:ENB blends were shifted to a lower temperature in relative to the rise in DCPD and ENB content,

respectively. Albeit the flammability characteristics (char yield) of the dual cross-linked hybrid thermosets were lowered compared to that of the pristine p(Bz-Nor) due to reduction in aromatic content, a systematic increment in the initial weight loss temperatures was observed with increasing DCPD/ENB content. Dual-cure networks based on ENB-based blends showed higher initial degradation temperatures and lower char yield than that of DCPD-based blends. The incorporation of lesser rigid cycloaliphatic crosslinks of DCPD exhibited a relative decrease in stiffness and glass transition temperatures in addition to the enhancement of the thermal stability of rubbery plateau modulus. For ENB-based systems, a systematic reduction in stiffness was observed in direct proportion to the ENB content, while on the other hand the glass transition temperatures increased, and was relatively higher than that of DCPD-based networks.

Future work in the second study will be geared towards quantifying cure kinetics using in-situ thermal FT-IR studies to logistically establish relationship between conversion based on cure time, cure temperature, catalyst concentration and network properties. Studies will be targeted towards optimizing the catalyst concentrations for different reactive blends to achieve the desired combination of rapid kinetics/conversion and superior thermo-mechanical properties. Future area of interest will be to synthesize a series of flexible norbornene functional benzoxazine monomers comprising of different core and side-chain length spacers for targeting low-temperature ROMP polymerization with enhanced ROMP reactivity, and establish controlled/sequential network synthesis.

In the third study, sequentially addressable hybrid polybenzoxazine networks were developed involving UV photopolymerization of meth(acrylates), followed by

thermally activated polymerization of benzoxazines. The progressive addition of BA diluent reduced the viscosity of the Bz-Meth monomer, rendering them highly processable. The gelation and vitrification kinetics of the co-monomer mixtures were enhanced with the inclusion of BA diluent. The highest limiting shear storage modulus value was obtained for equal weight mixtures of Bz-Meth and BA, which was a result of the superior network formation with faster diffusion-controlled termination kinetics in Bz-Meth in combination with higher extent of polymerization due to the presence of a more mobile BA. The initial degradation stability of the fully cured networks was improved with the addition of BA, while the char yield of the hybrid networks showed a systematic decrease with the BA mole content. The glass transition temperatures of UV cured and dually cured compositions of Bz-Meth:BA showed a systematic reduction in relative to the BA content, indicating enhanced flexibility.

Future work in the third study will be directed towards investigating the mechanical and shrinkage stress properties, and quantitatively examine the cure kinetics to determine the relative effect of network formation of the primary UV-cured network on the extent of benzoxazine polymerization. Future area of interest will be towards exploring a broad range of acrylate/methacrylate monomers with varying chemical structure, viscosity and functionality with an aim to achieve a broad array of material properties.

The application of dual-cure hybrid methodology in polybenzoxazines could be considered as a promising solution in overcoming the limitations of polybenzoxazines with an access to a broad array of improved and tailorable material properties. The simplistic synthetic methodologies and rich molecular design flexibility lay a strong

foundation for future developments with the creation of improved and novel polybenzoxazine materials for a variety of applications. Tremendous opportunities exist for long-term exploration of our work. Future area of interest is to develop dual-cure hybrid thermosets combining supramolecular reversible crosslinks and covalently crosslinked polybenzoxazines. Supramolecular polymers based on hydrogen bonding and metal-ligand interactions rely on weak and reversible non-covalent interactions, and thus allow a macroscopic response from change in network architecture using a variety of stimuli (temperature, light, pH, solvent, concentration etc.). Thus, the incorporation of reversible crosslinks within the thermosetting matrix will provide an access to a broad range of unique features including recyclability, stimuli responsiveness, self-healing ability and improved processing.

Overall, this approach could yield fundamentally different network structures, polymerization kinetics, thermo-mechanical properties, and processing control from benzoxazines. From the practical standpoint, this information would provide a platform to develop tailor made solutions for specific end-use applications in the areas of coatings, adhesives, sealants and high performance composites,

APPENDIX A

HYBRID DUAL-CURE POLYMER NETWORKS VIA SEQUENTIAL THIOL-ENE PHOTOPOLYMERIZATION AND THERMAL RING-OPENING POLYMERIZATION OF BENZOXAZINES

Synthesis of allyl based bis-benzoxazine (B-allyl)

In a 100 mL round bottom flask , were added a mixture of bisphenol-A (5.0 g, 0.02 mol) , allyl amine (2.5 g, 0.04 mol) and paraformaldehyde (2.6 g , 0.08 mol) poured into 44 mL of xylene (4 mL per gram of reactant). The solution was heated to 120 ^{o}C and maintained for 40 minutes with continuous stirring. The reaction mixture was cooled to room temperature and stirred over basic alumina for 15 minutes. The reaction mixture was then poured into a 100 ml round bottom flask and heated at 150 ^{o} C for 10 minutes and an excess of 0.4 g of paraformaldehyde was added with stirring and heating was continued for another 30 minutes. After cooling to room temperature, xylene was removed by distillation under reduced pressure. The crude product was dissolved in diethyl ether (25 mL), extracted with 3N NaOH (3 × 25 mL) to remove phenolic impurities, followed by washing with distilled water (3 × 25 mL). The solution was dried over anhydrous $MgSO_4$, filtered and diethyl ether was distilled out to yield a pale yellow viscous liquid. (2.5 g, 30 %).

^{1}H-NMR (300 MHz, $CDCl_3$, ppm): δ = 1.58 (s , -CH_3), 4.83 (s, -O-CH_2-N-), 3.94 (s, Ar-CH_2-N), 3.39 (d, -CH_2-), 5.26 (m, =CH_2), 5.96 (m, -CH=), 6.66 - 6.94 (m, aromatic CH).

^{13}C-NMR ($CDCl_3$, ppm, δ): 81.87 (-O-CH_2-N-), 54.54 (-N-CH_2-Ar), 41.68 (-CH_2-, allyl), 115.74 (=CH_2, allyl), 135.04 (-CH=, allyl).

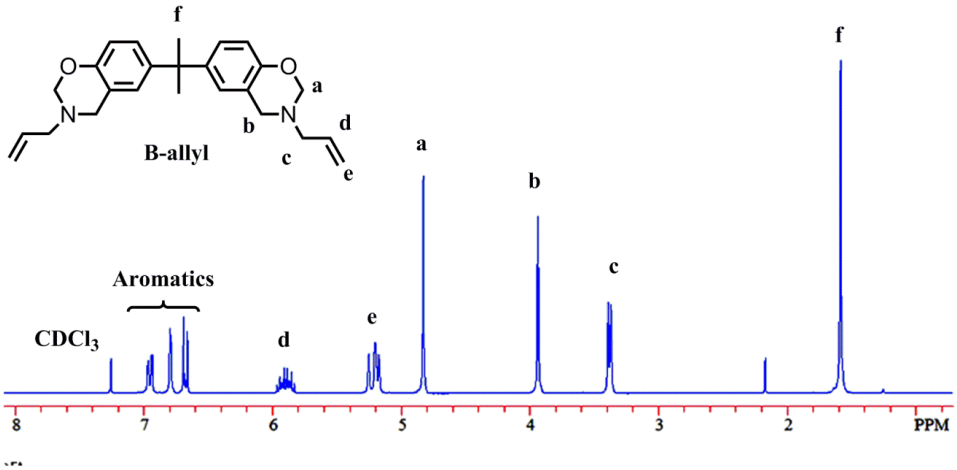

Figure A1. [1]H-NMR spectrum of allyl based bis-benzoxazine (B-allyl).

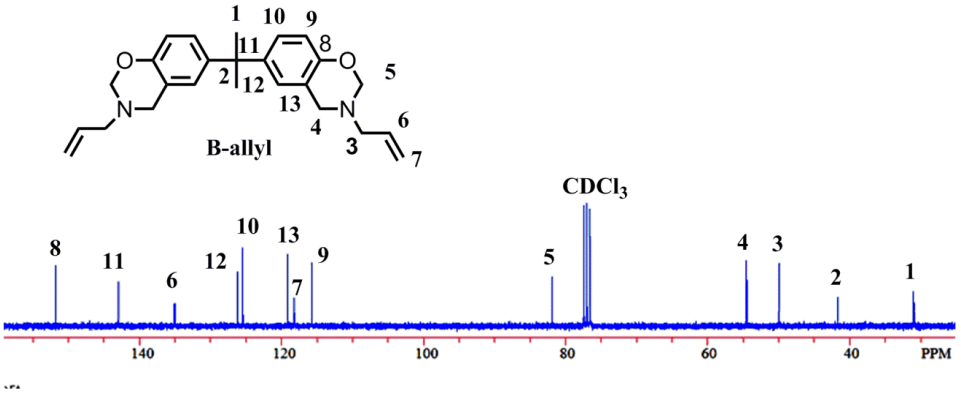

Figure A2. [13]C-NMR spectra of allyl based bis-benzoxazine (B-allyl).

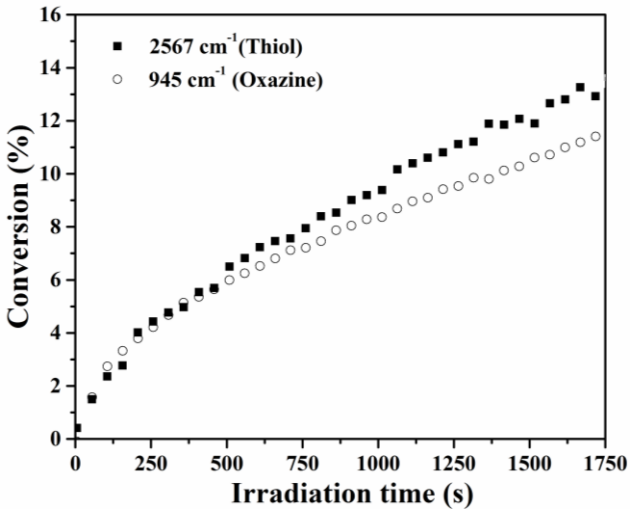

Figure A3. Real-time FTIR conversion plots using aniline based bis-benzoxazine exposed to UV radiation (36.0 mW/cm^2) at room temperature. Model studies were carried out using commercially available aniline based bis benzoxazine (Huntsman Araldite MT-35600) and glycol di-(3-mercaptopropionate) to understand the nature of benzoxazine ring-opening in the presence of thiol. Real-time FTIR kinetic studies were conducted under similar conditions to show that even in the absence of an alkene functional group, conversion of both thiol and benzoxazine ring (945 cm^{-1}) are still observed during the UV exposure.

*Figure A4***.** Photograph illustrating the ability to spin coat the liquid resins into thin films prior to sequential UV and thermal cure. The UV cure was carried out at room temperature for 20 min (365 nm, 36 mW/cm^2). The thermal cure was carried out at 180 ^{o}C in an air circulated oven for 3 h. The resin darkens towards a brownish-red color with increasing temperature.

APPENDIX B

DEVEOPMENT OF DUAL-CURE HYBRID COVALENTLY CROSSLINKED NETWORKS OF POLYNORBORNENE AND POLYBENZOXAZINE

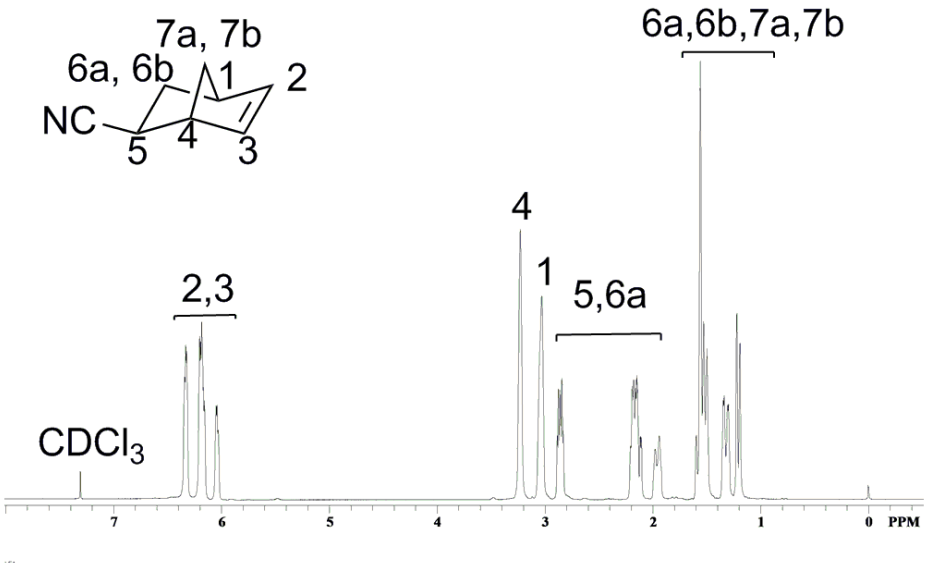

Figure B1. ^{1}H-NMR spectra of exo- and endo- mixtures of 5-norbornene-2-carbonitrile.

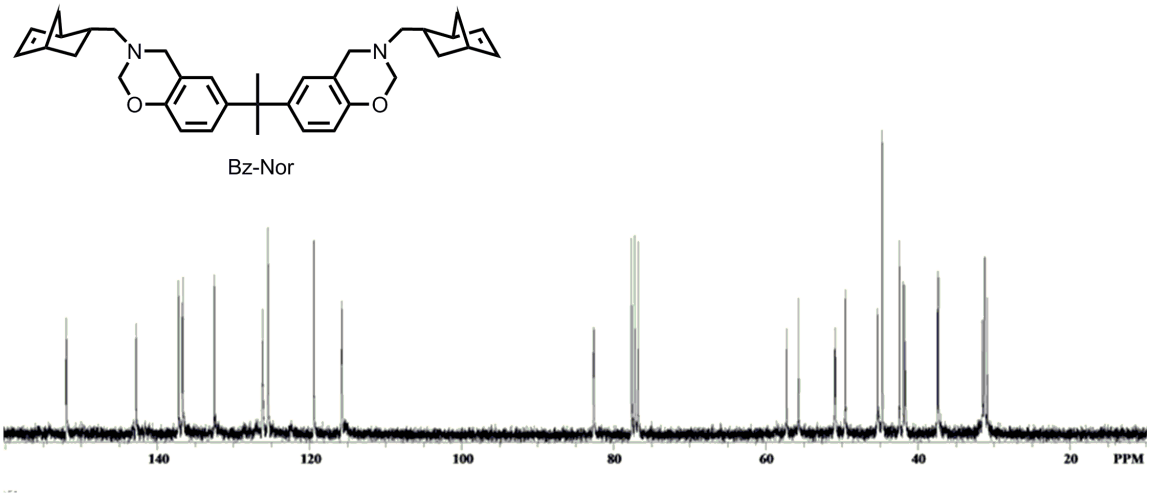

Figure B2. ^{13}C-NMR spectra of Bz-Nor monomer.

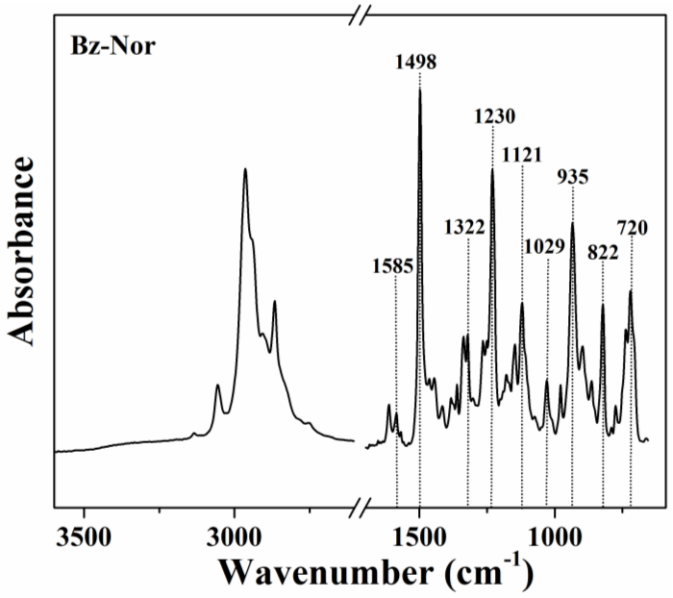

Figure B3. FT-IR spectra of Bz-Nor monomer resin.

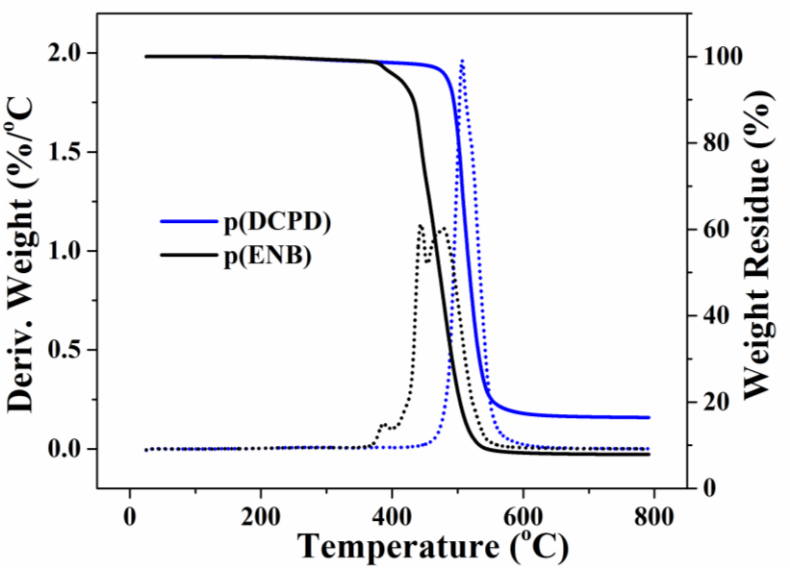

Figure B4. TGA profile of ROMP cured p(ENB) and p(DCPD) using Grubbs 3rd generation catalyst.

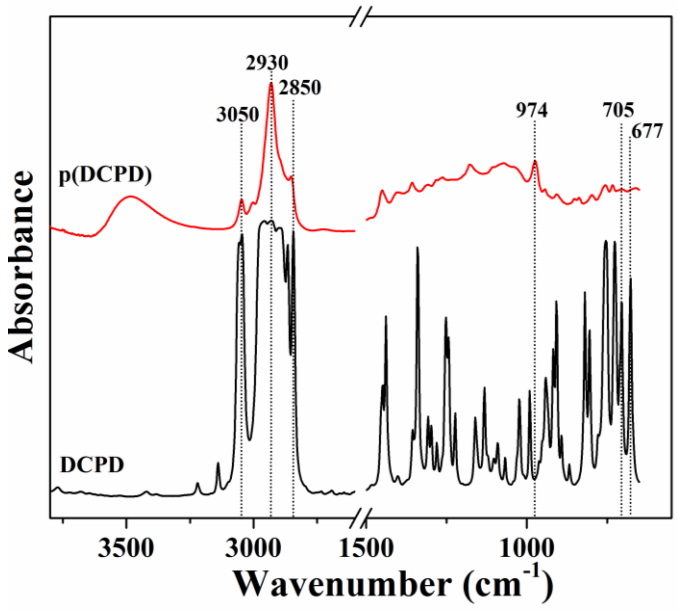

Figure B5. FT-IR spectra of DCPD monomer and p(DCPD) cured at 170 °C for 1h using Grubbs 3rd generation catalyst.

FT-IR, DCPD (KBr, cm^{-1}): 677-726 (out-of-plane =CH bending), 3010-3050 (sp^2 =C-H stretching), 2850-2930 (CH_2, sp^3 C-H stretching), 1340-1440 (=C-H bending)

FT-IR, pDCPD (KBr, cm^{-1}): 974 (out-of-plane trans C-H bending).

APPENDIX C

TUNABLE NETWORK PROPERTIES BASED ON DUAL-CURE HYBRID POLY(METHACRYLATE) AND POLYBENZOXAZINE NETWORKS

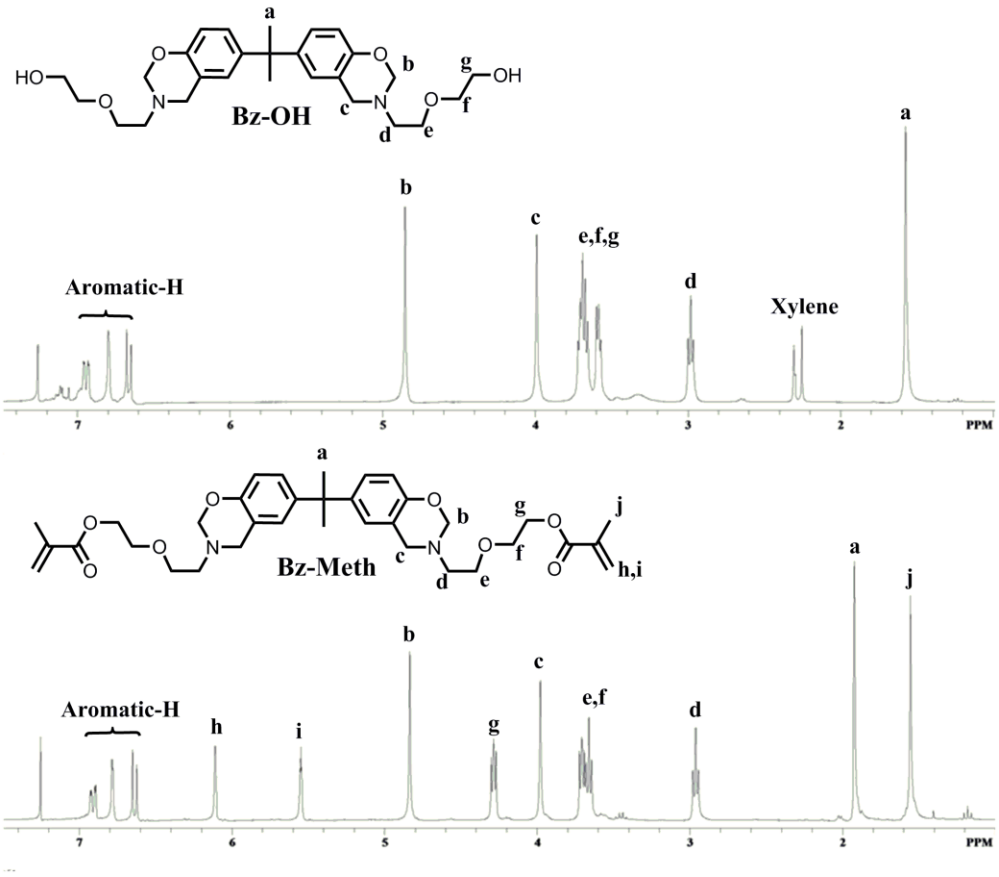

Figure C1. ^{1}H-NMR spectra of Bz-OH and Bz-Meth.

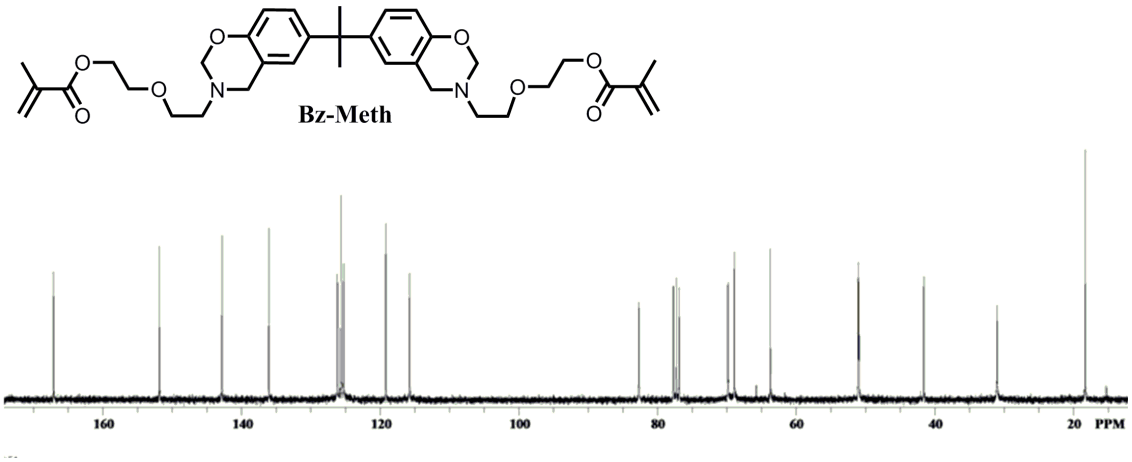

Figure C2. ^{13}C-NMR spectra of Bz-Meth monomer.

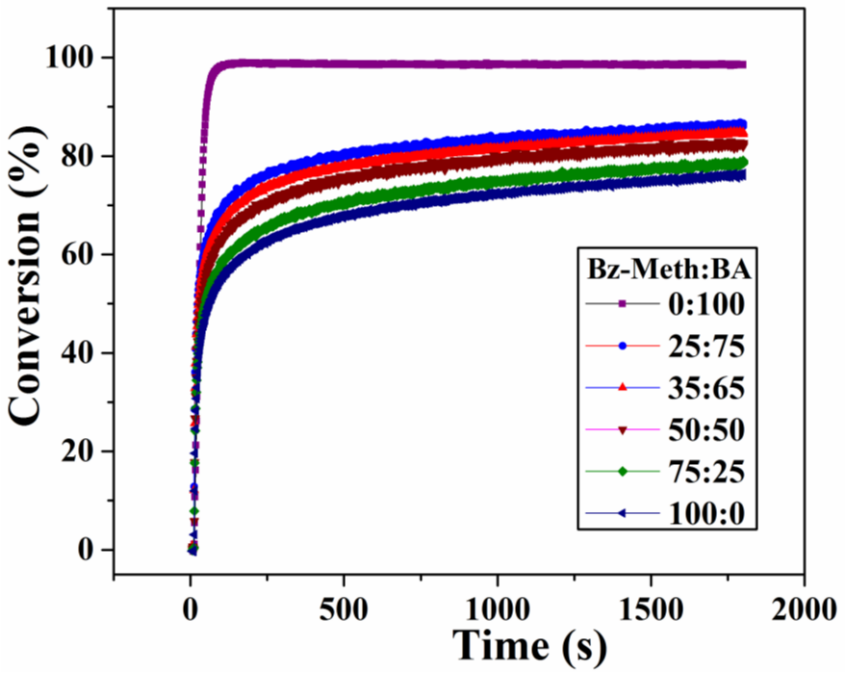

Figure C3. Double-bond (1637 cm^{-1}) conversion plots for Bz-Meth:BA formulations containing 2 wt% Irgacure 2020, irradiated with UV light (320-500 nm) for 1800 s using a light intensity of 20 mW/cm^2 at ambient temperature.

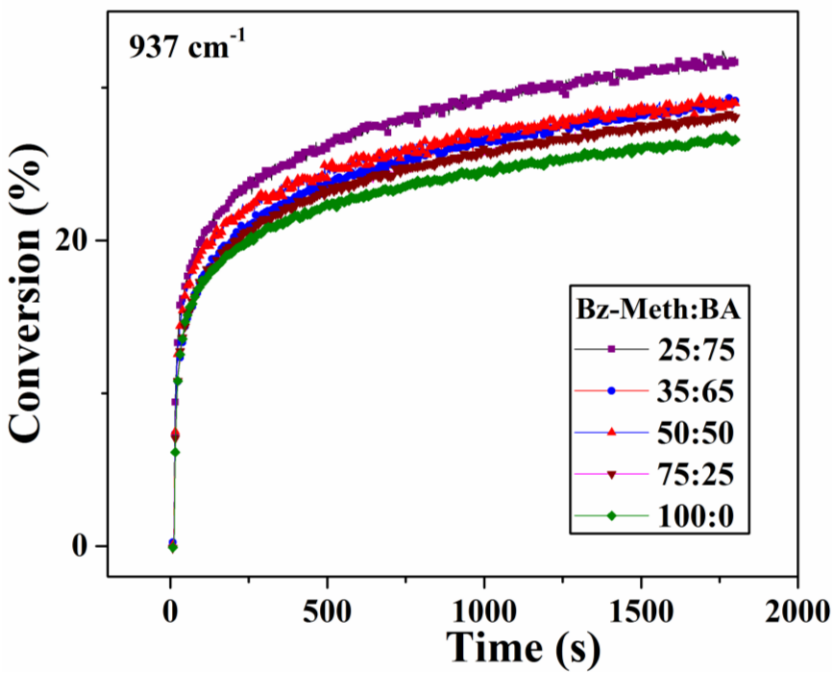

Figure C4. Real-time FTIR plots monitoring changes in the 937 cm^{-1} oxazine peak during UV curing of Bz-Meth:BA compositions using 3 wt% Irgacure 2020.

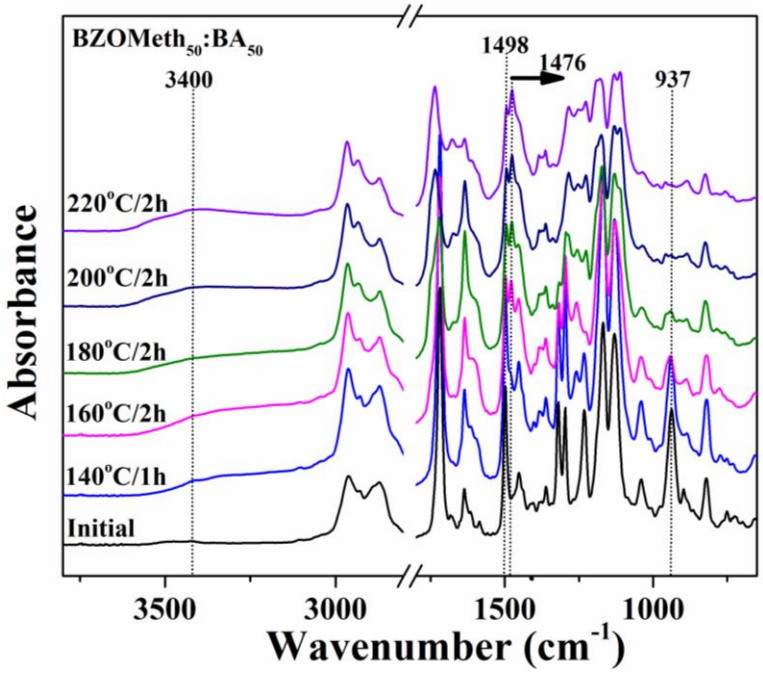

Figure C5. FT-IR spectra of thermally activated polymerization of Bz-$Meth_{50}$:BA_{50} after each stage of thermal step-cure under air atmosphere.

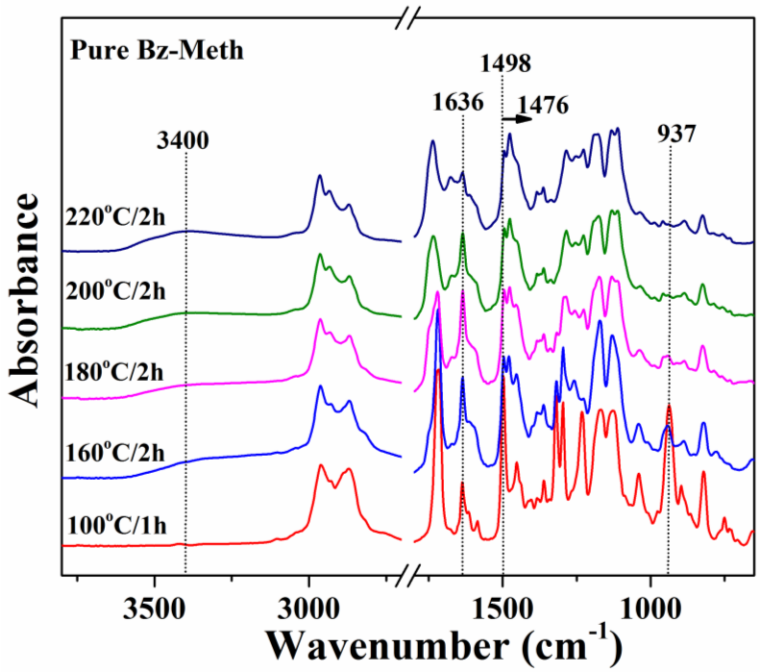

Figure C6. FT-IR spectra of thermally activated polymerization of pristine Bz-Meth resin after each stage of thermal step-cure under air atmosphere.